A Study of the Bloom's Syndrome Protein

A thesis submitted for the degree of
Doctor of Philosophy

Julia K. Karow

Linacre College
University of Oxford
Christmas 1999



Habe nun, ach!

Goethe, Faust I

...Who made heaven and earth, the sea, and all that therein is.

Ps. 146

Abstract

Julia K. Karow
Linacre College

Submitted for D.Phil.
Michaelmas 1999

A Study of the Bloom's Syndrome Protein

Bloom's syndrome is a rare autosomal recessive disorder characterised by an early onset of cancer of many types, erythematous lesions on sun-exposed skin, retarded growth, immunodeficiency and sub- or infertility. Cells from Bloom's syndrome patients have replication defects and an abnormally unstable genome manifested in chromosomal breaks and deletions and in an increased mutation rate. Most characteristically, these cells show elevated levels of sister-chromatid exchanges which probably result from homologous recombination events. Since the cells are not hypersensitive to DNA damaging agents, the defect is unlikely to be in one of the common DNA repair pathways. The gene mutated in Bloom's syndrome, *BLM*, was cloned in 1995 and found to encode a helicase from the RecQ family. This family is named after its *E. coli* member, RecQ, and includes at least five human genes. Three of these are mutated in inherited disorders; Bloom's syndrome, Werner's syndrome and Rothmund-Thomson syndrome.

In my DPhil project, I have investigated the enzymatic properties of the BLM protein. I have purified the protein in recombinant form and shown that it is a DNA-dependent ATPase and an ATP-dependent helicase with 3'-5' polarity. It binds and unwinds a variety of DNA structures, with a preference for tetraplex (G4)-DNA, Holliday junctions (recombination intermediates) and internal DNA bubbles. Furthermore, it is capable of branch migration, an activity distinct from its helicase activity. BLM forms oligomeric rings with fourfold and sixfold symmetry, both in a cell extract and as purified protein.

These results, in combination with the cellular phenotype of Bloom's syndrome and with evidence from the analysis of other RecQ homologues in model organisms such as yeast and *E. coli*, point to a role for BLM in somatic recombination (recombinational repair). Models for this function are discussed in this thesis.

Acknowledgements

Five years in England are coming to a close, of which my DPhil project of the last three years has been a particularly important time. Many people have contributed to my research in various ways, and many have opened up their country to me in a way that England will always remain my second home.

In particular, I would like to thank my supervisor, Prof. Ian Hickson. He was always approachable for discussions and gave valuable strategic advice for this project. Furthermore, he provided ample opportunity to develop my presentational and writing skills. In summary, he has been a good *Doktorvater*, as we say in Germany.
Dr. Chris Norbury deserves thanks for his admirable patience in response to numerous - some more, some less sophisticated - questions.
I am grateful to the Boehringer Ingelheim Fonds who sponsored my PhD project. Furthermore I would like to thank Prof. Adrian Harris for his financial support during the last three months of this work.

The members of the Hickson and Norbury laboratories, now "segregated", all provided a friendly and helpful atmosphere that made work enjoyable and – at times – endurable. The same is true for many people down the corridor who I would all like to thank.

For technical help at various stages of this project, I would particularly like to thank the following: Ronjon Chakraverty for his initial supervision, Phil North for advice on cloning and cell culture, Dominic Rothwell and Charles Redwood for their help with protein purification, Chris Ward and Robin Butler for introducing me to the Biocad, Alain van Gool and Jean-Yves Masson from Steve West's laboratory for detailed advice on substrate preparation, Rachael Murray for helping me to master the FPLC, Reg Boone for solving various urgent computer and printing problems, Richard Callaghan and Chris Burns from the Higgins laboratory for advice on enzymatic assays, and especially Leonard Wu for his tireless advice on many projects and for frequent discussions.

Special thanks go to Richard Crane and Yeun Shan Li for bringing music into my life and for being my friends.

Lots of love and support came from abroad – especially from Tom, who lived with me through all the ups and downs of a PhD. Finally, I would not have been able to advance this far without the love and help of my parents who I thank for all they did for me over many years.

Abbreviations

4NQO	4-nitroquinoline-1-oxide
ATP	adenosine 5'-triphosphate
ATPγS	adenosine 5'-O-(3-thiotriphosphate)
bp	base pairs
BS	Bloom's syndrome
BSA	bovine serum albumin
cDNA	complementary DNA
CS	Cockayne's syndrome
Da	Dalton
DNA	deoxyribonucleic acid
dsDNA	double-stranded DNA
DTT	dithiothreitol
ECL	enhanced chemiluminescence
EDTA	ethylenediaminetetraacetic acid
FPLC	fast liquid chromatography
GPA	glycophorin A
HEPES	N-(2-hydroxyethyl)piperazine-N'-[2-ethanesulfonic acid]
HRDC	helicase and RnaseD C-terminal
HU	hydroxyurea
kb	kilobase pairs
kDa	kilodaltons
LB medium	Luria-Bertani medium
MCM	minichromosome maintenance
NLS	nulcear localisation sequence
OD	optical density
ORC	origin of replication complex
PAGE	polyacrylamide gel electrophoresis
PCNA	proliferating cell nuclear antigen
PCR	polymerase chain reaction
PEG	polyethylene glycol

PML	promyelocytic leukaemia
RNA	ribonuleic acid
RNase	ribonuclease
RPA	replication protein A
RPC	replication protein C
RTS	Rothmund-Thomson syndrome
SCE	sister chromatid exchange
SDS	sodium dodecyl sulfate
SSB	single strand binding protein
ssDNA	single-stranded DNA
SV40	simian virus 40
TAE	Tris/acetate/EDTA
Taq	*Thermus aquaticus*
TBE	Tris/borate/EDTA
TE	Tris/EDTA
Tris	tris[hydroxymethyl]aminomethane
v/v	volume:volume ratio
w/v	weight:volume ratio
WS	Werner's syndrome
Y(E)PD	yeast extract peptone dextrose

Table of Contents

Abstract III
Acknowledgements IV
Abbreviations V
Table of Contents VII

Chapter 1 Introduction

1.1 General introduction 1
1.2 DNA replication 2
1.3 Genetic Recombination 3
1.3.1 Principles of DNA recombination 3
1.3.2 Homologous recombination 4
1.4 Helicases 6
1.4.1 Classification 6
1.4.2 Oligomeric state 7
1.4.3 Crystal structures 8
1.4.4 Polarity 12
1.4.5 Models for unwinding 12
1.4.6 Helicases in human disorders 13
1.4.6.1 Xeroderma pigmentosum 13
1.4.6.2 Cockayne's syndrome 15
1.4.6.3 Trichothiodystrophy 15
1.4.6.4 X-chromosome linked mental retardation syndrome (ATR-X) 16
1.5 The RecQ family of helicases 16
1.5.1 Overview 16
1.5.2 RecQ 21
1.5.3 RECQL 23
1.5.4 BLM 24
1.5.5 WRN 27

1.5.6 RECQL4 31
1.5.7 Sgs1 32
1.5.8 Rqh1 34
1.6 Human disorders resulting from defects in RecQ helicases 36
1.6.1 Bloom's syndrome 36
1.6.2 Werner's syndrome 38
1.6.3 Rothmund-Thomson syndrome 39
1.7 Aim of the project 40

Chapter 2 Materials and Methods

2.1 Chemicals and reagents 41
2.2 Cloning 41
2.2.1 Plasmids 41
2.2.1.1 *E. coli* cloning vector 41
2.2.1.2 *S. cerevisiae* expression vector 41
2.2.2 PCR (cloning) 42
2.2.3 PCR (screening) 42
2.2.4 Agarose gel electrophoresis 42
2.2.5 Purification of DNA from agarose gels 42
2.2.6 Ligation 43
2.2.7 *E. coli* strain 43
2.2.8 Competent cells 43
2.2.9 Transformation by electroporation 43
2.2.10 Small-scale preparation of plasmid DNA ("mini-prep") 44
2.2.11 Large-scale preparation of plasmid DNA ("maxi-prep") 44
2.2.12 Determination of DNA concentrations 45
2.2.13 Restriction enzyme digests 45
2.2.14 Sequencing 45
2.2.15 *S. cerevisiae* strain 46
2.2.16 Yeast transformation 46

2.3 Protein purification and analysis 46
2.3.1 Denaturing polyacrylamide gel electrophoresis 46
2.3.2 Western blotting 47

2.3.3 Antibodies 48
2.3.4 Yeast culture and protein induction 48
2.3.5 Yeast lysis 48
2.3.6 HeLa cell culture 49
2.3.7 HeLa cell lysis 49
2.3.8 Nickel chelate affinity chromatography 49
2.3.9 Determination of protein concentrations 50
2.3.10 Protein storage 50
2.3.11 Size exclusion chromatography 50
2.3.12 Electron Microscopy 50
2.3.12.1 Preparation of grids 50
2.3.12.2 Electron micrographs 51
2.3.13 Enzymatic assays 51
2.3.13.1 ATPase assays 51
2.3.13.2 Preparation of radiolabelled substrates 52
2.3.13.2.1 Gel purification of oligonucleotides 52
2.3.13.2.2 5'-labelling of oligonucleotides 52
2.3.13.2.3 Annealing and gel purification of small oligonucleotide substrates 52
2.3.13.2.4 Preparation of M13-based substrates 53
2.3.13.2.5 Preparation of long linear duplex substrate 54
2.3.13.2.6 Preparation of G4-DNA 54
2.3.13.3 Helicase assays 54
2.3.13.4 Bandshift assays 54

Chapter 3 Purification and initial characterisation of BLM

3.1 Introduction 55
3.2 Results 56
3.2.1 Cloning of the BLM expression construct 56
3.2.2 Overexpression and purification of BLM 57
3.2.3 Identification of BLM by western blotting 59
3.2.4 Characterisation of the ATPase activity of BLM 62
3.2.4.1 DNA dependence of the ATPase activity 62
3.2.4.2 Metal dependence of the ATPase activity 62

3.2.4.3 (2'-Deoxy)ribonucleoside 5'-triphosphate dependence of the NTPase activity 62
3.2.4.4 pH-dependence of the ATPase activity 62
3.2.4.5 Temperature dependence of the ATPase activity 67
3.2.4.6 Salt dependence of the ATPase activity 67
3.2.4.7 ATPase activity copurifies with BLM 67
3.2.4.8 Kinetic analysis of the ATPase activity 67
3.2.5 Helicase activity of BLM 72
3.2.6 Polarity of the helicase activity 72
3.3 Discussion 75

Chapter 4 Structure of BLM

4.1 Introduction 79
4.2 Results 80
4.2.1 Size-exclusion chromatography of purified BLM 80
4.2.2 Size-exclusion chromatography of extracts from yeast overexpressing BLM 82
4.2.3 Size-exclusion chromatography of HeLa cell extracts 82
4.2.4 Electron microscopy of BLM 85
4.2.5 Image analysis of BLM rings 85
4.3 Discussion 88

Chapter 5 Interaction of BLM with Holliday junctions

5.1 Introduction 93
5.2 Results 96
5.2.1 Unwinding of DNA substrates 96
5.2.1.1 HJ-X12 96
5.2.1.2 DS50 and DS52 96
5.2.1.3 HJ-X0 101
5.2.1.4 "Bubbles" and nicked substrates 101
5.2.1.5 G4-TP 106

5.2.1.6 Tailed substrates 109
5.2.1.7 Substrate comparison 112
5.2.2 Specificity of the BLM-Holliday junction interaction 114
5.2.3 Branch migration activity of BLM 116
5.3 Discussion 120

Chapter 6 Discussion

6.1 Summary of the key results 125
6.2 BLM – an "anti-recombinase" during replication? 126
6.2.1 BLM may remove "road blocks" to the replication fork 127
6.2.2 BLM may help stabilise stalled replication forks 129
6.3 BLM – a role in chromosome separation? 134
6.4 Outlook 136

Bibliography 137
Publications arising from this work 154

Chapter 1: Introduction

1.1 General introduction

In 1954, a New York physician named David Bloom published a paper in which he presented three cases of proportional dwarfs with sun-sensitive erythematous skin lesions resembling lupus erythematosus (Bloom 1954). He concluded "The occurrence of three almost identical cases suggests strongly a syndrome entity" – this syndrome would become known as "Bloom's syndrome" (BS). From 1960, cases of BS were systematically recorded worldwide and entered into the so-called "Bloom's Syndrome Registry" established by James German in New York. This registry was closed at the end of 1990 with 168 entries who have been continuously monitored since, including their families. In 1965, Bloom and German reported the occurrence of chromosome breakage in BS cells, and they speculated on the genetic nature of the disease (German *et al.* 1965). By 1969, German had observed an increase in cancer incidence in BS patients (German 1969). This turned out to be one of the main features of the disease: By 1996, 71 of the 168 patients in the registry had developed cancer, including tumours of all types. The year before, the gene mutated in BS, *BLM*, had been identified and cloned by German's group (Ellis *et al.* 1995). The protein encoded by this gene, BLM, turned out to be homologous to a class of DNA unwinding enzymes, the RecQ family of helicases.

Since there is evidence that BLM might be involved in DNA replication and recombination, these two processes will be briefly introduced first. This will be followed by a discussion of helicases in general and of human disorders resulting from defects in helicases. An

introduction to the key members of the RecQ family of helicases will be given, and the three human disorders associated with this family, Bloom's syndrome, Werner's syndrome and Rothmund-Thomson syndrome, will be presented.

1.2 DNA replication

DNA replication can be broadly divided into three stages: initiation, elongation and termination. It has been well characterised in *E. coli* and several viruses, including the eukaryotic virus SV40. (For recent reviews, see Campbell 1993, Stillman 1994, Huberman 1995, Sugino 1995, Bambara *et al.* 1997, Baker and Bell 1998.) Replication starts with the opening of DNA at an origin of replication. This is achieved by DnaA in *E. coli*, by the ORC proteins in yeast and by the T antigen in SV40. The single-stranded DNA thus created is stabilised by SSB in *E. coli* and by RPA in eukaryotes. A DNA helicase, DnaB in *E. coli* and large T in SV40, unwinds the DNA further at the replication fork. In eukaryotic cells, the replicative helicase has not been clearly identified yet although the MCM proteins are good candidates (Dutta and Bell 1997). An RNA primer is synthesised by DnaG (*E. coli*) or polymerase α/primase (eukaryotes) and extended by the polymerase III core (*E. coli*) or polymerase δ and probably ε (eukaryotes). In eukaryotes, polymerase switching is mediated by RFC. A "sliding clamp" is provided by the β subunit of polymerase III (*E. coli*) or by PCNA (eukaryotes). DNA synthesis is semiconservative, proceeds in 5'-3'direction and is semidiscontinuous, with a continuously synthesised leading strand and a discontinuously synthesised lagging strand. The RNA primers are removed by a nuclease (RnaseH in *E. coli* and eukaryotes, furthermore FEN-1 in

eukaryotes), the gaps are filled in by polymerase I (*E. coli*) or polymerase α (eukaryotes) and nicks are ligated by ligase (*E. coli*) or ligase I (eukaryotes).

When a replication fork encounters DNA damage, several scenarios are possible: If the damage consists of an adduct or an intrastrand crosslink, it may be bypassed and repaired by postreplicational gap repair. If the damage consists of a nick, this becomes a DSB once the fork has reached it, which is repaired by either homologous recombination or non-homologous end-joining (Kuzminov 1995, Kanaar and Hoeijmakers 1997, Kogoma 1997). Thirdly, the fork might get stalled and stabilised until the damage is repaired, whereupon replication can resume (Courcelle and Hanawalt 1999).

1.3 Genetic Recombination

1.3.1 Principles of DNA recombination

Genetic recombination is the exchange of DNA sequences between two DNA molecules. It occurs in all forms of life and serves to generate genetic diversity on the one hand and to repair damaged DNA on the other hand (West 1994). There are four major types of recombination (Heyer and Kohli 1994): site-specific recombination, general or homologous recombination, illegitimate recombination and transposition. In site-specific recombination, the exchange occurs between specific sites on the partner DNAs which otherwise bear no homology at all. In homologous recombination, the exchange can take place anywhere along the length of two homologous DNA molecules, although there may exist recombination "hot spots". Transposition is the transfer of DNA sequences from one site in the genome to another. Illegitimate recombination requires no specific sites and very little or no homology at all and leads to DNA rearrangements like insertions and deletions.

1.3.2 Homologous recombination

Homologous recombination serves both to generate genetic diversity (during bacterial conjugation or eukaryotic meiosis) and to repair DNA damage (DSB repair or postreplicational gap repair). It has at least six stages: 1) Initiation involving a nick, gap or double-strand break followed by formation of single-stranded DNA, 2) presynapsis, whereby the single-strand is activated for homology searching, 3) synapsis, the search for homology and pairing of homologous DNAs, 4) strand exchange leading to the formation of heteroduplex DNA, 5) establishment of Holliday junction intermediates and branch migration of the junction, and 6) resolution of the Holliday junction to give recombinant products (Camerini-Otero and Hsieh 1995).

Homologous recombination has been most extensively studied and is best understood in *E. coli*. Only now are we beginning to build up a picture of the process in eukaryotes, particularly in budding yeast. Historically, three distinct pathways of homologous recombination, the RecBCD pathway, the RecF pathway and the RecE pathway, had been defined in *E. coli*. The RecBCD pathway is the major pathway for conjugational recombination in *E. coli*, the RecE pathway is activated in *recBrecC* mutants by mutations in *sbcA*, and the RecF pathway is active in *recBCsbcBsbcC* mutants. However, the boundaries between these pathways are not as sharp as previously assumed, and there seem to exist several overlapping mechanisms (West 1994, Dunderdale and West 1994).

Initiation in *E. coli* starts with the formation of single-stranded DNA by RecBCD, RecQ/RecJ or RecE. RecBCD unwinds and degrades the DNA from a DSB until it reaches a χ-site, a recombination hotspot, where it nicks the DNA and pauses. Its nuclease activity is attenuated and it further unwinds the DNA to generate a single-stranded 3'-tail. Alternatively, RecQ starts

unwinding and forms single-stranded DNA, assisted by the single-strand specific exonuclease RecJ; or RecE, an exonuclease, forms a protruding DNA end. Next, RecA polymerises on the single-stranded DNA, forming a helical nucleoprotein filament. Its assembly may be assisted by RecF, RecO, RecR and SSB. This is followed by homology search and homologous pairing, maybe involving the formation of a DNA triplex (Camerini-Otero and Hsieh 1993, Rao *et al.* 1993). Reciprocal strand exchange and heteroduplex formation follow, leading to a so-called Holliday junction intermediate (Holliday 1964, Lilley 1997). A Holliday junction has recently been crystallised (Ortiz-Lombardía *et al.*1999) and found to have an X-stacked structure that needs to undergo a conformational change to allow isomerisation or migration. Branch migration of the junction extends the region of heteroduplex. This is mediated by the RuvABC complex, where two tetramers of RuvA specifically bind the Holliday junction and two hexamers of RuvB act as the "motor" of ATP-dependent branch migration (Parsons and West 1993, Parsons et *al.* 1995, West 1997). Branch migration can also be promoted by RecG, another junction-specific protein and, like RuvB (Tsaneva *et al.* 1993), a DNA-dependent ATPase and helicase (Lloyd and Sharples 1993a). Finally, the junction is processed by the RuvC dimer (Bennett *et al.* 1993, Ariyoshi *et al.* 1994) in the RuvABC complex, a junction-specific endonuclease or resolvase (and maybe by the RusA resolvase in the case of RecG (Mahdi *et al.* 1996)), to release either splice or patch recombinants. Other proteins involved in homologous recombination are DNA gyrase, DNA ligase and DNA polymerase I.

Structural homologues of a number of the *E. coli* recombination proteins have been identified in eukaryotes (e.g. for RecA: Shinohara *et al.* 1993). In *S. cerevisiae*, the *RAD52* epistasis group mediates homologous recombination. Rad51/RAD51 is one of several RecA homologues (Thacker 1999), and there is a large family of RecQ homologues (see below).

1.4 Helicases

1.4.1 Classification

Helicases are enzymes that disrupt the base-pairing of nucleic acids. This activity is coupled to the hydrolysis of nucleoside 5'- triphosphates (NTPs). The functions of helicases are manyfold: DNA helicases are required for DNA replication, recombination and repair (Lohman and Bjornson 1996), whereas RNA helicases participate in RNA splicing, RNA editing, rRNA processing, translation initiation, nuclear mRNA export and mRNA degradation (Lüking *et al.* 1998). The number of helicases reflects their ubiquitous functions: In 1997, there were twelve known helicases in *E. coli*, while 41 putative helicase genes had been identified in *S. cerevisiae* and 31 in humans.

Helicases belong to the large group of NTPases, members of which include the G-proteins, motor proteins (like myosin, kinesin, dynein) and the F_1-ATPase. They are characterised by the so-called "Walker A motif" or phosphate-binding loop and the "Walker B motif", which are necessary for NTP binding (Walker 1982). An invariant K in motif A is implicated in interactions with the β- or γ-phosphate of NTP. Helicases from superfamilies 1 and 2 (described below) usually possess a conserved DExx motif in the Walker B motif. The conserved aspartic acid in this motif is thought to bind a divalent metal ion, whereas the glutamic acid probably activates a water molecule for hydrolysis.

Helicases can be classified by their biochemical properties, e.g. directionality (see below), processivity, substrate preference, pathway involved or interaction with other proteins. The most exhaustive classification attempt to date based on amino acid sequence similarity comes from Gorbalenya and Koonin (1993). According to this scheme, helicases fall into four large superfamilies and two smaller families. Superfamily 1 contains proteins with seven

conserved motifs (I, Ia, II, III, IV, V, VI), including the Walker motifs (I and II). Motif III is implicated as a γ-phosphate sensor that transmits conformational changes to the DNA binding site (Dillingham *et al.* 1999). Recently, an 8th conserved motif has been added (Korolev *et al.* 1998). Furthermore, at least some members contain a TxGx motif implicated in ssDNA binding (Korolev *et al.* 1997). Well-characterised helicases belonging to this superfamily include PcrA from *B. stearothermophilus* as well as the Rep and UvrD proteins from *E. coli.* Helicases from superfamily 2 contain a similar set of seven conserved motifs and the TxGx motif. They include the DEAD-family (containing eIF-4A) and the DEAH-family of RNA helicases, the Snf2-family, the Rad3-family and the RecQ-family. Some of these families contain additional conserved regions outside the seven helicase motifs. A well-characterised member of this superfamily is the RNA helicase of hepatitis C virus (HCV). Superfamily 3 contains mostly viral helicases with only three conserved motifs (including the Walker A and B motifs). One of its well-studied members is SV40 T antigen. Another superfamily, here designated as superfamily 4, contains ATPases of diverse functions and includes RuvB, the branch migration protein from *E. coli.* Six of the seven helicase motifs from superfamily 2 have been identified in RuvB (Mézard *et al.* 1999). Helicases related to DnaB, the replicative helicase in *E. coli*, including the bacteriophage helicases T7gp4 (or T7 gene 4 helicase/primase) and T4gp41, comprise family 4. This family shows a total of five conserved motifs. Family 5 includes the proton-translocating ATPases as well as the *E. coli* transcription termination factor Rho.

1.4.2 Oligomeric state

Most helicases characterised to date are oligomeric, in the majority of cases either dimeric or hexameric. PcrA is unusual in that it is believed to act as a monomer (Velankar *et al.* 1999). Examples of dimeric helicases include *E. coli* Rep, which dimerises upon binding to single-stranded or double-stranded DNA, and *E coli* UvrD, which possibly also forms higher

oligomers. Both are members of superfamily 2. Hexameric helicases include replicative helicases from family 4 (DnaB-like), e.g. *E. coli* DnaB, bacteriophage T7 helicase/primase, bacteriophage T4 gp41; SV40 T antigen (superfamily 3), a viral replicative helicase; *E. coli* transcription-termination protein Rho (family 5); plasmid-encoded RepA; bovine papilloma virus type 1 E1 protein and E. *coli* branch migration protein RuvB (superfamily 4). Many of these have been studied by electron microscopy which revealed their hexameric ring structures (DnaB: San Martín *et al.* 1995, Yu *et al.* 1996b; RuvB: Stasiak *et al.* 1994; E1: Fouts *et al.* 1999; RepA: Scherzinger *et al.* 1997; T7gp4: Egelman *et al.* 1995; SV40 T antigen: Mastrangelo *et al.* 1989, San Martín *et al.* 1997; Rho: Gogol *et al.* 1991). While RuvB is known to encircle double-stranded DNA, single-stranded DNA passes through the hole of T7gp4, and the DNA wraps around the ring of Rho. Fig. 1.1 shows several electron micrographs of T7gp4, averaged images and a model.

1.4.3 Crystal structures of helicases

To date, the crystal structures of four intact helicases have been determined. The first view of a helicase at atomic resolution was that of the monomeric helicase PcrA from *B. stearothermophilus* in the presence of ADP. PcrA consists of two domains (1 and 2), each composed of two subdomains (1A, 1B, 2A, 2B) (Subramanya *et al.* 1996). Subdomains 1A and 2A contain a central parallel β-sheet surrounded by α-helices and are homologous to each other and to the ATP-binding domain of the *E. coli* recombination protein RecA. Subdomain 1B is inserted into 1A, and 2B into 2A; both are primarily α-helical and share no structural homology. The nucleotide-binding pocket is located at the bottom of a cleft between domains 1A and 2A and is formed by several of the motifs conserved among superfamilies 1 and 2.

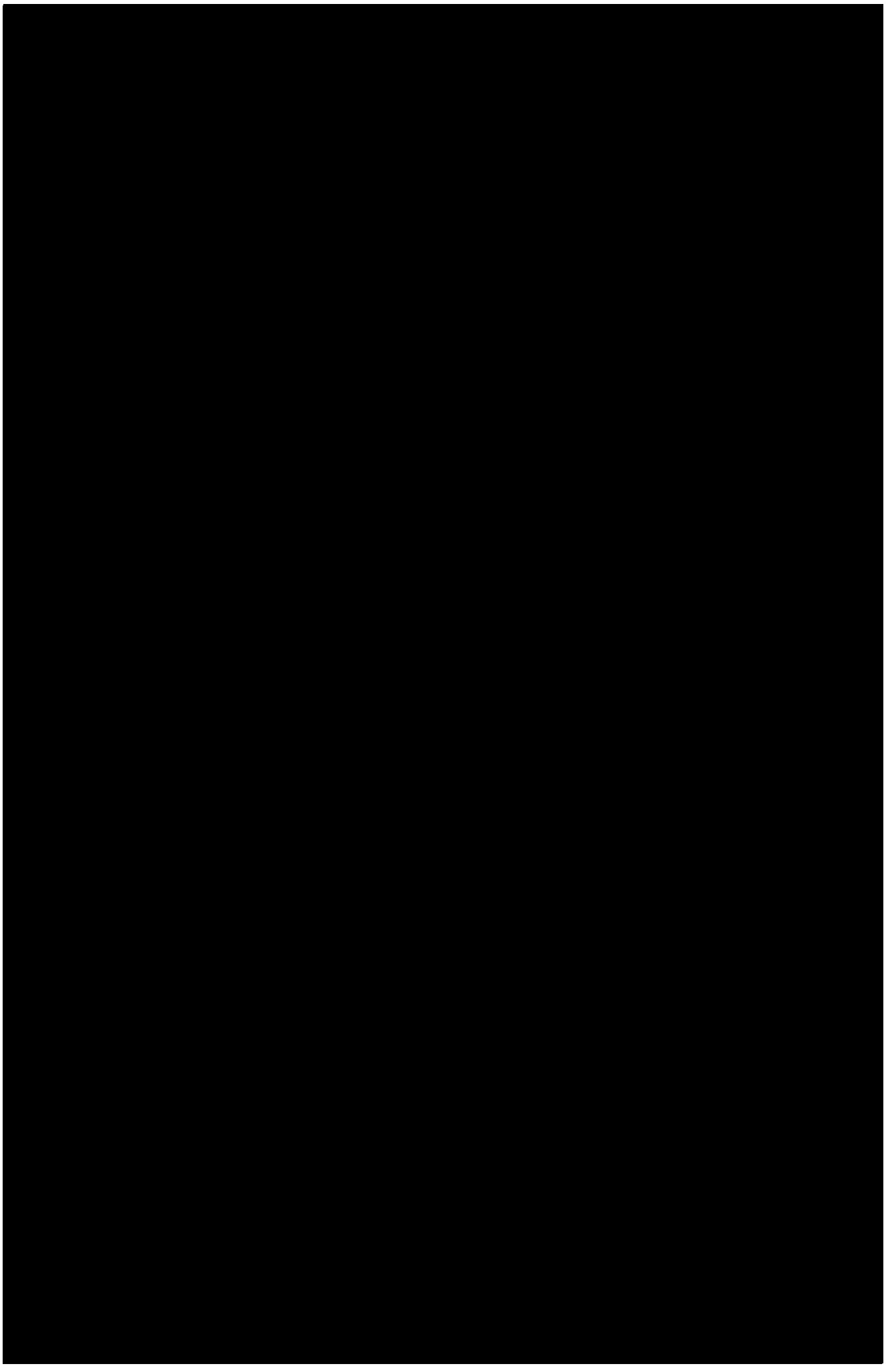


Fig. 1.1. Electron micrographs and model of bacteriophage T7gp4 (helicase/primase).(A) Electron micrographs and averages of (a and b) T7 4A' (helicase and primase) and (d and e) T7 4B (helicase only). Exact sixfold symmetry has been imposed on b and e to generate c and f, respectively. (B) Electron micrograph (a) and average (b) of T7 4A' protein covering M13mp8 ssDNA. (C) Reconstructed T7 4B hexamer. On the right, half of the structure has been removed; the rod indicates the path of ssDNA. (Reproduced from Egelman *et al.* 1995.)

Recently, PcrA was also crystallised in the presence of single-stranded DNA (Velankar *et al.* 1999), revealing two different structures, a "substrate" complex and a "product" complex (Fig. 1.2).

The second helicase crystallised was the C-terminal domain of the NS3 protein of hepatitis C virus (HCV), containing the RNA helicase, a bifunctional protease/RNA helicase (Yao *et al.* 1997). This helicase consists of three domains, two of which are homologous to 1A and 2A of PcrA and to RecA, whereas the third and C-terminal domain is different. Two more crystal structures of NS3 have been reported since (Cho *et al.* 1998, Kim *et al.* 1998), the latter in the presence of RNA.

E. coli Rep helicase was crystallised bound to single-stranded DNA (Korolev *et al.* 1997) and found to have a domain structure similar to that of PcrA. Two conformers, an "open" and a "closed" structure, were found that differed in the position of domain 2B which had undergone a rotation in the "closed" form. This movement of domain 2B might play a role in the translocation of the Rep helicase along DNA. In the "open" Rep structure, parts of domain 1A and 1B form a groove that is part of the ssDNA binding site. Interestingly, although Rep had previously found to be dimeric (dimerisation induced by DNA binding), it appears as a monomer in the crystals, with two monomers binding to each oligonucleotide.

Finally, a C-terminal fragment of the helicase domain of bacteriophage T7 helicase/primase (T7gp4), a hexameric helicase from family 4, was recently crystallised (Sawaya *et al.* 1999). It forms a helical filament resembling that of *E. coli* RecA. When viewed in projection along the helical axis of the crystals, six subunits of the helicase domain resemble hexameric rings. The structure of the T7 helicase domain is similar to that of RecA and the F_1-ATPase, a finding that had been predicted previously (Yu and Egelman 1997). Nucleotides bind

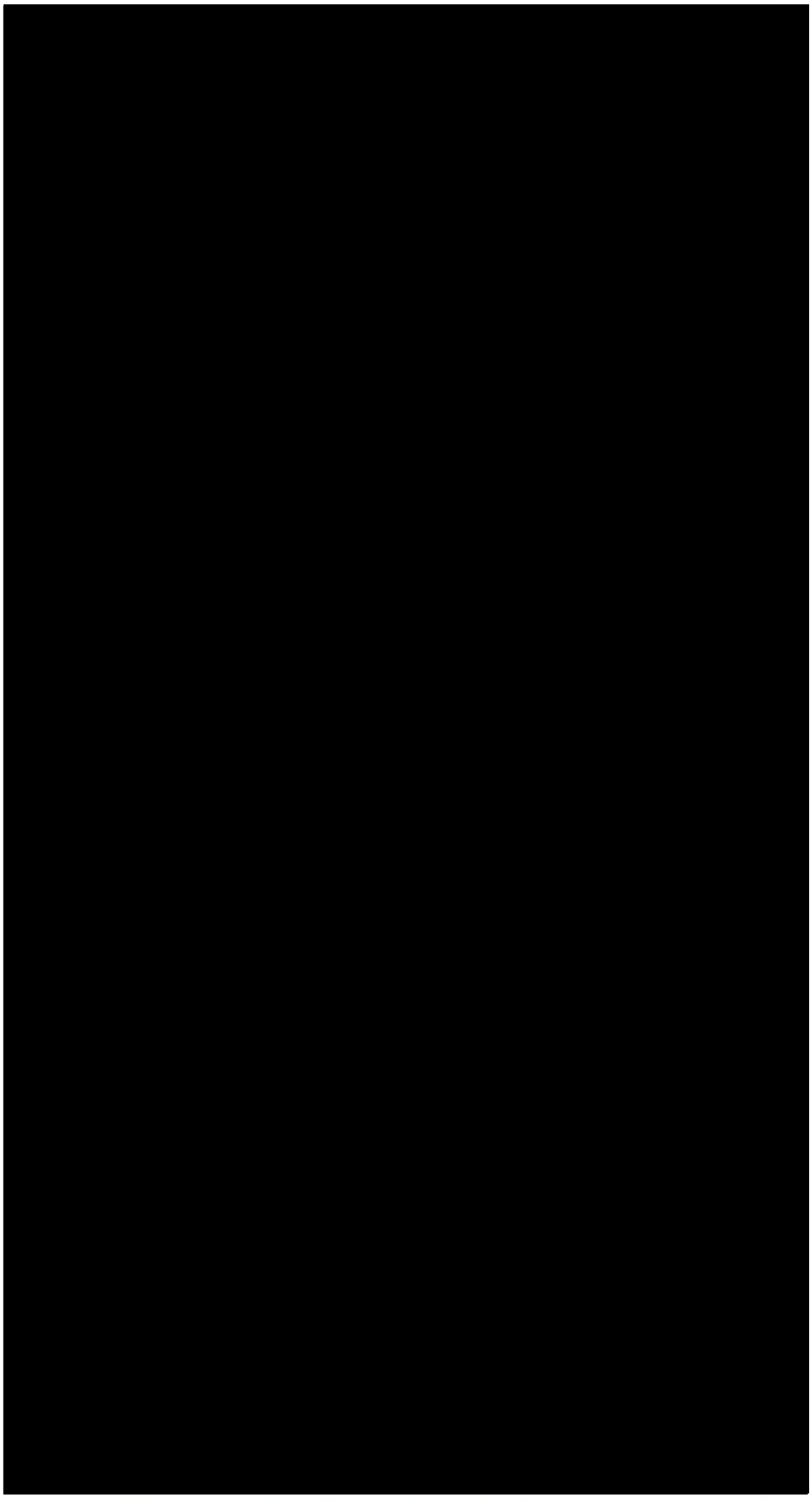


Fig. 1.2. Crystal structure of PcrA helicase in the presence of DNA. Domain structure of (A) the product complex and (B) the substrate complex. Domains 1A, 2A, 1B and 2B are indicated in A and shown in different colours. The DNA is shown in magenta, sulphate (in A) and ADPNP (in B) are shown in yellow. (Reproduced from Velankar *et al.* 1999.)

at the interface between two subunits, similar to the two nucleotide-binding domains in PcrA, Rep and NS3. Residues within helicase motif H4, which are implicated in DNA binding, are located near the centre of the hexamer. The subunit interface consists of two regions, a helix that reaches out to the neighbouring subunit and several loops near the nucleotide binding site. Thus, hydrolysis of NTPs could easily be coupled to a rotation of subunits with respect to each other and could change the DNA binding properties of all subunits.

The unifying theme of these structures seems to be the presence of two RecA-like domains or subdomains. Since superfamilies 1 and 2 contain both helicases with 3'-5' and with 5'-3' polarity, it is conceivable that the orientation of the RecA subdomains within the helicase determines its polarity (Bird *et al.* 1998b).

1.4.4 Polarity

Most DNA helicases start unwinding from a single-strand and display a preference for its backbone polarity in relation to the duplex. This preference defines the polarity or directionality of a helicase as 3'-5' or 5'-3'. The polarity is therefore undefined for helicases that initiate unwinding only from blunt-ended or forked DNA. Experimentally, the directionality of a helicase is usually defined by an unwinding assay using a partially duplex DNA with ssDNA in its centre and double-stranded portions at both ends. The oligonucleotide that is preferentially removed by the helicase defines its polarity.

1.4.5 Models for unwinding

Two main models (described in Fig. 1.3) have been proposed for the unwinding mechanism of helicases: the "inchworm" and the "active rolling" model (reviewed in Bird *et al.* 1998a). The "inchworm" model proposes that a helicase "melts" two DNA strands as it moves along duplex DNA. This model is compatible with a monomeric helicase that can bind single- and double-stranded DNA

at the same time. Interestingly, in the crystal structures, PcrA, HCV NS3 and Rep all appear monomeric (however, it cannot be excluded that this represents an artifact of the crystallisation process). The "active rolling" model, on the other hand, assumes a dimer (or a multiple thereof) with alternating affinities of the two subunits for ss and dsDNA, depending on the binding and hydrolysis of ATP. This dimer "rolls" along the DNA. This model postulates an oligomeric protein in which each subunit can bind either single-stranded or double-stranded DNA but not both simultaneously.

1.4.6 Helicases in human disorders

There are seven recessive human disorders in which helicases are defective (reviewed in Ellis 1997). In Bloom's syndrome, Werner's syndrome and Rothmund-Thomson syndrome, members of the RecQ-family are dysfunctional. These disorders will be discussed in greater detail below. The other disorders, xeroderma pigmentosum, Cockayne's syndrome, trichothiodystrophy (for a recent review of these three, see Bootsma *et al.* 1998) and X-chromosome linked mental retardation syndrome (ATR-X) (reviewed by Gibbons and Higgs 1996) will be briefly described here.

1.4.6.1 Xeroderma pigmentosum

Xeroderma pigmentosum (XP) is characterised by skin abnormalities and photosensitivity, cataracts, a greatly increased risk of skin cancer and, in some cases, neurological abnormalities. Cells from XP patients are hypersensitive to UV light, they show an increased mutation rate post-irradiation and decreased repair of pyrimidine dimers. Genes acting in the nucleotide excision repair (NER) pathway (Sancar *et al.* 1996), the major pathway for the repair of bulky DNA adducts and lesions caused by UV-irradiation, are mutated in XP and fall into seven complementation groups. Two of these genes, *XPB (ERCC3)* and *XPD* (*ERCC2*), encode helicases (Weber *et al.* 1990, Weeda *et al.* 1990, Ma *et al.* 1994, Sung *et al.* 1993). Both are



Fig. 1.3. Models for helicase unwinding.
The two most widely used models for unwinding of DNA by helicases are shown. The *active rolling model* (upper half) postulates the presence of at least two subunits (or a multiple thereof), coloured in red and yellow. The relative affinity of these subunits for single- or double-stranded DNA is modulated by the nucleotide (NTP, NDP or none) bound to them. Thus, each subunit successively binds no DNA/dsDNA/ssDNA, "rolling" along the DNA. The *inchworm model* (lower half) requires the presence of at least one subunit (shown in red) which possesses two DNA binding sites. Thus, it is capable of binding to single- and double-stranded DNA simultaneously. The affinity of the binding sites for DNA changes depending on the nucleotide bound to the protein. Thus, the protein successively binds ssDNA and no DNA/ss and ds DNA/ssDNA. (Reproduced from Velankar *et al.* 1999.)

part of TFIIH, a six-protein complex with a dual role: As part of NER, it unwinds DNA at a site of a lesion prior to excision of the damaged strand. Furthermore it is involved in the initiation of transcription, unwinding DNA to permit RNA polymerase II access (Schaeffer *et al.* 1993, Feaver *et al.* 1993, Friedberg 1996).

1.4.6.2 Cockayne's syndrome

The dual role of TFIIH mentioned above may explain why certain kinds of mutations in *XPB* or *XPD,* affecting both functions of the protein, lead to a combined phenotype of XP and another disorder, Cockayne's syndrome (CS) (Cooper *et al.* 1997). CS individuals are growth deficient, photosensitive, show skeletal abnormalities, cataracts and mental degeneration. Their cells are hypersensitive to UV light, and repair of DNA lesions of the transcribed strand is reduced. The developmental abnormalities found in CS probably result from a defect in transcription; however, they might be caused by a defect in the repair of oxidative damage. The reduced repair of the transcribed DNA strand points to a problem in transcription-coupled repair, suggesting that TFIIH has a function in this process. Besides *XPB* and *XPD*, three other genes can be affected in CS, one of which, *CSB/ERCC6*, belongs to the SWI2/SNF2 family of helicases (Troelstra *et al.* 1992, Selby and Sancar 1997). Although it possesses the seven helicase motifs of superfamily 2, CSB has failed to show DNA unwinding activity (Selby and Sancar 1997). It interacts with various components of the NER machinery and has DNA-stimulated ATPase activity. In yeast, SWI2/SNF2 is part of the SWI/SNF complex, which is involved in transcriptional activation. Presumably, it makes the DNA accessible for transcription by displacing histones from the promoter regions of genes (Owen-Hughes *et al.* 1996).

1.4.6.3 Trichothiodystrophy

A further syndrome resulting from certain mutations in *XPB* or *XPD* is trichothiodystrophy (TTD) (Weeda *et al.* 1997, Broughton *et al.* 1994, Takayama *et al.* 1996). This disorder is

characterised by sulphur-deficient brittle hair, growth deficiency, mental retardation, subfertility and photosensitivity in some cases. Cells from TTP patients show increased UV light sensitivity and decreased repair of pyrimidine dimers. Since TTP shares some symptoms with CS, it is likely that the transcriptional functions of the two helicases are impaired in this syndrome. Notably, only XP, not CS or TTP, shows an increase in cancer. One other gene, *TTPA*, can be mutated in trichothiodystrophy.

1.4.6.4 X-chromosome linked mental retardation syndrome (ATR-X)

ATR-X is caused by mutations in another SWI2/SNF2-like gene, *ATRX* (also *XNP*, *XH2, RAD54L*) (Gibbons *et al.* 1995, Gibbons and Higgs 1996, Picketts *et al.* 1996). This disorder is characterised by α-thalassemia, developmental delay, severe mental retardation and genital abnormalities. The gene product of *ATR-X* is possibly also involved in transcriptional regulation, as a component of the SWI/SNF complex.

1.5 The RecQ family of helicases

1.5.1 Overview

This rapidly expanding family of helicases belongs to superfamily 2 and was named after its *E. coli* member RecQ. It is highly conserved across species, with members identified in bacteria (*E. coli, H. influenzae, B. subtilis*), fungi (*S. cerevisiae, S. pombe, U. maydis*), plants (*A. thaliana*), animals (invertebrates: *D. melanogaster, C. elegans*; vertebrates: *X. laevis, M. musculus*) and humans. To date, there are five known members in humans, four in *C. elegans* and two in *D. melanogaster*. Unicellular organisms seem to possess fewer RecQ helicases than do multicelluar ones: only one member is known in *E. coli*, *S. cerevisiae* and *S. pombe*. This

suggests there has been a diversification of function in evolution. Interestingly, three of the human members are associated with genetic disorders: BLM with Bloom's syndrome, WRN with Werner's syndrome and RECQL4 with some cases of Rothmund-Thomson syndrome. A selection of RecQ family members is shown in Fig. 1.4.

All family members share a central helicase "domain" composed of approximately 360 - 400 amino acids, which contains the seven conserved motifs of superfamily 2, including a DExH box in motif II. A sequence alignment of this region from several RecQ family members is shown in Fig. 1.5. Similarity between RecQ members is largely restricted to this region. Directly C-terminal to this and sometimes regarded part of the "helicase domain" is a region of extended homology called RecQ-Ct or RQC which is unique to this family and not present in other DExH helicases (Morozov *et al.* 1997). This region seems to be present in almost all members characterised (with the notable exception of RECQL4), despite a previously published claim that only the large RecQ members possess it (Stewart *et al.* 1997). It contains a number of cysteine residues and resembles a zinc finger DNA binding domain. Members of a subclass of RecQ which include the eukaryotic members except for WRN share additional cysteines and other conserved residues in this region (Bahr *et al.* 1998). Several RecQ members possess an HRDC (Helicase and Rnase D C-terminal) domain in their C-terminal half. This domain contains a number of conserved bulky hydrophobic residues. Since it is conserved in some helicases and in RnaseD, all being proteins that bind to RNA or DNA, it might have a role in nucleic acid binding. To date, five RecQ members have been purified and studied in terms of their enzymatic activities *in vitro*. Results from these studies are summarised in Table 1.1.

Depending on whether or not they contain extensive additional N- and C-terminal regions, RecQ helicases can be divided into two classes. One class contains members of 1050-1500 amino acid length with extended, highly charged N- and C-terminal regions, the function(s) of which are only beginning to be defined now. This class includes BLM, WRN and

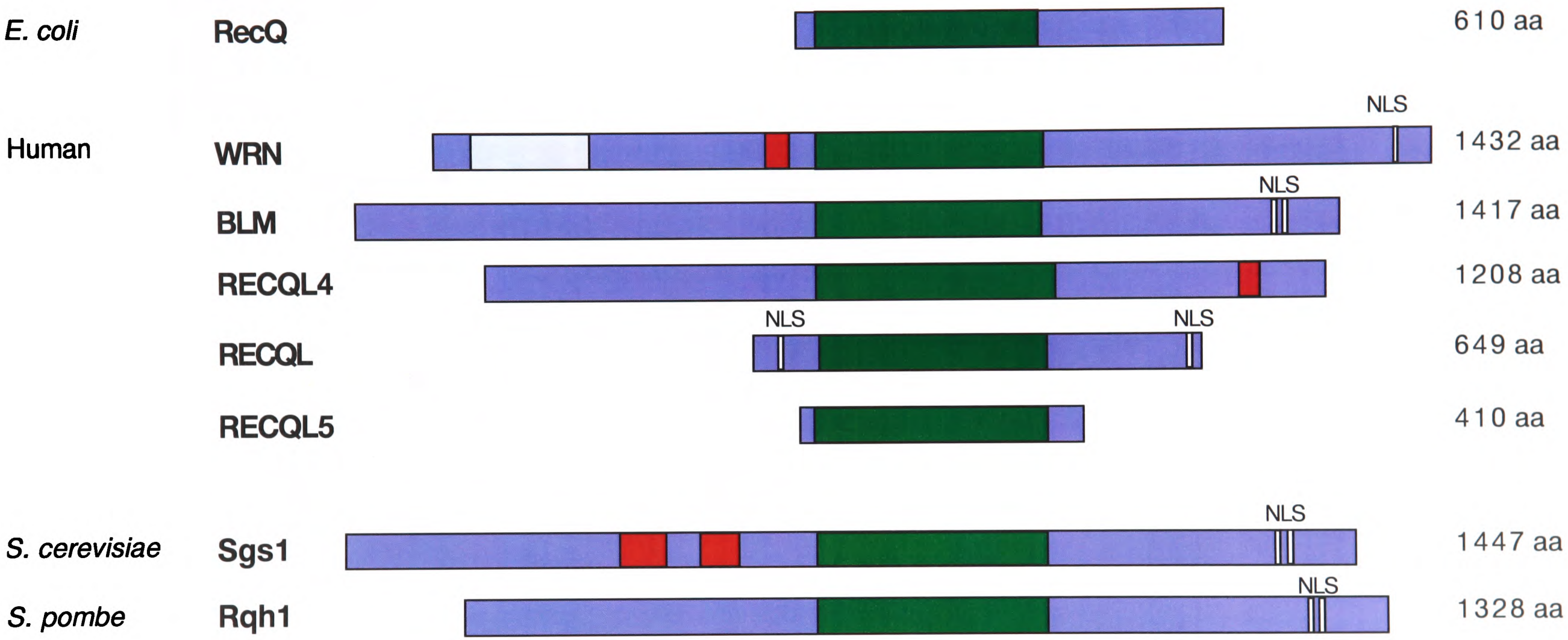


Fig. 1.4. Schematic representation of RecQ family members. Species and protein names are indicated on the left. The conserved central helicase domains (including the regions of extended homology where appropriate) are shown as green boxes. The light blue box in WRN marks the exonuclease domain. The red boxes represent acidic patches, and nuclear localisation signal sequences (NLS) are indicated. (HRDC domains are not shown). The size of each protein is shown on the right.

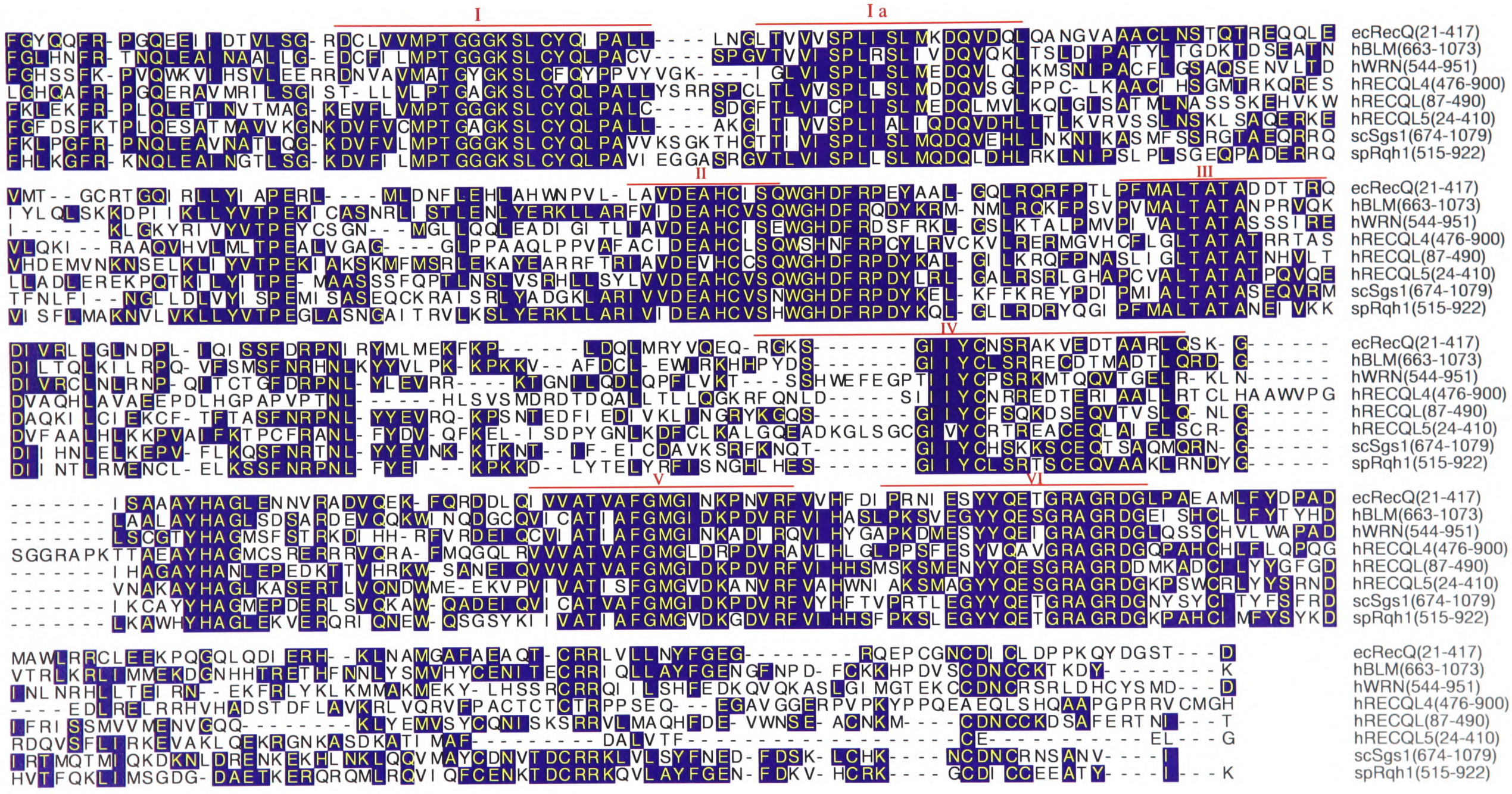


Fig. 1.5. Sequence alignment of RecQ family members.
The alignment was performed using the CLUSTAL V method (Higgins and Sharp 1989). The helicase "domains" and the regions of extended homology (RecQ-Ct) are shown. Identical residues are coloured in blue, the seven conserved helicase motifs are indicated in red. Protein names and residue numbers are shown on the right. Ec = *E. coli*, h = human, sc = *S. cerevisiae*, Sp = *S. pombe*.

Table 1. Properties of purified RecQ helicases

	RecQ	WRN	BLM	Sgs1	RECQL
Associated disorders	n.a.	Werner's syndrome	Bloom's syndrome	n.a.	unknown.
No. of amino acids	610	1,432	1,417	1,447	659
Directionality of unwinding	3'-5'	3'-5'	3'-5'	3'-5'	3'-5'
Helicase substrates[a]	• 3'- and 5'-overhangs • fork • blunt-ended • 3- and 4-way junctions • covalently-closed plasmid	• 3'-overhang • DNA/RNA hybrid • G4-DNA from fragile X syndrome repeat sequence • 4-way junctions[b]	• 3'-overhang • fork • bubbles[c] • various G4-DNAs • 3[b]- and 4[c]-way junctions	• 3'-overhang • fork • DNA/RNA hybrid • 3- and 4-way junctions • various G4-DNAs	• none reported
Genetic interactions	RecF pathway	unknown	unknown	topoisomerases I and III	unknown
Physical interactions	unknown	RPA, p53	topoisomerase IIIα[b] RAD51[b] RPA[b]	topoisomerases II and III	Qip1, Rch1 (importin-alpha homologues)

[a] in addition to standard substrates (oligonucleotide annealed to single-stranded circle, or short oligonucleotides annealed to each end of linear single-stranded DNA)

[b] our unpublished data

[c] see chapter 5 of this thesis

RECQL4 from humans, BLM from *D. melanogaster*, three *C. elegans* homologues, Sgs1 from *S. cerevisiae* and Rqh1 from *S. pombe*. The second class contains proteins of 400-800 amino acid total length, consisting of little more than the core helicase domain, and includes RecQ from bacteria, human RECQL and RECQL5, and one *C. elegans* homologue. However, this distinction is not as strict as previously assumed, since a *Drosophila* homologue of RECQL5 was recently found to have three isoforms, two of 54 kDa and one of 121 kDa (Sekelsky *et al.* 1999). Furthermore, this classification by size does not necessarily reflect evolutionary relationships: A recent analysis showed that RECQL, which only possesses a short N-terminal segment, is more closely related in this area to *C. elegans* K02F3.1, which has a long N-terminal region, than to the short bacterial RecQ proteins (Kusano *et al.* 1999). According to this study, the two yeast homologues, Sgs1 and Rqh1, are more closely related to BLM than to WRN, a finding that may be relevant for the use of yeast as a model system for BS or WS.

1.5.2 RecQ

The *recQ* gene locus was first identified as a mutant from a screen for increased resistance to thymineless death (TLD) in *E. coli* (Nakayama *et al.* 1984). Knowing that mutants of *recF*, a gene in the RecF pathway of recombination in *E. coli*, were also TLD-resistant, the authors transferred the *recQ* mutation into a *recBC sbcB* background. In this strain, the RecBCD pathway, the major pathway of conjugational recombination in *E. coli*, is defective and the RecF pathway is somehow activated by a mutation in exonuclease I. Similar to *recF*, the *recQ* mutation in this background results in increased sensitivity to UV light and deficient conjugational recombination. However, contrary to *recF*, there is no increase in UV sensitivity of *recQ* in a wild-type background. Furthermore, mutations in *recQ* lead to an increase in

illegitimate recombination, measured by the frequency of formation of two transducing phages in *E. coli*, which is independent of the RecBCD, RecF or RecE recombination pathway (Hanada *et al.*1997).

The *recQ* gene was subsequently cloned (Nakayama *et al.* 1985, Irino *et al.* 1986); it encodes a protein of 610 amino acids (approximately 67 kDa) with a conserved helicase and RecQ-Ct region (amino acids 23-417). The protein was overexpressed and purified from *E. coli* (Umezu *et al.* 1990) and shown to possess DNA-dependent ATPase activity and DNA unwinding activity with 3'-5' polarity. In an ATPase assay, Mn^{2+} and Ca^{2+} can almost fully, and Zn^{2+} can partially substitute Mg^{2+}. Furthermore, dATP, but not GTP, can replace ATP. The enzyme is able to unwind a 71mer and a 143mer annealed to single-stranded M13 phage and, at high concentrations, a 143 nt duplex blunt-ended substrate as well as a substrate designating 5'-3' polarity. A later study showed that RecQ is markedly stimulated by *E. coli* single-strand binding protein (SSB) and by bacteriophage T4 single-strand binding protein gp32 (Umezu *et al.* 1993). Furthermore, RecQ was found to initiate homologous pairing *in vitro* in the presence of RecA and SSB, forming joint molecules (Harmon and Kowalczykowski 1998). However, this activity can probably be completely attributed to its ability to unwind blunt-ended DNA. Also, RecQ is able to dissociate joint molecules formed in its absence. Its substrate specificity seems to be weak, since it binds and unwinds a variety of synthetic short substrates with less than tenfold difference, including a 4-way junction (Holliday junction), a 3-way junction, a fork, a 3'-tailed substrate, a 5'-tailed substrate and a 63 nt blunt-ended substrate. Only a 48 nt blunt-ended substrate is not efficiently unwound (Harmon and Kowalczykowski 1998). Recently, RecQ in combination with *E. coli* or yeast topoisomerase III was found to possess a strand passage activity (Harmon *et al.* 1999). Initially, the authors found that RecQ is able to unwind covalently closed double-stranded DNA molecules. This activity specifically stimulates topoisomerase III to fully catenate these substrates. Neither another helicase with a similar

activity (UvrD) nor single-stranded regions in one of the substrates are able to yield the same results, suggesting a specific functional interaction between RecQ and topoisomerase III. However, a physical interaction between the two enzymes has not been shown. A different activity of RecQ was recently reported by Courcelle and Hanawalt (1999): Following UV-induced damage, RecQ and RecJ process the nascent lagging strand at blocked replication forks prior to the resumption of DNA synthesis.

1.5.3 RECQL

RECQL ("RecQ-like") was first purified as one of five DNA-dependent ATPase activities in HeLa cells and was designated helicase Q1 (Seki *et al.* 1994). Intriguingly, its elution profile is altered in XP-C deficient cells although purified RECQL does not complement the repair defect of these cells. The purified protein has a molecular mass of 73 kDa and DNA-dependent ATPase activity with a preference for ATP or dATP and single-stranded DNA as the cofactor. Furthermore it is active as a helicase, unwinding a short oligonucleotide annealed to single-stranded M13. Both activities are insensitive to up to 200 mM NaCl. In a second, independent purification, RECQL coeluted with a factor (TCF) that forms a ternary complex with the *c-fos* promoter serum response element (SRE) and the serum response factor (SRF), although it is not identical with the TCF (Puranam and Blackshear 1994). The RECQL gene was independently cloned by two laboratories and found to encode a protein of 649 amino acids (Seki *et al.* 1994) and 659 amino acids (Puranam and Blackshear 1994), differing in the last 45 and 35 amino acids, respectively. The helicase and RecQ-Ct region stretches from amino acids 87-490. Both groups located the gene to chromosome 12p12. Furthermore, Blackshear's group showed by immunofluorescence that RECQL is located in the nucleus where it gives a speckled appearance and shows some filaments that seem to outline the nucleolus. This is in accordance with the N-terminal nuclear localisation signal sequence (NLS) of the protein (KKIK; amino acids 44-47). A further putative NLS was found near the C-terminus (amino acids 642-645) (Matsumoto *et al.* 1998). RECQL

mRNA is most abundant in lung, kidney, heart and skeletal muscle and almost absent in brain. More recently, RECQL was found to interact with Qip1 and Rch1, both homologues of the NLS-receptor importin-alpha (Seki *et al.*1997). A mouse homologue of RECQL was located to chromosome 6 (Puranam *et al.* 1995). Two isoforms of a mouse homologue of RECQL were recently cloned, one of which (Q1alpha) is expressed in all tissues examined and carries the same N-terminal NLS as human RECQL, the other of which lacks this sequence and is exclusively expressed in testis (Wang *et al.* 1998).

1.5.4 BLM

The gene mutated in BS was first assigned to chromosome 15 (McDaniel and Schultz 1992) and was subsequently regionally mapped to band 15q26 (German *et al.* 1994). It was finally cloned in 1995 by a novel approach called somatic crossover point mapping (SCP) (Ellis *et al.* 1995). This relied on a curious observation: A subpopulation of blood lymphocytes from some BS patients shows a low sister chromatid (SCE) exchange rate, in contrast to the majority of lymphocytes which display the characteristically high rate (see 1.6.1). In some cell lines derived from these low SCE cells, polymorphic loci distal to *BLM* had become homozygous, whereas polymorphic loci proximal to *BLM* had remained heterozygous. This suggested that a wild-type *BLM* had been recreated through recombination between a paternally and a maternally inherited *BLM* allele mutated at different sites. By comparing polymorphic loci in cells with high SCEs and with low SCEs from a single patient (SCP mapping), *BLM* was localised to a 250 kb region. Further screening of cDNA libraries led to the discovery of *BLM*.

The gene encodes a protein of 1417 amino acids with a predicted molecular mass of 159 kDa. The central helicase "domain", including the RecQ-Ct region of extended homology, runs from amino acids 649-1073. The N- and C-terminal regions of the protein are rich in acidic, basic and polar amino acids and in serine. Both these regions contain a binding site for

hTOPOIIIα, with the N-terminal binding site residing within amino acids 1-212 and the C-terminal site within amino acids 966-1417 (Wu *et al.* 2000). A bipartite nuclear localisation signal (NLS) was discovered in the C-terminus (RKRKK, amino acids 1334-1338 and RSKRRK, amino acids 1344-1349), the more C-terminal of which is sufficient to target BLM to the nucleus (Kaneko *et al.* 1997). Recently, an N-terminal fragment of BLM (amino acids 1-431) was found to form hexamers and dodecamers, suggesting that it contains an oligomerisation region (Beresten *et al.* 1999). This is in accordance with our own results that BLM forms oligomeric rings (Karow *et al.* 1999 and chapter 4 of this thesis).

The gene is expressed in a variety of tissues and haematopoietic cell lines, including placenta, spleen, small intestine, B-, T-, myelomonocytic and megakaryocytic cell lines, but especially in thymus and testis (Kitao *et al.* 1998; Kaneko *et al.* 1999). This is also true for murine *BLM*, which is most highly expressed in spleen, thymus, ovary and testis, but also in lung and cerebrum (Chester *et al.* 1998).

BLM was found by us to possess DNA-dependent ATPase activity and helicase activity with 3'-5' polarity (Karow *et al.* 1997 and chapter 3 of this thesis). This result was confirmed by Neff (Neff *et al.* 1999) who also discovered that BLM, when introduced into a BS cell line lacking the *BLM* gene, reduces the frequency of SCEs. Similar results were obtained by Ellis and colleagues (Ellis *et al.* 1999). Furthermore, we found that BLM very efficiently unwinds G4-DNA (Sun *et al.* 1998 and chapter 5 of this thesis).

In the cell, BLM is found in both small foci and in diffuse patches in the nucleus and is absent in a BS cell line (Neff *et al.* 1999). Moreover, it colocalises with PML, a protein that acts as a growth and tumour suppressor, to so-called PML nuclear bodies. Interestingly, BLM is delocalised in PML-/- cells which, like BS cells, show increased levels of sister chromatid

exchanges (Zhong *et al.* 1999). In mouse spermatocytes, BLM colocalises with replication protein A (RPA), forming discrete foci along the synaptonemal complexes of homologously paired chromosomes in late zygoneme of meiotic prophase (Walpita *et al.* 1999). *BLM*, when expressed in budding yeast, suppresses the increased homologous and illegitimate recombination in an *sgs1* mutant (*SGS1* being the only homologue in budding yeast) and reduces its increased sensitivity to hydroxyurea. Moreover, it restores the slow growth phenotype of a *top3* mutant when expressed in a *top3sgs1* double mutant (Yamagata *et al.* 1998).

65 mutations have been identified in the *BLM* gene of 137 BS individuals (James German, personal communication) of which sixteen have been published so far (German and Ellis 1998; Foucault *et al.* 1997). They include five missense mutations (Q672R, I843T, C901Y, C1055S and C1036P), six nonsense mutations (S186X, K272X, R364X, S595X, Q645X, Q700X), two frameshift mutations (514-1-X and 735-4-X) and three exon-skipping mutations (exon 2 skipped, exon 6 skipped, exons 11 and 12 skipped). The 735-4-X frameshift mutation occurs in all BS individuals with Ashkenazi Jewish background and results from a deletion of ATCTGA and insertion of TAGATTC at nt 2281. It represents a founder effect since this mutation is found at a highly elevated frequency in the Ashkenazi Jewish population (Li *et al.* 1998). The three exon-skipping mutations result in a small out-of-frame peptide, a protein truncated around amino acid 370 and a protein truncated near amino acid 770. Thus, the majority of mutations lead to a truncation of the protein and a product lacking the full set of seven helicase motifs (residing within amino acids 649-987). Therefore, these truncated proteins probably do not have helicase activity. Proteins carrying two of the missense mutations, Q672R and C1055S, were expressed in BS cells and fail to reduce the sister chromatid exchanges; they also lack helicase displacement activity (Neff *et al.* 1999). Moreover, three of the missense mutations (Q672R, I843T and C1055S) were introduced at the equivalent positions of the mouse homologue of *BLM* (accidentally, not the original Q672R but a Q672P mutation was

introduced), and the resulting proteins have no ATPase or helicase activity (Bahr *et al.* 1998). Missense mutations C1055S and C1036P change cysteines in the putative DNA-binding domain and might therefore affect DNA binding. Also, the level of topoisomerase IIα was reduced in a patient with mutation C1036P, suggesting that BLM might transcriptionally regulate topoisomerase IIα (Foucault *et al.* 1997). Intriguingly, no mutations of the coding sequence of BLM could be found in a number of patients (J. German, personal communication). Furthermore, one allele in a BS patient was found to be wild type but was not expressed (Foucault *et al.*1997). Thus, there might exist yet unidentified mutations in the promoter area of the *BLM* gene, or in other genes that affect the expression of *BLM* or encode proteins that interact with BLM. Alternatively, these examples could represent cases of misdiagnosis of BS.

A mouse homologue of human BLM was cloned by two groups (Seki *et al.* 1998; Bahr *et al.* 1998). One of them identified it by virtue of its ability to interact with the ATFa transcription factor and found it to encode a protein of 1426 residues with 78% overall identity to human BLM (Bahr *et al.* 1998). Mouse embryos homozygous for a targeted deletion of the *BLM* gene (upstream of the helicase region) are developmentally retarded and die by day 13.5 *in utero* with severe anaemia (Chester *et al.* 1998). The growth retardation can be explained by a wave of increased apoptosis in the epiblast in early embryogenesis. Erythrocytes and their precursors in the embryos are abnormal in shape and show micronuclei. BLM-/- fibroblasts show high levels of SCEs. However, heterozygous mice appear normal at least during the first year of life.

1.5.5 WRN

WRN, the gene mutated in Werner's syndrome, was identified by positional cloning (Yu *et al.* 1996a). It is expressed in all tissues tested, especially in pancreas, placenta, muscle and heart.

WRN encodes a protein of 1432 amino acids (168 kDa) with a "helicase domain"and RecQ-Ct area at amino acids 544-951. In its N-terminal region, it possesses a duplication of 27 amino acids (424-477) and an acidic patch consisting mainly of D and E residues (amino acids 507-526). This region has recently been shown to act as a transcriptional activator (Balajee *et al.* 1999). Furthermore, there is a nuclease "domain" within amino acids 80-231 that is homologous to bacterial RNase D and to a 3'-5' proofreading exonuclease domain of bacterial DNA polymerase I (two conserved residues are present at position 82 and 84). The C-terminal region contains an HRDC domain at amino acids 1150-1229. WRN possesses a nuclear localization signal in its C-terminal region (amino acids 1370-1375) (Suzuki *et al.* 1997; Matsumoto *et al.* 1998). Two studies report that WRN is located in the nucleolus (Marciniak *et al.* 1998, Gray *et al.* 1998), however, two other reports claim a wider distribution in the nucleoplasm (Shiratori *et al.* 1999, Balajee *et al.* 1999). A more recent publication from one of the latter groups shows that WRN is located in both the nucleoplasm and the nucleoli (Kitao *et al.* 1999a). In one study, serum starvation or exposure to the genotoxin 4NQO reduces nucleolar WRN, possibly causing it to translocate from the nucleolus to the nucleoplasm (Gray *et al.* 1998). This effect can be blocked by sodium orthovanadate (Na_3VO_4), a thyrosine phosphatase inhibitor, suggesting that WRN localisation is regulated by its phosphorylation state.

WRN has been overexpressed and purified from baculovirus (Suzuki *et al.* 1997; Shen *et al.* 1998b; Gray *et al.* 1997; Orren *et al.* 1999). It has DNA-dependent ATPase activity with a preliminary hydrolysis rate of 6.7 μmol ATP/μg protein/ min (equivalent to a k_{cat} of approximately 1,000,000 min^{-1}) according to one study (Suzuki *et al.* 1997) and a k_{cat} of 50-200 min^{-1} according to two others (Brosh *et al.* 1999, Orren *et al.* 1999). Its affinity for single-stranded DNA is higher than for double-stranded DNA, and it does not show increased affinity for several types of damaged DNA (Orren *et al.* 1999). Furthermore it has helicase unwinding activity, displacing a 20mer annealed to a 46mer, and a 24mer, a tailed and untailed 40mer and

an 18mer RNA annealed to ssM13. This helicase activity has 3'-5' polarity and can be sustained by ATP, dATP, CTP and dCTP but only weakly by GTP, dGTP, UTP or TTP. Strand displacement by WRN is stimulated by single-strand binding proteins (SSBs) from several species, including *E. coli* SSB, T4 gp32 and human RPA, with RPA being the most efficient stimulator. More recently, a direct interaction between WRN and RPA has been reported, and WRN is able to unwind substrates up to 849 bp in length in the presence of RPA but not of the other single-strand binding proteins (Brosh *et al.* 1999). Interestingly, helicase activity is retained in a mutant carrying a truncation from nucleotides 3370-3464, a mutation commonly found in Japanese patients with WS. Like BLM, WRN shows some preference for unwinding G4-DNA. While it has been reported that this activity is restricted to tailed G4-DNA substrates based on a trinucleotide repeat sequence (Fry and Loeb 1999), I found that WRN also dissociated G4-DNA based on a telomeric sequence and an IgG switch region sequence (data not shown).

Several laboratories found the N-terminal region of WRN to possess exonuclease activity that can be separated from its helicase activity. An N-terminal domain of WRN (amino acids 1-333 or amino acids 1-368) retains exonuclease activity on a partially duplex substrate (Huang *et al.* 1998, Shen *et al.* 1998a). It hydrolyses the recessed strand of the substrate, is stimulated by ATP and does not act upon single-stranded DNA, a blunt-ended duplex or a protruding strand (Kamath-Loeb *et al.* 1998). Two groups determined its directionality to be 3'-5' (Huang *et al.* 1998, Kamath Loeb *et al.* 1998). However, Suzuki and colleagues found the directionality to be 5'-3' (Suzuki *et al.* 1999). They reported that the exonuclease activity acts on DNA duplexes and DNA/RNA heteroduplexes and is dependent on active unwinding by the WRN helicase.

A mouse homologue of the *WRN* gene has been cloned and found to encode a protein of 1401 amino acids (157 kDa) highly homologous to human WRN (Imamura *et al.*1997). One of the main differences between the two is the absence of the repeat of the 27 amino acid acidic region in the N-terminal part of human WRN in the mouse homologue. Furthermore, unlike its human counterpart, mouse WRN does not localise to the nucleolus but shows diffuse nuclear staining (Marciniak *et al.* 1998). A mouse deficient in active WRN (lacking helicase motifs III and IV) has been created and appears normal during the first year of life (Lebel and Leder, 1998). ES cells are not hypersensitive to a variety of DNA damaging agents but may display a somewhat higher mutation rate and marginally increased sensitivity to topoisomerase inhibitors. Furthermore, fibroblasts from WS mouse embryos show reduced proliferation. Copurification studies from the same report suggest WRN may interact with a replication complex. This is interesting, because a WRN homologue, called focus-forming activity 1 (FFA-1), has been discovered in *X. laevis* egg extracts that shows helicase activity and is required for the formation of replication foci (Yan *et al.* 1998). A role for WRN in recombination was suggested by a study showing that WRN can suppress the increase in illegitimate recombination of an *sgs1* mutant (Yamagata *et al.* 1998). Spillare and colleagues have reported an interaction between WRN and p53 (Spillare *et al.* 1999). WRN binds to the carboxyl terminal part of p53, and the amount of p53-mediated apoptosis in WS fibroblasts is reduced. The latter effect can be reverted when wild type WRN is expressed in these cells. Blander *et al* (1999) also reported an interaction between the carboxy terminal half of WRN and a small part of p53 near its C-terminus. Overexpression of WRN increases the amount of p53-dependent transcription. Interestingly, p53 also seems to downregulate the expression of WRN (Yamabe *et al.* 1998).

Some studies suggest WRN has a role in transcription. WRN, when fused to the Gal4 DNA binding domain, can activate a reporter gene bearing the *GAL1* promoter in a yeast assay system, and critical residues for this activity reside within amino acids 315-403 and, in

combination with these, in amino acids 404-1041 (Ye *et al.* 1998). Transcription in several WS cell lines is reduced to 40-60 % of that observed in normal individuals and can be complemented by the addition of normal cell extracts to chromatin from WS cells. Markedly, this transcriptional defect of WS cells does not affect RNA polI transcription. Purified WRN, but not mutant WRN lacking either helicase function or the 27 amino acid N-terminal direct repeat (residues 424-477), is able to stimulate RNA polII transcription in an *in vitro* assay. Finally, in a one-hybrid-study, both wild type WRN and the 27 amino acid repeat by itself were strong activators of transcription (Balajee *et al.* 1999).

Nineteen different WRN mutations have been described so far (Moser *et al.* 1999). They all lead to a truncation of the protein at various points. More than 50 % (10) of them map in the C-terminal half of WRN, beyond the helicase and RecQ conserved region. Strikingly, unlike in Bloom's syndrome, missense mutations are absent. In some Japanese patients, only one or no *WRN* allele was found to be mutated; this could point to a misdiagnosis, a sequencing error or a mutation affecting the promoter region of WRN, or a yet unidentified gene, the product of which either regulates WRN expression or interacts with the WRN protein.

1.5.6 RECQL4

The *RecQ4/RECQL4* gene (hereafter called *RECQL4*) is one of the most recent additions to the RecQ-family of helicases. It was cloned in 1998, based on an EST sequence, and encodes a protein of 1208 amino acids (133 kDa predicted molecular mass) (Kitao *et al.* 1998). Besides the conserved helicase "domain" (amino acids 475 – 825), the protein contains an acidic region in the C-terminal half. Interestingly, it lacks the RecQ-Ct region of extended homology. The *RECQL4* gene was mapped to chromosome 8q24.3. Northern blot analysis showed that it is expressed in a variety of tissues, especially in testis and thymus. Recently, RECQL4 was found to be mutated in four cases of Rothmund-Thomson syndrome (RTS) (Kitao *et al.* 1999b,

Lindor *et al.* 1999). The mutations found result in truncations yielding proteins of 550, 686, 756 and 830 amino acid lengths. Except for the last one of these, none of predicted proteins contains a full set of helicase motifs. In two RTS patients with mutated RECQL4 genes, the transcripts are specifically downregulated. However, no mutations in RECQL4 were found in four other patients, suggesting either a misdiagnosis, or a mutation in the promoter region or in a different gene. The protein is located in the nucleus (Kitao *et al.* 1999a). Recently, a mouse homologue of RECQL4 has been identified (Kitao *et al.* 1999a).

1.5.7 Sgs 1

SGS1 ("slow growth suppressor") was first discovered as a mutation suppressing the growth defect and hyperrecombination in rDNA of *top3* mutants in *S. cerevisiae* (Gangloff *et al.* 1994). In the same publication, the authors report that an N-terminal fragment (amino acids 1-500) of Sgs1 is sufficient to interact with yeast topoisomerase III in a two-hybrid system. Interestingly, the Gal4 activation domain was not present in this assay, suggesting that the Sgs1-fragment alone was acting as a transcription factor. Another group found that a helicase-defective mutant but not a C-terminal truncation of *SGS1* could complement an *sgs1* null mutant in a *top3* mutant background, suggesting that the C-terminal region of Sgs1 interacts with topoisomerase III (Lu *et al.* 1996). A recent study reported that this interaction is conserved between species, since Sgs1 also interacts with human topoisomerase IIIβ (Ng *et al.* 1999). In a different two-hybrid-screen, a fragment of Sgs1 (amino acids 434-792) was found to interact with a putative leucine zipper region in the C-terminal domain (amino acids 1109-1163) of *S. cerevisiae* topoisomerase II (Watt *et al.* 1995). Another genetic study suggests that mutated *sgs1* reduces the growth rate of *top1* mutants lacking topoisomerase I (Lu *et al.* 1996). *sgs1* mutants show a reduced growth rate, reduced spore viability, increased mitotic chromosome nondisjunction and high levels of meiotic missegregation (Watt *et al.* 1995). The mutation also

leads to an increase in mitotic intra- and interchromosomal recombination at several loci, including the rDNA locus, and to an increase in illegitimate recombination (Gangloff *et al.* 1994, Watt *et al.* 1996, Yamagata *et al.* 1998). Furthermore, loss of *SGS1* causes premature ageing of yeast cells, indicated by a reduced life-span, cell enlargement, premature sterility and a redistribution of the Sir protein silencing complex from telomeres to the nucleolus (Sinclair *et al.* 1997). Moreover, the nucleoli of *sgs1* cells are enlarged and fragmented. These changes are probably due to the accumulation of extrachromosomal rDNA circles (ERCs), a possible cause of ageing in yeast (Sinclair and Guarente 1997).

The gene *SGS1* encodes a protein of 1447 amino acids (predicted molecular mass 164 kDa). It includes two acidic blocks in the N-terminal region (amino acids 400-475 and 510-596) (Gangloff *et al.* 1994), a helicase "domain" and RecQ-Ct region (amino acids 674-1079), a HRDC domain in the C-terminal region (amino acids 1272-1351) (Morozov *et al.* 1997) and a putative bipartite nuclear localisation sequence (amino acids 1331-1333 and 1346-1348) (Matsumoto *et al.* 1998). An N-terminal fragment (amino acids 400-1268) of Sgs1 has been overexpressed and purified from yeast and characterised *in vitro* (Bennett *et al.* 1998). It possesses DNA-dependent ATPase activity stimulated by single-stranded and double-stranded DNA in both circular and linear form. However, it preferentially binds forked DNA over single-stranded and double-stranded DNA, which does not require Mg^{2+} or NTPs. It also possesses helicase unwinding activity (Lu *et al.* 1996, Bennett *et al.* 1998). This requires Mg^{2+} (which can be replaced by Mn^{2+} or Ca^{2+} but not Zn^{2+}) and ATP (replaceable by dATP but not GTP, TTP or UTP) and is very sensitive to the salt concentration in the buffer with a 50 % reduction at 30-40 mM NaCl or KCl compared to the absence of salt. The polarity of Sgs1 is 3'-5'. SSB stimulates its helicase activity, especially on a long substrate of 558 nt which it only unwinds to a small extent in the absence of SSB. Furthermore, Sgs1 is capable of unwinding a RNA-DNA heteroduplex. A recent footprinting study showed that Sgs1 interacts specifically with a junction

between a duplex DNA and its 3' single-stranded extension (either a tail or a gap) (Bennett *et al.* 1999). It binds and unwinds substrates with a 3'-tail of at least 8 nt and fails to interact with double-stranded or 5'-tailed substrates. Furthermore, it unwinds double-stranded substrates with a gap of at least 2 nt. Also, it dissociates a synthetic four-way junction (Holliday junction) into its four constituent strands.

1.5.8 Rqh1

rqh1+ was identified as a mutant called *hus2-22* in a screen for hydroxyurea (HU)-sensitive checkpoint mutants (Enoch *et al.* 1992). The cells show sensitivity to UV and ionising radiation as well as an aberrant mitosis resulting in a "cut" ("cell untimely torn") phenotype following exposure to hydroxyurea. Subsequently, the gene was cloned from a genomic library by complementation of the UV sensitivity (Stewart *et al.* 1997) and renamed *rqh1+* (for RecQ helicase). It encodes a 1328 amino acid protein with a helicase and RecQ-Ct region ranging from amino acids 515 to 922 and a potential bipartite NLS near the C-terminus (amino acids 1272 – 1274 and 1296 – 1299) (Matsumoto *et al.* 1998). The mutation in *hus2-22* cells is a truncation at amino acid 790, resulting in a loss of the two last helicase motifs. A second mutant called *rad12-502*, which was found in a screen for radiation sensitive mutants, was physically mapped and turned out to be a defect in *rqh1* as well (Murray *et al.* 1997). Here, a point mutation (T543I) had occurred in helicase motif I. One study shows that cells bearing the *rad12-502* mutation are not sensitive to ionising radiation (Murray *et al.* 1997), however, this was not confirmed by another study (Davey *et al.* 1998). Furthermore, these cells were less sensitive to UV than the *hus2-22* mutants or a *rqh1* null mutant. No enzymatic activity of the Rqh1 protein has been reported yet. *rqh1* null mutants show no obvious defects under normal growth conditions. Unlike checkpoint mutants, they do arrest in S-phase after HU treatment or UV irradiation. They also complete DNA replication after S-phase arrest but are defective in the subsequent chromosome segregation. This suggests *rqh1+* is not required for S-phase arrest but

for the recovery from this arrest. Furthermore, *rqh1* mutants show increased rates in homologous recombination after HU treatment (Stewart *et al.* 1997). Rqh1 was found to be neither involved in the nucleotide excision repair (NER) pathway, nor in the UV dimer endonuclease (UVDE) pathway of UV damage repair, and it does not interact with the UVDE enzyme. Rather, it seems to be involved in the same UV tolerance response as several recombinational repair proteins. Its function is dependent on the six *rad* checkpoint genes but is not necessary to initiate or propagate the checkpoint-dependent signal to Cds1, the kinase that defines the pathway resulting in DNA damage tolerance during S-phase. Nevertheless, genetic analysis shows that *rqh1* functions in the Cds1-mediated pathway and not in the Chk1-dependent mitotic arrest pathway. Finally, the *rad12-502* mutation shows a genetic interaction with genes involved in the elongation phase of DNA replication including DNA polymerase subunits, polymerase-associated proteins and ligase. A different study of *rqh1/rad12*$^+$ found that it upregulates basal activity of the UVDE enzyme, whereas *rad9*$^+$ downregulates it. *Rqh1/rad12*$^+$ also acts in an overlapping pathway with *rad9*$^+$. Overexpression of *rqh1/rad12*$^+$ or deletion of *rad9* both lead to an S-phase checkpoint defect (Davey *et al.* 1998). A deletion of the gene encoding topoisomerase III (*top3*$^+$) is lethal but can be suppressed by a deletion of *rqh1*$^+$ (Goodwin *et al.* 1999, Maftahi *et al.* 1999). This is similar to the genetic interaction observed between *sgs1* and *top3* in budding yeast, suggesting that this interaction has been conserved in evolution.

1.6 Human disorders resulting from defects in RecQ helicases

1.6.1 Bloom's syndrome

Bloom's syndrome (BS) was first described in 1954 (for a recent review, see German and Ellis 1998). It is an extremely rare, autosomal recessive disorder with approximately 200 cases known worldwide. BS individuals are of well-proportioned small size and are highly predisposed to cancer at an early age. Additionally, they may show the following features: Head and face often have a characteristic appearance with prominent nose and ears. Often sun-sensitive erythematous skin lesions appear which are limited to the face and dorsa of the hands and forearms (areas that are usually exposed to the sun). Patients suffer from immunodeficiency leading to frequent infections of the ears and respiratory tract. Affected males do not produce any spermatozoa, females can be fertile but have an early onset of the menopause. Skin areas of hypo- and hyperpigmentation are present in abnormal numbers. The three major complications are cancer, chronic lung disease and diabetes mellitus; cancer being by far the most common cause of death. By the year 1996, 71 of the 168 persons in the Bloom's syndrome registry had been diagnosed with cancer, 29 of them with more than one primary tumour, and 50 of these patients had died of cancer. The tumours are not restricted to a certain type but represent the whole spectrum of human cancers, with a premature onset (the mean age of cancer diagnosis is 24.7 years).

BS is caused by a mutation at a single locus, *BLM* (for a description of the gene and the mutations, see section 1.5.4). Although the carrier frequency in the general population is extremely low, it has reached approximately 1% within the Ashkenazi Jewish population through a founder effect (Li *et al.* 1998). Therefore, about one third of known BS individuals descend from Ashkenazi Jews.

Somatic cells from BS individuals have an abnormally unstable genome (German 1993, Kuhn *et al.* 1986), including chromatid gaps, breaks and rearrangements as well as micronuclei (Rosin and German 1985). Furthermore, their mutation rate is elevated, as measured at specific loci, e.g. the *HPRT* locus on the X-chromosome (Vijayalaxmi *et al.* 1983) and the *GPA* (glycophorin A) locus on chromosome 4 (Kyoizumi *et al.* 1989, Langlois *et al.* 1989). BS cells also have a particular tendency for recombination between chromosomes, both homologues and sister chromatids (Groden *et al.* 1990). Indeed, the diagnostic feature of BS is the increased number of sister-chromatid exchanges (SCEs) (50-100/metaphase in BS cells versus less than 10 in wild type cells). They can be easily demonstrated by growing BS cells in medium containing bromodeoxyuridine (BrdU) for two cell cycles to allow for differential staining of the sister chromatids. Exchanges between two homologues, on the other hand, appear as four-armed symmetrical configurations in metaphase, so-called quadriradial structures. They are found in approximately 1% of BS T lymphocytes but only extremely rarely in normal cells. The hypermutability of BS defines it as a "somatic mutational disorder". This phenotype explains the extreme susceptibility of BS patients to cancer, essentially a genetic disease relying on an accumulation of mutations in oncogenes or tumour suppressor genes. It also explains the small body size of the patients, probably resulting from excessive death of mutated cells during development.

Despite their genome instability phenotype, BS cells are generally not hypersensitive to DNA damaging agents, including UV radiation, ionising radiation and alkylating agents, suggesting they do not carry a defect in one of the main DNA repair pathways such as nucleotide excision repair, double-strand break repair, base excision repair or DNA mismatch repair. However, BS cells do grow slowly, with a reduced rate of transit through S-phase (Hand and German 1975) and delayed DNA maturation (Ockey and Saffhill 1986). They also show abnormal replication intermediates (Lönn *et al.* 1990) suggesting a defect of BS cells in replication.

Bloom's syndrome serves as a model showing the clinical consequences of an excessive somatic mutation rate and helping us understand the basis of the maintenance of genomic stability in human cells.

1.6.2 Werner's syndrome

This rare autosomal recessive disorder was first described in 1904 by the German physician Otto Werner in his doctoral thesis "Über Katarakt in Verbindung mit Sklerodermie" (Werner 1904 and Werner (translation Hoehn) 1985). (For a recent review, see Schellenberg *et al.* 1998). The prevalence of Werner's syndrome (WS) in the general population has been estimated from 1 in 22,000 to 1 in 1,000,000. WS individuals usually develop normally until puberty when they lack the adolescent growth spurt, remaining small. Subsequently they develop cataracts, skin with scleroderma-like appearance and hair loss, all features of premature ageing. Most patients show an excess of hyaluronic acid in their urine. Other symptoms found in a subset of patients include hypogonadism, osteoporosis, diabetes mellitus and vascular diseases. Persons with WS also have a greatly elevated risk of developing a wide variety of cancers. However, there is an overrepresentation of nonepithelial cancers, with a ratio of epithelial to nonepithelial cancers of 1:1 versus 10:1 in the general population. Cancers commonly found include soft-tissue sarcomas, osteosarcomas, melanomas and thyroid carcinomas. Cancers, followed by myocardial infarcts and cerebrovascular incidents are the most common causes of death, at a mean age of 47 years.

WS fibroblasts have a limited potential for division and show early senescence (similar to fibroblasts from normal elderly donors) (Martin *et al.* 1970). WS cells also exhibit genomic instability, in particular an elevated level of chromosomal breakage, deletions and rearrangements (Salk *et al.* 1982, Salk *et al.* 1981, Salk *et al.* 1985) and an increased somatic mutation rate at the *HPRT* locus (Fukuchi *et al.* 1985, Fukuchi *et al.* 1989, Monnat *et al.*

1992). Also, they show a prolonged S phase, a reduced rate of DNA replication and increased distances between origins of replication (Fujiwara *et al.* 1977, Takeuchi *et al.* 1982, Hanaoka *et al.* 1983). However, they do not have a defect in DNA repair since they are not hypersensitive to a variety of DNA damaging agents (Stefanini *et al.* 1989), with the notable exception of 4-nitroquinoline-1-oxide (4NQO) (Gebhart *et al.* 1988, Ogburn *et al.* 1997).

Werner's syndrome is caused by a mutation in the *WRN* gene locus (see section 1.5.5 for a more detailed discussion). There is great interest in this disease as a model for ageing, since it shows many of the usual features of ageing prematurely. However, unlike often in normal ageing, the central nervous system appears to be spared in WS. Also, the overrepresentation of non-epithelial cancers is not typical of normal ageing. Because of the high cancer incidence combined with the genome instability in WS, WRN may provide a clue to the maintenance of replicative capacity and genome stability in humans.

1.6.3 Rothmund-Thomson syndrome

This syndrome was first described by the German physician August Rothmund in 1868 (Rothmund 1868) and by the British doctor Sidney Thomson in 1923 and 1936 (Thomson 1923, Thomson 1936). Rothmund described ten cases of young patients with poikiloderma and a high incidence of juvenile cataracts, whereas Thomson reported three similar cases of poikiloderma of whom two showed bony abnormalities. Meanwhile, more than 200 cases have been reviewed in the literature (Vennos and James 1995), and Rothmund-Thomson syndrome (RTS) has been established as a rare autosomal recessive disease. The symptoms include poikiloderma, skeletal abnormalities, a high incidence of juvenile cataracts, short stature, hair loss and an increase in both cutaneous and noncutaneous malignancies, especially osteosarcomas. The onset of the disease is within the first three years of life, and the life span is usually normal. These clinical signs are somewhat heterogenous, and there is no reliable

laboratory test, which makes a differential diagnosis difficult. Cytogenetic studies have been small so far and include some reports of DNA repair defects (e.g. excision repair: Vasseur *et al.* 1999) and of chromosomal instability (Lindor *et al.* 1996, Miozzo *et al.* 1998). Recently it was reported that some RTS patients carry mutations of *RECQL4*, a member of the RecQ family of helicases (Kitao *et al.* 1999b).

1.7 Aim of the project

The aim of this study was to clarify why the lack of *BLM* in BS patients leads to genomic instability, often resulting in cancer, or, in other words, to determine the role(s) of BLM in the cell. The approach chosen was the biochemical characterisation of the BLM protein *in vitro*. Chapter 2 contains the methods used, Chapter 3 describes the overexpression, purification and initial enzymatic characterisation of recombinant BLM. Chapter 4 reports an investigation of the structure of BLM, Chapter 5 explores its interaction with a number of DNA substrates, including Holliday junctions, which are key intermediates of recombination. Chapter 6 summarises the results and proposes models for the role of BLM in the cell.

Chapter 2: Materials and Methods

2.1 Chemicals and reagents

All chemicals came from either Sigma or BDH. All enzymes were purchased from Roche (formerly Boehringer Mannheim) unless otherwise stated. Radioisotopes were obtained from Amersham.

2.2 Cloning

2.2.1 Plasmids

2.2.1.1 *E. coli* cloning vector

pT7Blue (Novagen) was used for modifying and cloning the *BLM* cDNA.

2.2.1.2 *S. cerevisiae* expression vector

pYES2 (Invitrogen), a multicopy shuttle vector, was used to overexpress *BLM* in *S. cerevisiae*. The gene is under the regulation of the *GAL1* promoter and expression is induced by the addition of galactose. Selection in *E. coli* is via ampicillin resistance and in *S. cerevisiae* by the *URA3* marker.

2.2.2 PCR (cloning)

Primers JK3 and R2 were used to amplify the N-terminus (1.4 kb) of the *BLM* cDNA using 5 cycles. Primers JK4 and S9 were used to amplify the C-terminus (0.5 kb) of the *BLM* cDNA using 7 cycles. PCR conditions were 2 min, 94°C; 1 min, 55°C (JK3/R2) or 48°C (JK4/S9); 3 min (JK3/R2) or 2 min (JK4/S9), 72°C; 0.5 min, 94°C (the last three steps were repeated for the given number of cycles); 1 min, 55°C (JK3/R2) or 48°C (JK4/S9); 10 min, 72°C. Expand polymerase was used in the manufacturer's buffer.

2.2.3 PCR (screening)

5 µl of an overnight bacterial culture were mixed with 25 pmol primers, 2.5 U *Taq* DNA polymerase, 0.4 mM dNTP in *Taq*-buffer in a total reaction volume of 50 µl. PCR conditions were 2 min, 95°C (initial lysis); 1 min, 48-55°C; 3 min, 72°C; 30 s, 95°C (10 cycles); 10 min, 72°C (extension).

2.2.4 Agarose gel electrophoresis

DNA was mixed with DNA loading buffer (30% (w/v) sucrose, 0.1 M EDTA, 0.01% (w/v) bromophenol blue) and loaded onto a 0.8-1.5% agarose gel in TAE or TBE buffer containing 0.5 µg/ml ethidium bromide. Gels were run at a constant current of 50-100 mA. The DNA was visualised by UV light.

2.2.5 Purification of DNA from agarose gels

DNA was purified from agarose gels using a "Gene-clean-II" kit (BIO 101) according to the manufacturer's instructions. In brief, the agarose containing the DNA was excised under long-wave UV light and dissolved in 6 M NaI (containing TBE modifier in the case of a TBE

agarose gel) at 55 °C. Silica matrix which binds DNA was added. After three washes with buffer containing 50% ethanol, the DNA was eluted in water.

2.2.6 Ligation

Ligations were carried out at a 1:40 - 1:100 molar ratio of vector to insert using 50-100 ng linearised vector. Reactions furthermore contained 1 U T4 ligase and 1 mM ATP in the manufacturer's T4 ligase buffer in a total reaction volume of 10 µl. The ligation reaction was allowed to proceed for 24 hours at 16°C.

2.2.7 *E. coli* strain

DH10B (Gibco), genotype: F⁻ *ara*D139 Δ(*ara, leu)*7697 Δ*lac*X74 *gal*U *gal*K *mcr*A Δ(*mrr* – *hsd*RMS – *mcr*BC) *rps*L *dor* ϕ80d*lac*ZΔM15 *end*Al *nup*G *rec*Al

2.2.8 Competent cells

E. coli DH10B cells were grown to log phase in SOB medium. They were rapidly chilled and washed twice with Millipore water before being resuspended in 2-3 ml 10% glycerol/l culture. Subsequently, cells were snap-frozen and stored at -80°C until use (up to 6 months).

2.2.9 Transformation by electroporation

10 ng of plasmid DNA or 0.7 µl of a ligation reaction were mixed with 50 µl electrocompetent cells and transferred to an electroporation cuvette. The cells were transformed with a Gene Pulser electroporator (BioRad) at 2.5 kV, 25 µF and 400 Ω. Immediately afterwards, the cells

were diluted in SOC medium and grown for 30 min at 37°C. Cells were then spread onto LB-agar plates containing 0.1 mg/ml ampicillin and grown at 37°C overnight.

2.2.10 Small-scale preparation of plasmid DNA ("mini-prep")

DNA was prepared by alkaline lysis followed by either propan-2-ol precipitation or silica chromatography. Small-scale overnight cultures of *E. coli* in LB medium containing 0.1 mg/ml ampicillin were harvested and resuspended in solution I (25 mM Tris/Cl pH 8.0, 10 mM EDTA, 50 mM glucose). After alkaline lysis in solution II (0.2 M NaOH, 1% SDS) and neutralisation with solution III (3 M potassium acetate, pH 4.8), the lysate was centrifuged and the supernatant was incubated with RNaseA to remove RNA. A chloroform/isoamylalcohol extraction was performed to remove the enzyme. The DNA was then precipitated with propan-2-ol, centrifuged, washed with ethanol, air-dried and resuspended in water. Alternatively, solution I already contained RNaseA. After centrifugation of the lysate, the supernatant was mixed with a silica-based matrix that binds DNA (Qiagen). The suspension was applied to a mini-column and washed with a buffer containing 50% ethanol. The DNA was eluted with water.

2.2.11 Large-scale preparation of plasmid DNA ("maxi-prep")

Plasmid DNA on a large scale (>100 µg) was prepared by alkaline lysis followed by either propan-2-ol precipitation and caesium chloride banding to remove nicked DNA or by binding to and elution from an anion exchange resin followed by propan-2-ol precipitation. 400 ml overnight cultures of *E. coli* in LB/ampicillin were harvested by centrifugation and resuspended in solution I (see 2.2.10). After alkaline lysis and neutralisation, the lysate was

centrifuged and the supernatant filtered. The DNA was precipitated with propan-2-ol, resuspended in TE buffer and mixed with a CsCl solution (54% w/w) in TE buffer containing ethidium bromide. The samples were centrifuged at 500,000 x g for 3 hours and the plasmid band was removed. After isoamyl alcohol extraction of the ethidium bromide, the plasmid DNA was precipited with ethanol and resuspended in TE buffer. Alternatively, the cleared cell lysate was applied to an anion exchange column (Qiagen) which was washed with a medium-salt wash buffer. The DNA was eluted in a high-salt buffer and precipitated with propan-2-ol.

2.2.12 Determination of DNA concentrations

The DNA concentration was routinely determined by measuring the absorption (optical density, OD) at 260 nm. It was assumed that $1OD_{260}$ equals 50 µg/ml of double-stranded DNA and 33 µg/ml of single-stranded DNA. Alternatively, the DNA was run out on an agarose gel and stained with ethidium bromide, and the concentration was estimated by comparison with a standard.

2.2.13 Restriction enzyme digests

Generally, 5 µg of plasmid DNA were digested using 10 U of restriction enzyme in the manufacturer's buffer in a total reaction volume of 20 µl for 1-4 h at 37°C.

2.2.14 Sequencing

Expression constructs were sequenced using the chain termination (Sanger dideoxy) method. Samples were run on a semi-automated sequencer (ABI PRISM 377). The sequencing PCR reaction contained one primer, AmpliTaq DNA polymerase (Perkin-Elmer), deoxynucleotides

and low concentrations of dideoxynucleotides differentially labelled with fluorescent tags. The sequence was analysed using the program Sequencher.

2.2.15 *S. cerevisiae* strain

S. cerevisiae strain JEL 1 (α *leu*2 *trp*1 *ura*3-52 *prb*1-1122 *pep*4-3 Δ*his*3::*PGAL10-GAL4*) was used for the overexpression of BLM.

2.2.16 Yeast transformation

Yeast cells were grown to mid-log phase (OD_{600} = 0.4-0.6) in 50 ml YPD medium and harvested by centrifugation. The cells were washed once each in water and in lithium buffer (0.1 M lithium acetate, 0.1 M Tris-Cl pH 7.5, 50 mM EDTA) and resuspended in 0.5 ml lithium buffer. 1 μg of plasmid DNA was mixed with 50 μg of sonicated salmon sperm DNA in less than 20 μl and added to 200 μl yeast suspension. 1.2 ml of PEG solution (lithium buffer containing 40% PEG 3350 or 4000) was added and the mixture was shaken for 30 min at 30°C. After incubation at 42°C for 15 min, the cells were pelleted and resuspended in 100 μl water. They were spread onto complete supplement mixture agar plates lacking uracil for selective growth of transformants and incubated at 30°C for 2-5 days.

2.3 Protein purification and analysis

2.3.1 Denaturing polyacrylamide gel electrophoresis

Protein samples were boiled for 2 min at 98°C in protein sample buffer (60 mM Tris-Cl pH 6.8, 1% (w/v) SDS, 1% (v/v) 2-mercaptoethanol, 5% (v/v) glycerol, 0.005% (w/v)

bromophenol blue) and loaded onto SDS-polyacrylamide gels. The separating gel contained 0.375 M Tris-Cl pH 8.8, 0.1% SDS, between 8% and 12% polyacrylamide (acrylamide: bisacrylamide 37.5:1). The stacking gel contained 0.125 M Tris-Cl pH 6.8, 0.1% SDS, 6% polyacrylamide (37.5:1). Generally, Mini-Protean gels (BioRad) were used. The electrophoresis running buffer consisted of 25 mM Tris, 190 mM glycine and 0.1% SDS. Gels were run at a constant current of 20-40 mA. Proteins were visualised by staining the gel with Coomassie solution (0.1% (w/v) Coomassie brilliant blue, 10% acetic acid, 20 % methanol) and destaining with 10% acetic acid, 20% methanol.

2.3.2 Western blotting

Proteins were separated on denaturing polyacrylamide gels as described above and transferred to a nitrocellulose membrane by either wet or semi-dry blotting. In the first case, proteins were blotted onto Hybond-C super nitrocellulose membrane (Amersham) in transfer buffer I (50 mM Tris, 350 mM glycine, 20% (v/v) methanol) using a Trans-Blot cell (BioRad) at 15 V for 16 h at 4°C. Semi-dry blotting onto Hybond ECL nitrocellulose membrane (Amersham) was performed in transfer buffer II (48 mM Tris, 39 mM glycine, 1.3 mM SDS, 10% (v/v) methanol) using a semi-dry blotter (Hoefer) for 2 h at 36 mA at room temperature. Membranes were incubated with blocking buffer (10% dried milk in PBSA, 0.3% Tween 20) for at least 1 h. Incubation with the first antibody, diluted in blocking buffer, was for 1 h. This was followed by at least 3 washes in wash buffer (up to 1% dried milk in PBSA, 0.3% Tween 20). The membrane was then incubated for 1 h with the second antibody, which was conjugated to horseradish peroxidase and diluted in blocking buffer. After at least three rinses in wash buffer, the protein was detected by enhanced chemiluminescence (ECL) using an ECL kit

(Amersham) according to the manufacturer's instructions. This detection relies on the oxidation of luminol catalysed by horseradish peroxidase; the light emitted during this reaction can be detected by autoradiography.

2.3.3. Antibodies

The antibody used to detect BLM was IHIC33, an affinity-purified rabbit polyclonal antibody raised against amino acids 1-449 of BLM. Alternatively, the protein was detected with a mouse monoclonal anti-histidine-tag antibody (Dianova). The secondary antibodies used were anti-rabbit-HRP-conjugated antibody and anti-mouse-HRP-conjugated antibody (DAKO).

2.3.4 Yeast culture and protein induction

Yeast JEL1 cells containing pJK1 (see chapter 3) were grown at 30°C in dextrose-free YPD medium containing 2% raffinose up to an OD_{600} of 0.7. For induction of BLM expression, galactose was added to a final concentration of 2%, and the cells were cultured for another 24 h at 20°C. Cells were harvested by centrifugation, washed in 50 mM sodium phosphate buffer (pH 7.0) and stored at -80°C until required.

2.3.5 Yeast lysis

All steps were performed at 4°C. Yeast cells were defrosted and resuspended in an equal volume of lysis buffer (50 mM sodium phosphate pH 7.0 or 50 mM HEPES-OH pH 7.0, 0.5 M or 1 M KCl, 10% glycerol, EDTA-free protease inhibitors (Roche, according to instructions)). 0.5 x the total volume glass beads (acid-washed, 425-600 µm) was added, and the cells were lysed by vortexing for 10 x 30 s with incubations of 30 s on ice after each

burst. To remove solid particles, the lysate was centrifuged at 30,000 x g for 30 min and filtered through a 0.8 μm filter.

2.3.6 HeLa cell culture

HeLa S3 cells were grown in RPMI medium supplemented with 5% fetal calf serum. Logarithmically growing cells were harvested by centrifugation and stored at -80°C until used.

2.3.7. HeLa cell lysis

All steps were performed at 4°C. 10^8 frozen HeLa S3 cells were resuspended in an equal volume of lysis buffer (50 mM Tris-Cl pH 7.5, 0.5 M KCl, 1 mM DTT, 0.1 mM EDTA, 20% glycerol, protease inhibitors (Roche)). 0.5 x the total volume glass beads (acid-washed, 425-600 μm) was added, and the cells were lysed by vortexing for 30 s. Lysates were precleared by a 10 min centrifugation at 30'000 x g.

2.3.8 Nickel chelate affinity chromatography

The cleared yeast lysate was loaded onto a Poros MC20 column (1.7 ml bed volume) using a BioCAD workstation (Perkin Elmer). Prior to loading, the column had been charged with several bed volumes of 0.1 M $NiSO_4$, saturated with 5 bed volumes of 1.5 M imidazole in running buffer (50 mM phosphate pH 7.0, 0.25 M NaCl or 50 mM HEPES-OH pH 7.2, 0.25 M KCl) and equilibrated with 15 mM imidazole in running buffer. After loading, the column was washed with 15 bed volumes of 50 mM imidazole in running buffer. BLM was eluted in one of two ways: either a 50-1500 mM imidazole gradient in running buffer was applied over 8 bed volumes, or BLM was eluted with 250 mM EDTA in running buffer over 10 bed

volumes. Fractions of 1 ml were collected and dialysed at 4°C either for 2-16 h against buffer containing 60 mM Tris-Cl pH 7.5, 0.1 M NaCl, 1 mM EDTA, 1 mM 2-mercaptoethanol or against buffer containing 50 mM HEPES-OH pH 7.2, 0.25 M KCl, 1 mM EDTA, 1 mM 2-mercaptoethanol.

2.3.9 Determination of protein concentrations

Protein concentrations were determined using the BioRad Coomassie assay with BSA as a standard. Briefly, 10 µl of protein were mixed with 250 µl diluted and filtered assay solution in a microtiter plate. Subsequently, OD_{595} was determined within one hour.

2.3.10 Protein storage

BLM was stored in 25% glycerol at -80°C.

2.3.11 Size exclusion chromatography

Gel filtration was performed using a fast protein liquid chromatography (FPLC) superose 6 column (Pharmacia). The running buffer contained 50 mM Tris-Cl pH 7.5, 0.5 M KCl, 1 mM DTT and 0.1 mM EDTA. Samples (cell extracts or purified protein) of 200 µl were applied, the flow rate was 0.5 ml/min.

2.3.12 Electron Microscopy

2.3.12.1 Preparation of grids

Protein was applied onto an air-glow-discharged, carbon coated, 400 mesh nickel grid (Agar Scientific) and negatively stained by floating on a drop of 1% (w/v) uranyl acetate for 20s. Excess stain was blotted off and the grid was air-dried.

2.3.12.2 Electron micrographs

Grids were examined in a JEOL 1010 transmission electron microscope at 80 kV or 100 kV. Micrographs of the grids were taken at 30,000 x - 50,000 x magnification and selected negatives were digitised using an Emil linear CCD densitometer at a step size of 14 μm (equivalent to 2.8 Å on the specimen). Images of protein molecules were selected by the operator.

2.3.13 Enzymatic assays

2.3.13.1 ATPase assays

ATPase activity was determined by measuring the release of inorganic phosphate by a colourimetric assay according to Chifflet *et al.* (1988). The reaction buffer contained 50 mM Tris-Cl pH 7.5, 4 mM $MgCl_2$, 2 mM ATP, 25 μg/ml (76 μM) sheared salmon sperm DNA, 50 μg/ml BSA, 50 mM NaCl, 1 mM DTT and various amounts of protein in a total reaction volume of 50 μl. After a 30 min incubation at 37°C, the reaction was stopped with 150 μl 12% SDS. Subsequently, 200 μl of a freshly prepared solution containing 0.5% (w/v) ammonium molybdate, 3% (w/v) ascorbic acid and 0.5 M HCl was added and the samples were incubated for 5 min at 20°C. After adding 300 μl of a solution containing 2% (w/v) sodium metaarsenite, 2% (w/v) sodium citrate and 2% (v/v) acetic acid, the samples were incubated for 10 min at 37°C. Finally, the absorbance of the reaction mixture was measured at 850 nm. Inorganic phosphate was used as a standard.

2.3.13.2 Preparation of radiolabelled substrates

2.3.13.2.1 Gel purification of oligonucleotides

Oligonucleotides were mixed with formamide sample buffer (80% (v/v) formamide in TBE buffer), heated for 2 min at 98°C and loaded onto an 8% denaturing polyacrylamide gel in TBE buffer. The gel was run for 2 h at 200 V in TBE buffer at 4°C. The DNA was visualised by UV shadowing: the gel was placed on a thin layer chromatography plate and viewed under long-wave UV. The gel area containing the DNA was excised with a and cut into small pieces. It was incubated for 16 h in 0.5 M sodium acetate (pH 5.0), 10 mM magnesium acetate and 2.5 mM EDTA. After centrifugation, the DNA in the supernatant was recovered by ethanol precipitation.

2.3.13.2.2 5'-labelling of oligonucleotides

The labelling reaction contained 200 ng oligonucleotide, 5-10 U T4 polynucleotide kinase (Pharmacia), 25 µCi (0.85 pmol) [γ-^{32}P]-ATP in the manufacturer's buffer in a total volume of 10 µl. After an incubation for 30 min at room temperature, the reaction was stopped by adding 60 µl of 20 mM Tris-Cl pH 7.5, 0.1 M NaCl, 10 mM EDTA (STE buffer). Oligonucleotides were separated from unincorporated ATP using a NucTrap push column (Stratagene) according to the manufacturer's instructions.

2.3.13.2.3 Annealing and gel purification of small oligonucleotide substrates

One 5'-labelled oligonucleotide was annealed to a fivefold excess of the appropriate unlabelled oligonucleotide(s) by incubating them for 3 min at 90°C, 10 min at 65°C, 10 min at 37°C and 10 min at room temperature in a PCR machine. The annealing reaction mixture was applied to

a 10% nondenaturing polyacrylamide gel (acrylamide: bisacrylamide 40:1) in TBE buffer and run at 200 V for 2 h. The gel area containing the substrate was then visualised by autoradiography and excised. The DNA was electroeluted either by using a Biotrap (Schleicher & Schuell) according to the manufacturer's instruction or by placing the gel slice into dialysis tubing and applying 80-100 V in 0.5 x TBE buffer for 2-4 h at 4°C. In either case, the solution containing the DNA was recovered and dialysed against 10 mM Tris-Cl pH 8, 10 mM EDTA, 50 mM NaCl for 1 h at room temperature. The substrates were stored at -20°C until used. Their concentrations were determined by relating their radioactivity to the specific radioactivity of the 5'-labelled oligonucleotide incorporated in them.

2.3.13.2.4 Preparation of M13-based substrates

An oligonucleotide was annealed to single-stranded M13mp18 (New England Biolabs) and 3'-labelled by incubation with 2 U of Klenow polymerase and 20 μCi of [α-^{32}P]dCTP (Amersham) in the appropriate buffer for 30 min at 37°C. Unincorporated nucleotides were removed using a NucTrap column (Stratagene).

A substrate for the determination of the directionality of BLM was created by annealing a 90-mer to single-stranded M13mp18 and digesting the product with *Sal*I. All available 3'-ends were subsequently labelled using Klenow polymerase, [α-^{32}P]dCTP and dTTP as described above.

2.3.13.2.5 Preparation of long linear duplex substrate

A 0.5 kb linear duplex substrate was produced by digesting pYES2 DNA with *Pst*I, gel-purification of the product from an agarose gel and 3'-^{32}P-endlabelling of the fragment using terminal transferase.

2.3.13.2.6 Preparation of G4-DNA

Approximately 50 µg of oligo G4-TP (see Table 5.1) were first boiled and then chilled on ice. Subsequently, they were incubated at 1 M NaCl in a total volume of 40 µl at 60°C for 48 hours. After the incubation, the DNA was precipitated with ethanol, resuspended in 40 µl TE buffer and stored at -20°C until used. For helicase assays, approximately 200 ng G4-DNA were 5'-labelled using polynucleotide kinase (see 2.3.13.2.2).

2.3.13.3 Helicase assays

In helicase assays, the release of a labelled oligonucleotide from a substrate was measured. Unless otherwise stated, the reaction mixture contained 50 mM Tris-Cl pH 7.5, 2 mM $MgCl_2$, 2 mM ATP, 0.1 mg/ml BSA and various amounts of DNA substrate and BLM. After incubation at 37°C, samples were routinely run on 10% nondenaturing polyacrylamide gels (acrylamide: bisacrylamide 40:1) at room temperature. Product formation was visualised by autoradiography and quantified using a Phosphorimager.

2.3.13.4 Bandshift assays

Proteins and DNA were incubated in 20 mM triethanolamine-HCl pH 7.5, 2 mM $MgCl_2$, 1 mM ATPγS, 0.1 mg/ml BSA and 1 mM DTT at room temperature for 20-30 min. In some cases, protein-DNA complexes were fixed with 0.25% glutaraldehyde for 10 min at 37°C and visualised by autoradiography after nondenaturing polyacrylamide gel electrophoresis through a 5% gel in TBE buffer.

Chapter 3: Purification and initial characterisation of BLM

3.1 Introduction

At the beginning of this project, in autumn 1996, the sequence of the *BLM* gene had been published for one year (Ellis *et al.* 1995). It is homologous to a family of DNA helicases called the RecQ family which is named after its *E. coli* member, RecQ. Each member possesses a region spanning 360-400 amino acids that contains the seven conserved helicase motifs that mark the SF2 superfamily of DNA and RNA helicases (Ellis *et al.* 1995, Sekelsky *et al.* 1999, Gorbalenya and Koonin 1993). The majority of mutations in *BLM* found in BS patients up to then were predicted to be loss-of-function mutations that would destroy the putative helicase activity of the enzyme. Four of the mutants encode putative products of 185, 271, 515 and 739 amino acids, none of which contains a complete set of the seven helicase domains. Two mutants encode full-length proteins with amino acid substitutions at residues conserved in RecQ helicases (I843T, Q672R), and one encodes a protein with a substitution in the C-terminal region (1055 C-S). Therefore, the predicted helicase activity seemed to be of great importance for the normal function of the protein and hence seemed to be worth studying.

In order to demonstrate and characterise the proposed helicase activity of the BLM protein, I set out to purify it in recombinant form using an *S. cerevisiae* expression system that had been well established in our laboratory. This system had been successfully used to

overexpress and purify recombinant human topoisomerases IIα and IIβ previously (Wasserman *et al.* 1993, Austin *et al.* 1995). Two modifications were made to the ends of BLM to facilitate its overexpression, purification and detection: residues 2-1417 were fused to the first five amino acids of yeast topoisomerase II, and a hexahistidine tag was added to the C-terminus. The N-terminal modification had proved to increase the expression level of human topoisomerase IIα in the past (Ian Hickson, personal communication). The reason for this is not entirely clear, but we assume that the yeast N-terminus somehow stabilises a human protein overexpressed in yeast, or that it enhances translation efficiency. The C-terminal hexahistidine tag allows purification of the protein by metal chelate affinity chromatography and its detection by anti-histidine tag antibodies. This chapter describes the cloning of the BLM expression construct, the overexpression and purification of BLM protein and the initial characterisation of its ATPase and helicase activities.

3.2 Results

3.2.1 Cloning of the BLM expression construct

At the beginning of this project, the BLM cDNA had already been PCR-cloned from a human B-cell cDNA library and inserted into the yeast/*E. coli* shuttle vector pYES2 (Ronjon Chakraverty, DPhil thesis 1998). This vector allows overexpression of proteins in *S. cerevisiae* under the control of the *GAL1* promoter. Five silent base changes from the published sequence (Ellis *et al.* 1995) had been detected in this clone, four of which probably represent polymorphisms because they were found in several independently generated cDNAs. For overexpressing BLM, I added a yeast Kozak consensus sequence upstream of the coding sequence by PCR cloning. Furthermore, I replaced the initiation codon with the first five codons of the *S. cerevisiae*

topoisomerase II (*TOP2*) gene, and I added a C-terminal hexahistidine tag. In order to minimise the number of errors introduced by the polymerase, I used the smallest possible number of PCR cycles and I recloned the gene as three contiguous fragments. In detail, to generate the N-terminal modification with the inclusion of the yeast Kozak consensus sequence, I amplified a 1.4 kb 5' fragment of the *BLM* cDNA using the 5' primer JK3 (5' AGAGAGGGATCCCTAACCA**TGTCAACTGAACCG**GCTGCTGTTCCTCAAAATAAT-3') and the 3' primer R2 (5'-TCCTAGGGTGGTAGTCAGTAAACA-3'). Primer JK3 contains a *Bam*HI site (underlined), a yeast Kozak consensus sequence (TAACC) and the first five codons of the yeast *TOP2* open reading frame (bold). A *Bam*HI-*Eco*RI fragment of this PCR product replaced the corresponding region in the original pYES2-BLM expression construct. To generate the C-terminal modification, I amplified a 0.5 kb fragment of the 3' end of the *BLM* cDNA using the 5' primer S9 (5'-CTCAAGAAGCTTGCAGAATC-3') and the 3' primer JK4 (5'-AGAGAGCTCGAGTCA*__GTGGTGGTGGTGGTGGTG__TGAGAATGCATATGAAGG CTT-3'). Primer JK4 contains a *Xho*I site (underlined), a stop codon (asterisk) and 6 codons for histidine residues (bold). A *Hind*III-*Xho*I fragment of this PCR product replaced the corresponding fragment in the original pYES2-BLM expression construct. The 1.4 kb *BamH*I-*Eco*RI 5'-fragment, a 2.4 kb *Eco*RI-*Hind*III fragment from the original pYES2-*BLM* construct and the 0.5 kb *Hind*III-*Xho*I 3'-fragment were used in a three-way ligation with pYES2 cut with *Bam*HI and *Xho*I to create pJK1. Sequencing of the product revealed two additional base changes in the BLM open reading frame representing silent mutations introduced by PCR.

3.2.2 Overexpression and purification of BLM

S. cerevisiae JEL1, a protease-deficient yeast strain, was transformed with pJK1. The cells were grown at 30°C in complete medium (YPD minus dextrose) containing 2% raffinose as a carbon source. At an OD_{600} of 0.7, expression of recombinant BLM protein was induced by

adding galactose to 2% final concentration. Cells were allowed to express BLM for 24 h at 20°C. Preliminary experiments had suggested that the yield of BLM was higher at this reduced temperature. Cells were harvested by centrifugation, washed in phosphate buffer and snap-frozen in liquid nitrogen for storage at –80°C until they were used. For purification, cells from 2 litres of yeast culture were resuspended in lysis buffer, and 0.5 volumes of glass beads per volume of cell suspension were added. Cells were then lysed by manual vortexing. After clearing the cell lysate by centrifugation and filtration, soluble proteins were applied to an immobilised metal affinity chromatography (IMAC) column (POROS MC20) charged with Ni^{2+} using a BioCAD workstation. The Ni^{2+}-ions bound to the resin show high affinity primarily to histidine residues. Therefore, histidine-rich proteins or proteins containing an artificial histidine tag will bind strongly to this resin. They can be eluted with either imidazole, which competitively binds to the Ni^{2+} ions, or with EDTA, which strips the metal ions off the column with the protein bound to them. Before applying the cell lysate, the column had been washed with a high concentration of imidazole, which reduces the binding of nonspecific proteins. After loading the supernatant, the column was washed with buffer containing 50-80 mM imidazole. At this imidazole concentration, the majority of BLM remained bound to the column while weakly bound proteins were washed off. The protein was then eluted in one of two ways. Either a linear imidazole gradient (50-1500 mM) was applied, or an EDTA step (250 mM) was used. Fig. 3.1 shows a typical example of a BLM purification using the latter method for elution. The majority of BLM eluted in a narrow peak of approximately 4 ml. If imidazole was used as the eluent, BLM eluted at 100-350 mM imidazole (see also Fig. 3.9). The purified protein migrated with an apparent M_r of 180,000 in SDS-PAGE. Judged by Coomassie blue staining, the protein was nearly homogeneous; silver staining revealed a number of contaminants of various sizes present at very low concentrations (data not shown). The yield of purified BLM was between 0.05 mg and 0.25 mg per litre of yeast culture, the most concentrated fractions contained 0.1-0.16 mg/ml (0.625-1 nM) protein. Fractions containing BLM were dialysed against storage buffer. After

dialysis, the protein was quantified with BSA as a standard. Afterwards, the fractions were stored at –80°C in 25% glycerol. Numerous attempts were made to concentrate BLM before dialysis. These included the use of centrifugation concentration devices or the extraction of water from a dialysis bag by a hygroscopic powder. They all failed due to a loss of the protein by its precipitation on the membrane of the concentration device or the dialysis bag. For the same reason, dialysis generally led to a decrease in protein concentration. This effect seemed to be more pronounced in the presence of a salt concentration of <250 mM in the buffer. Furthermore, any attempt to employ a second purification step failed due to the loss of the protein, which could be neither detected in the flow-through nor in the eluate. This suggests that the protein had precipitated either on the column or in the column tubing, or that it had been degraded during the second purification step.

3.2.3 Identification of BLM by western blotting

To identify BLM, samples from the precleared yeast cell lysate prior to purification and from the eluate were western-blotted using two different antibodies. Fig. 3.2 A shows that IHIC33, an affinity-purified polyclonal rabbit antibody raised against an N-terminal fragment of BLM, recognised a 180 kDa protein as well as a 100 kDa protein in both fractions, and two additional smaller proteins in the yeast cell lysate. Fig. 3.2 B shows that a monoclonal anti-histidine tag antibody recognised a single 180 kDa species both in the lysate and in the eluate.

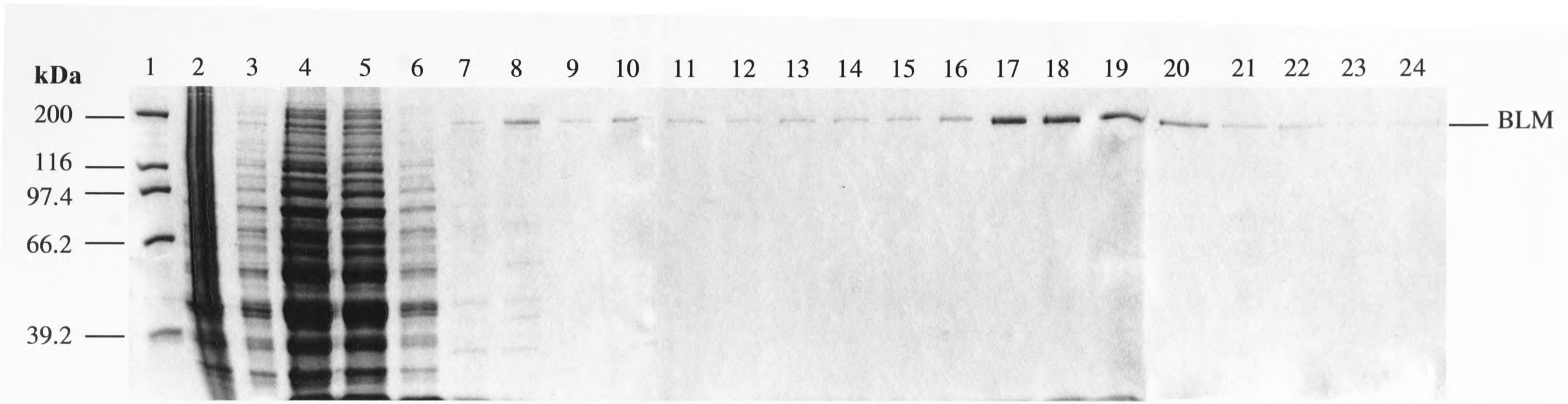


Fig. 3.1. Purification of BLM. A cleared cell lysate from two litres of yeast culture overexpressing BLM was passed over a POROS MC20 column loaded with Ni^{2+}. After washing the column with buffer containing 80 mM imidazole, proteins bound to the column were eluted by a 250 mM EDTA step. Elution fractions of 1 ml were collected and 10 µl were subjected to SDS-PAGE using a 10% gel, followed by staining with Coomassie blue. Lane 1, marker; lane 2, yeast cell lysate; lane 3, yeast cell lysate after centrifugation; lanes 4 and 5, wash fractions; lanes 6-24, elution fractions.

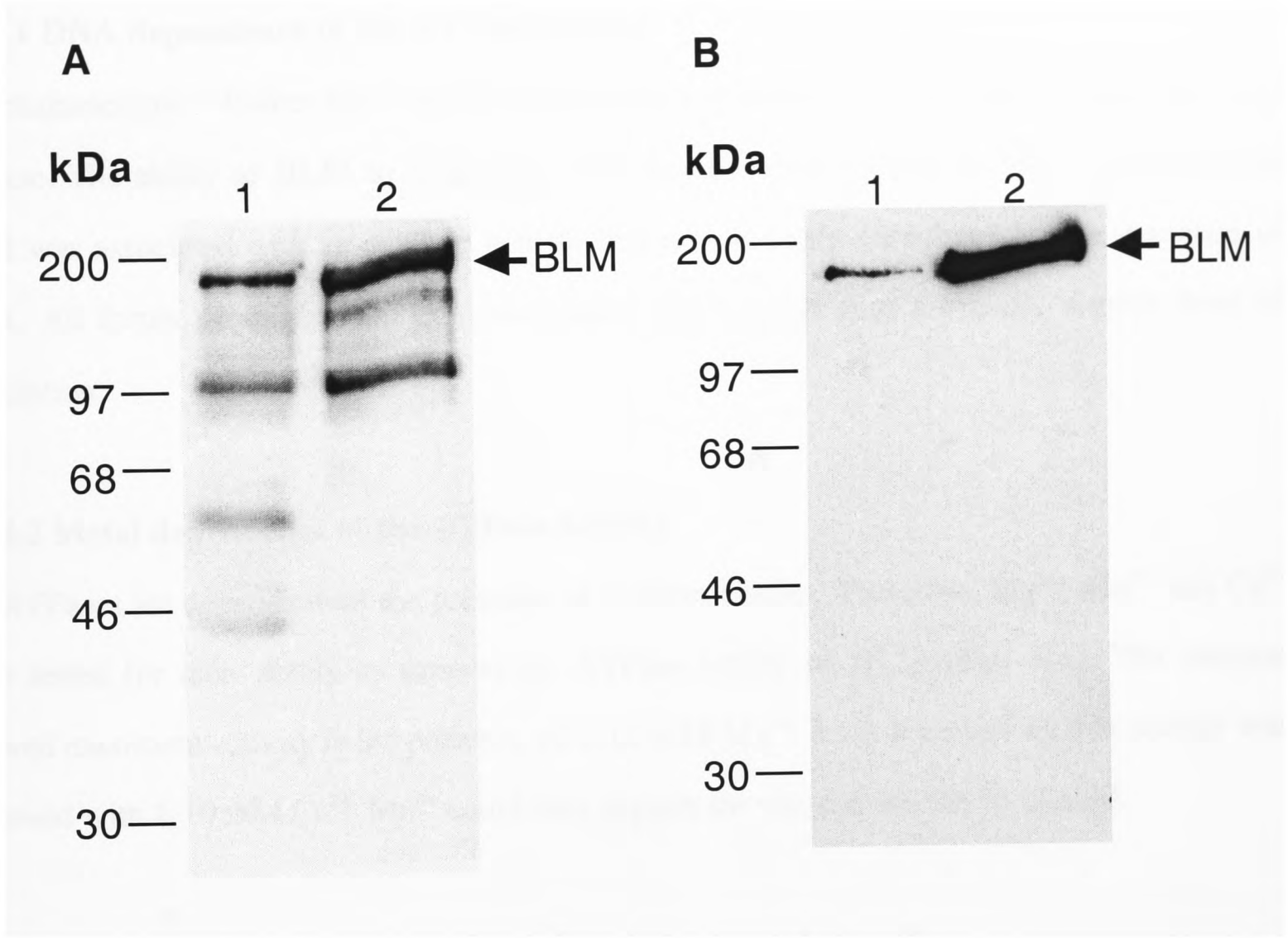


Fig. 3.2. Identification of BLM by western blotting.
(A) rabbit polyclonal antibody (IHIC 33) raised against an N-terminal fragment of BLM, (B) anti-histidine-tag antibody. Lanes: 1, yeast cell lysate; 2, purified BLM.

3.2.4 Characterisation of the ATPase activity of BLM

3.2.4.1 DNA dependence of the ATPase activity

The characteristic "Walker box" motifs in the primary sequence of BLM make it likely to be an ATPase. The ability of BLM to hydrolyse ATP was therefore examined. Fig. 3.3 shows that BLM was associated with an ATPase activity that was strongly stimulated by the presence of DNA. All forms of single- and double-stranded DNA tested gave a broadly similar level of stimulation.

3.2.4.2 Metal dependence of the ATPase activity

All ATPases are dependent on the presence of divalent cations. Therefore, Mg^{2+}, Mn^{2+} and Ca^{2+} were tested for their ability to support the ATPase activity of BLM (Fig. 3.4). The enzyme showed maximum activity in the presence of 2-10 mM Mg^{2+}. Less than half of this activity was achieved with 1-10 mM Ca^{2+}. Mn^{2+} could only support the enzyme activity at <2 mM.

3.2.4.3 (2'-Deoxy)ribonucleoside 5'-triphosphate dependence of the NTPase activity

Some ATPases can hydrolyse ribonucleoside or deoxyribonucleoside triphosphates (NTPs or dNTPs) other than ATP. Therefore, the ability of BLM to use these substrates was tested (Fig. 3.5 A and B). ATP and dATP were hydrolysed most efficiently by BLM. CTP or dCTP only yielded about 25% of this activity. No other substrate was hydrolysed to a significant extent.

3.2.4.4 pH dependence of the ATPase activity

In order to find the optimum pH for the ATPase activity, BLM was assayed in buffers of different pH (Fig. 3.6). The pH optimum was found to be between pH 7.5 and pH 8.5. Virtually no ATPase activity was found at pH 5 or 10.5.

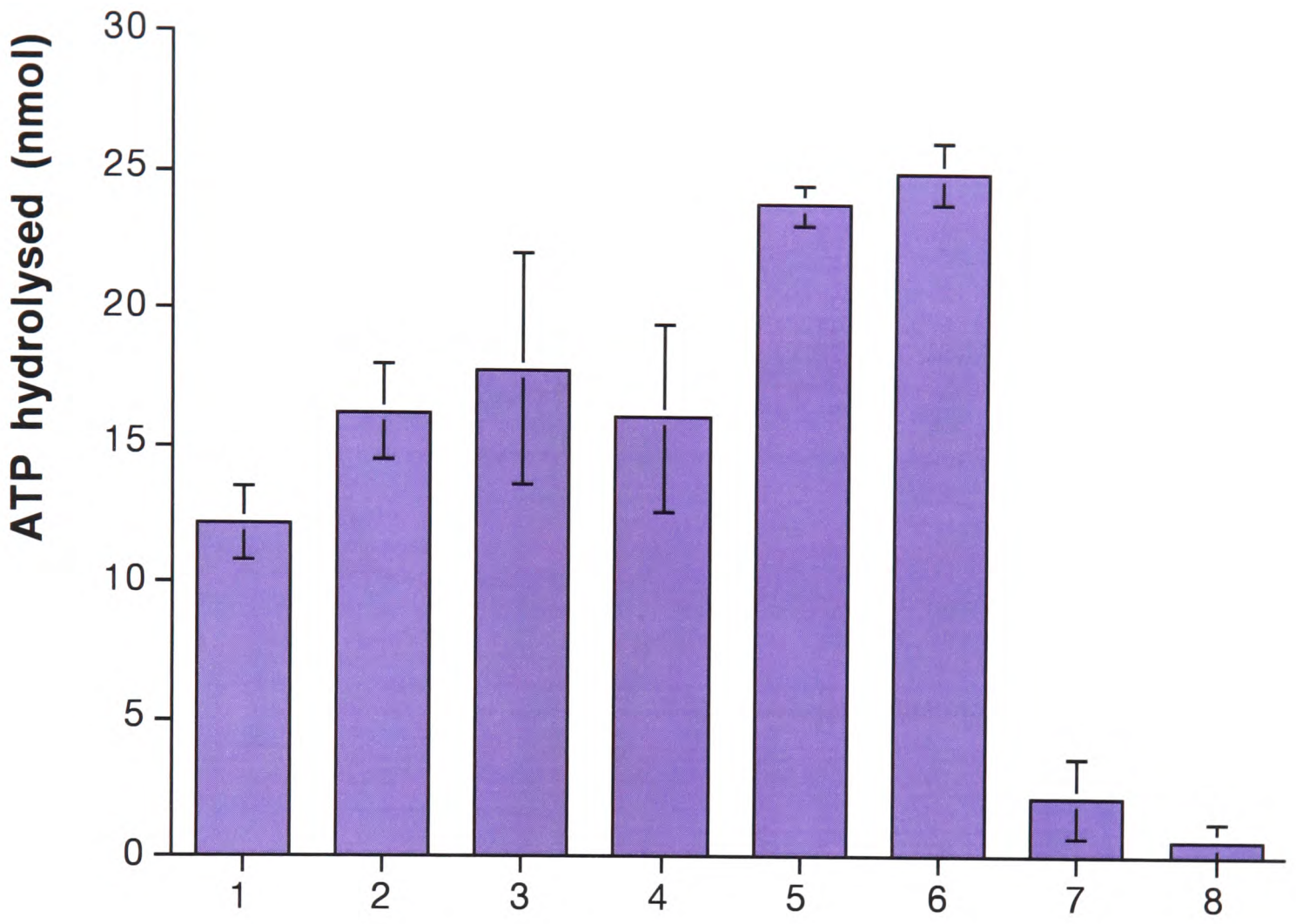


Fig. 3.3. BLM is a DNA-stimulated ATPase.
DNA was present at 76 μM (nucleotides), the incubation time was 30 min. The types of DNA used were a 17mer oligonucleotide (1), a 90mer oligonucleotide (2), M13 single-stranded circular DNA (3), supercoiled plasmid DNA (4), native salmon-sperm DNA (5) and heat-denatured salmon-sperm DNA (6). Controls were no DNA (7) and heat-inactivated BLM (8). Each value repesents the average of three experiments, the error bars show the deviations from the mean.

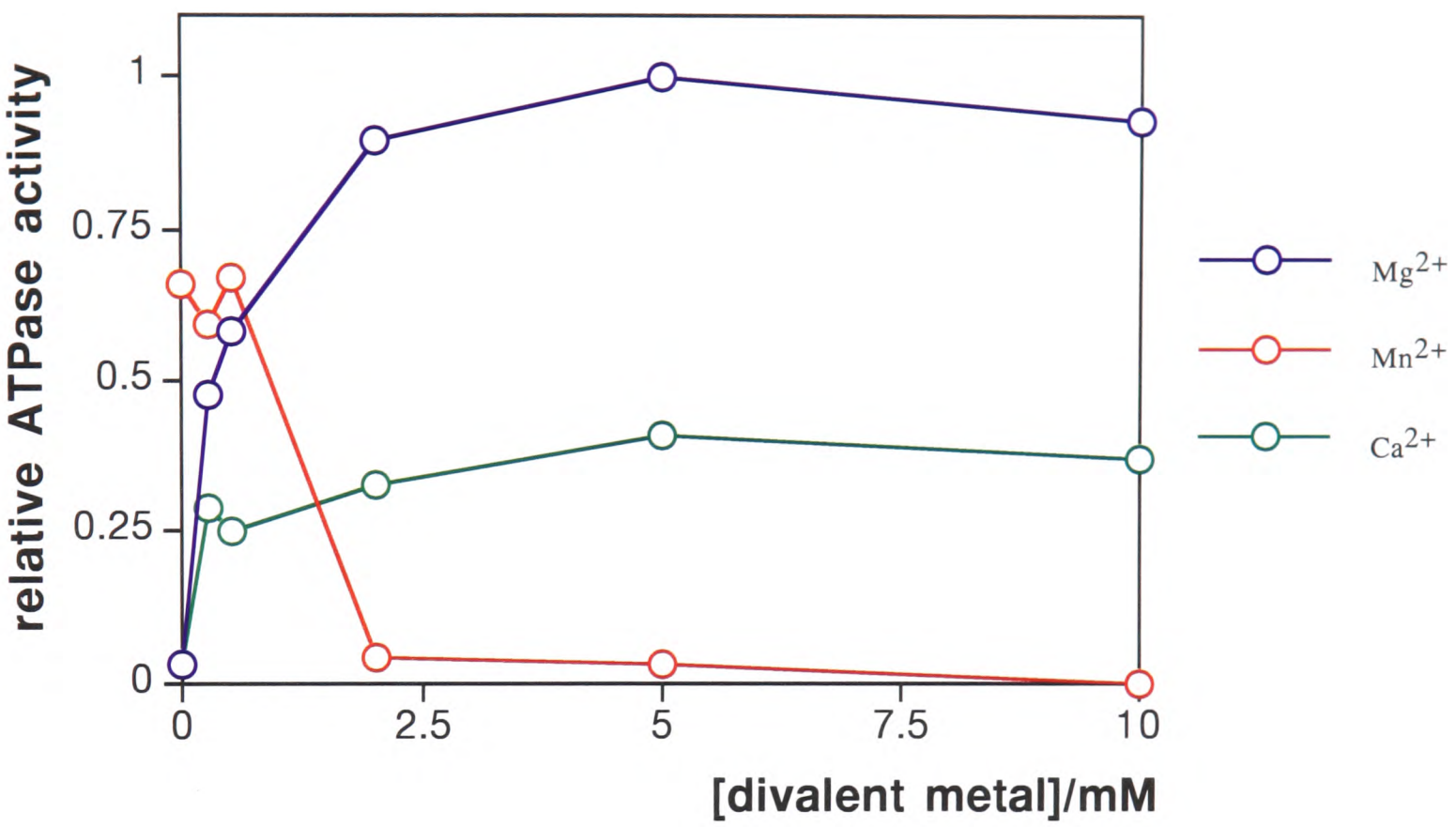
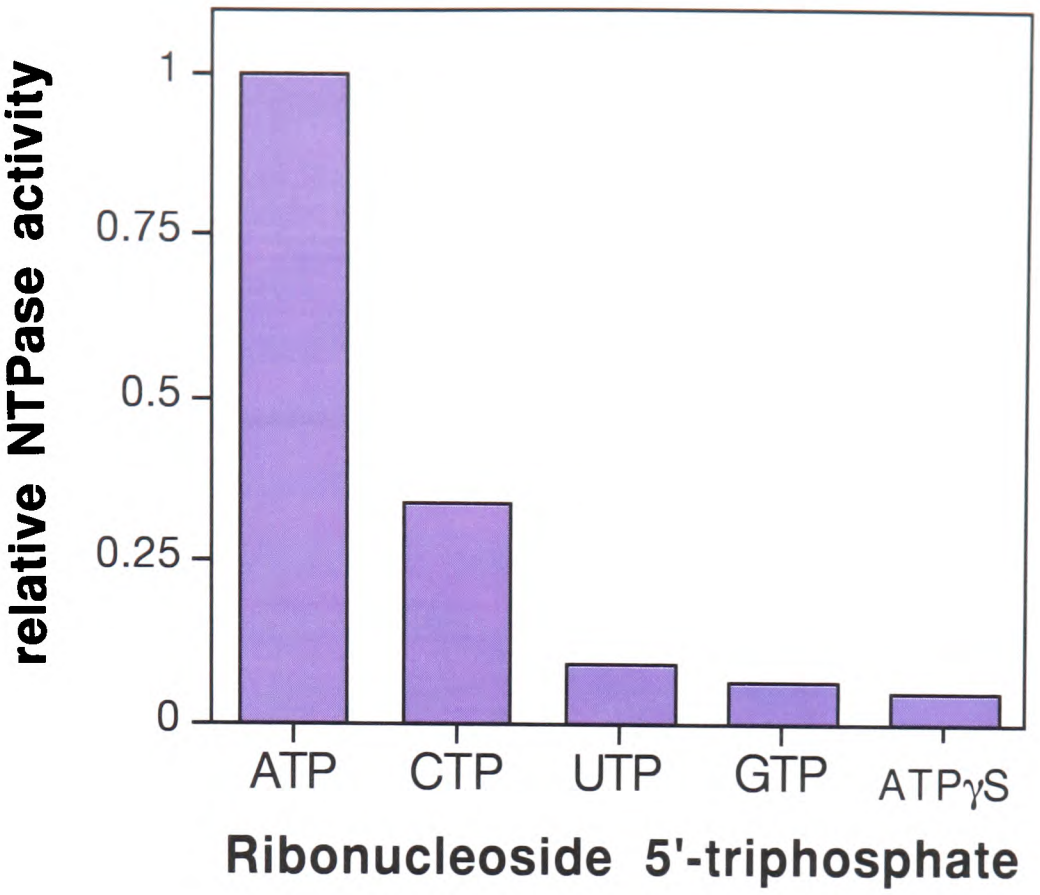


Fig. 3.4. Divalent metal dependence of the ATPase activity of BLM. ATPase activity was measured in the presence of 0-10 mM $MgCl_2$, $MnCl_2$ or $CaCl_2$. 9 nM BLM were incubated for 30 min. A representative example is shown. The maximum ATPase activity of BLM in the presence of $MgCl_2$ has arbitrarily been assigned a value of 1.

A



B

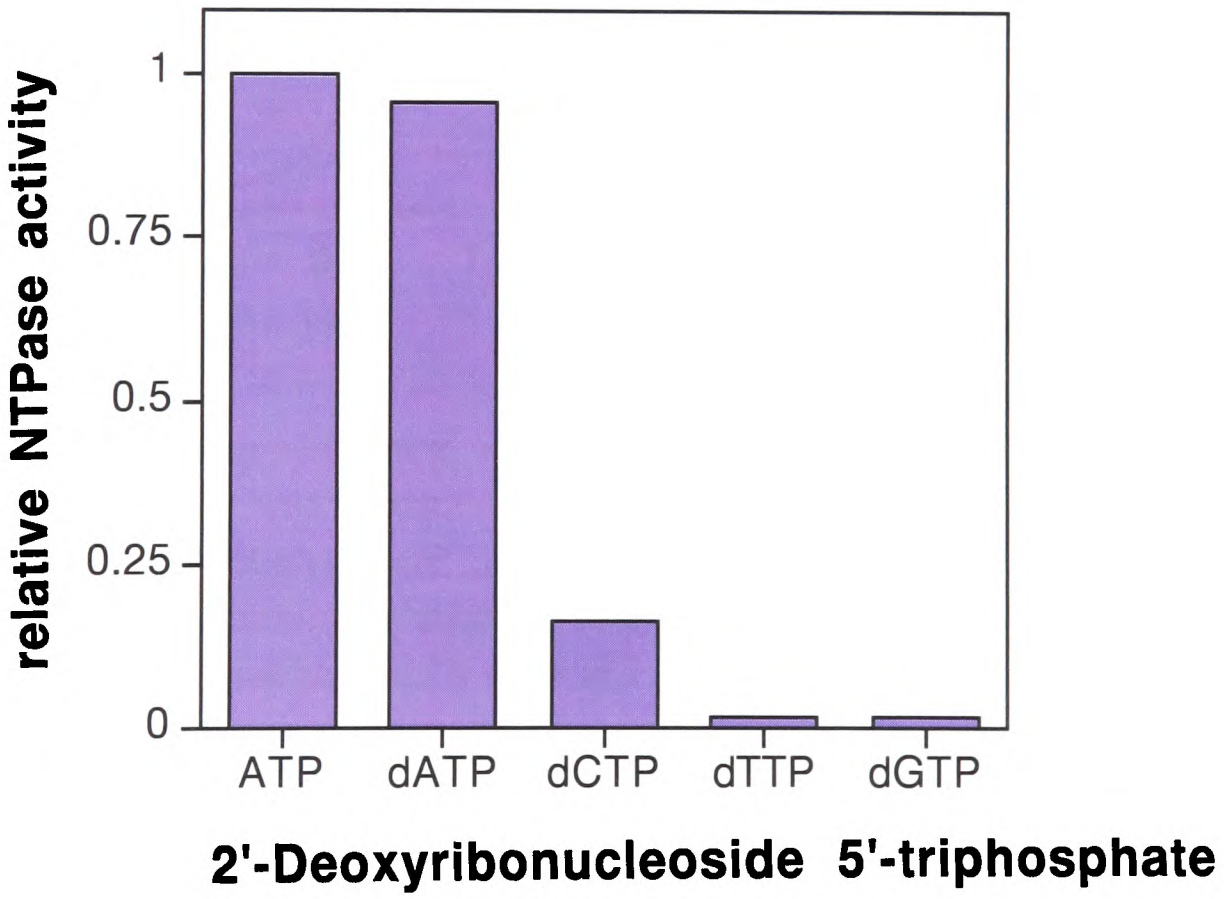


Fig. 3.5. (2'-Deoxy)ribonucleoside 5-triphosphate dependence of the NTPase activity of BLM. NTPase activity was measured in the presence of 2 mM NTPs (A) or dNTPs (B). 10 nM BLM were incubated for 30 min. A representative example is shown. The maximum NTPase activity in the presence of ATP has arbitrarily been assigned a value of 1.

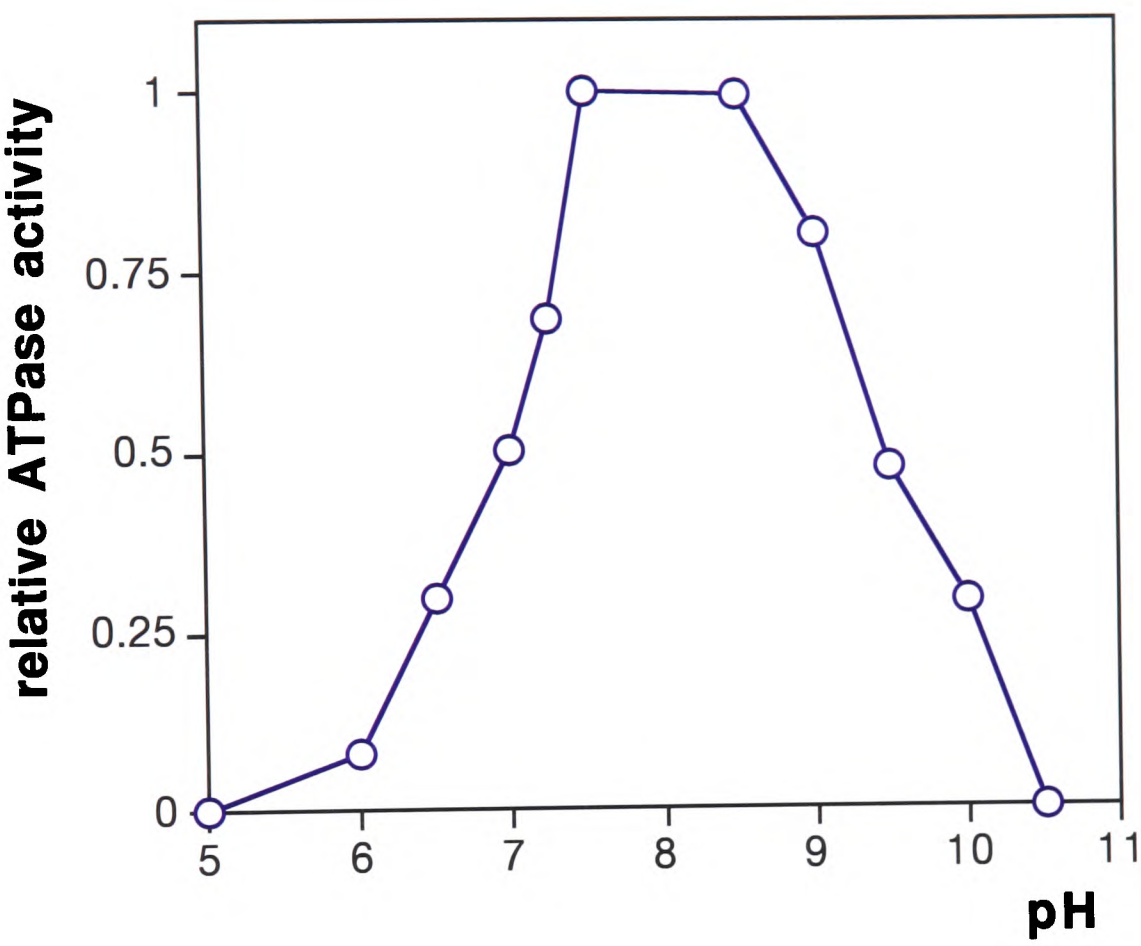


Fig. 3.6. pH-dependence of the ATPase activity of BLM.
ATPase activity was measured at different pH values ranging from pH 5 to pH 10.5. Reactions were incubated for 30 min at 10 nM BLM. A representative example is shown. The maximum ATPase activity in this assay has arbitrarily been assigned a value of 1.

3.2.4.5 Temperature dependence of the ATPase activity

BLM was assayed at different temperatures to find the optimum temperature for ATP hydrolysis (Fig. 3.7). The ATPase activity peaked at 42°C.

3.2.4.6 Salt dependence of the ATPase activity

The ATPase activity of BLM was tested in the presence of three different salts, NaCl, KCl or NH_4Cl, ranging from 0-150 mM in concentration (Fig. 3.8). The activity did not differ between these three salts and did not change over the concentration range tested.

3.2.4.7 ATPase activity copurifies with BLM

To confirm that the DNA dependent ATPase activity found was associated with the BLM protein, fractions from a BLM purification using an imidazole gradient elution were assayed for ATPase activity and subjected to SDS-PAGE. Fig. 3.9 shows that there was a strong correlation between the quantity of BLM protein in each fraction (panel A) and the level of ATPase activity (panel B).

3.2.4.8 Kinetic analysis of the ATPase activity

The rate of ATP hydrolysis was measured as a function of the ATP concentration. Approximately 3 nM BLM were assayed in the presence of 4 mM $MgCl_2$, 76 μM (nucleotides) DNA and 0-4 mM ATP for 20 min. Previous experiments had shown that the rate of cleavage was linear during this interval (data not shown). The ATP cleavage reaction followed Michaelis-Menten kinetics (Fig. 3.10) with a maximum velocity of 0.67 nmol P_i/min, a Michaelis constant (K_M) of 0.3 mM ATP and a turnover number (k_{cat}) of approximately 4000 min^{-1}.

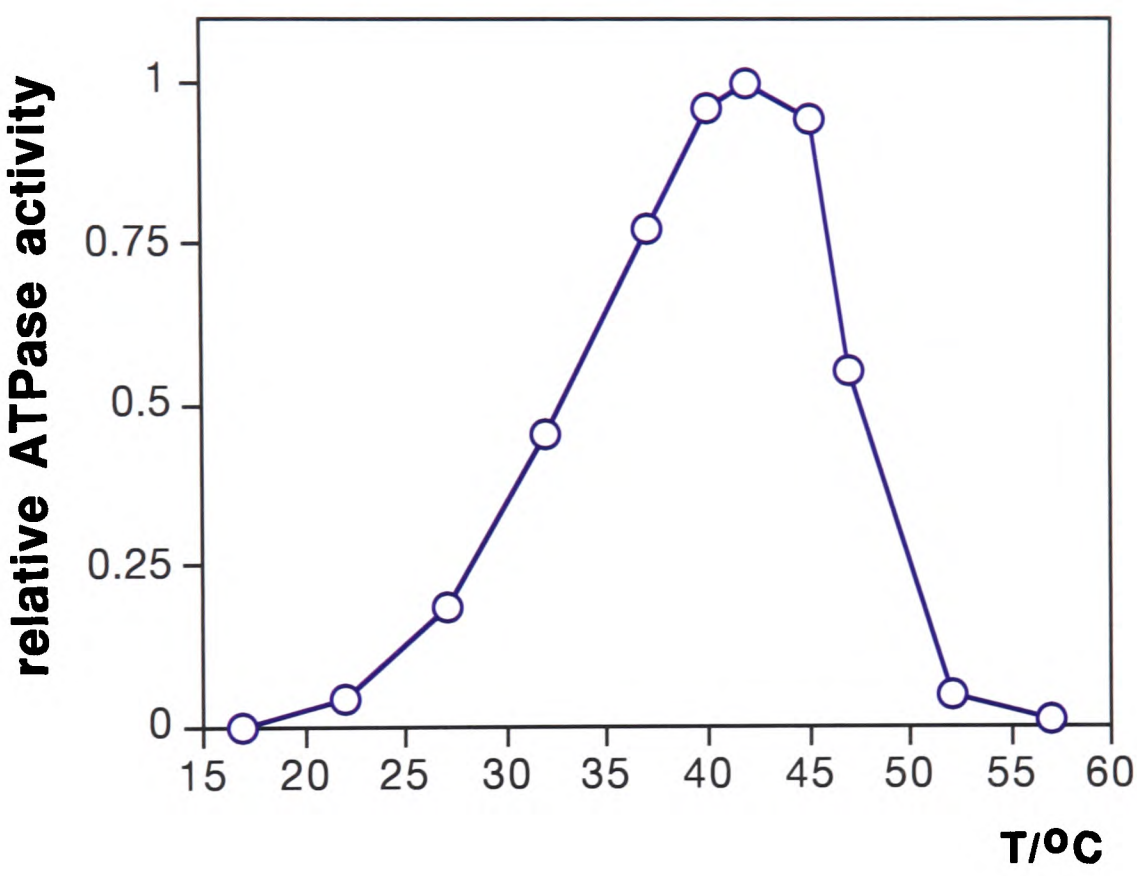


Fig. 3.7. Temperature dependence of the ATPase activity of BLM. ATPase activity was measured at different temperatures ranging from 17°C to 57°C. Reactions were incubated for 30 min at 10 nM BLM. A representative example is shown. The maximum ATPase activity in this assay has arbitrarily been assigned a value of 1.

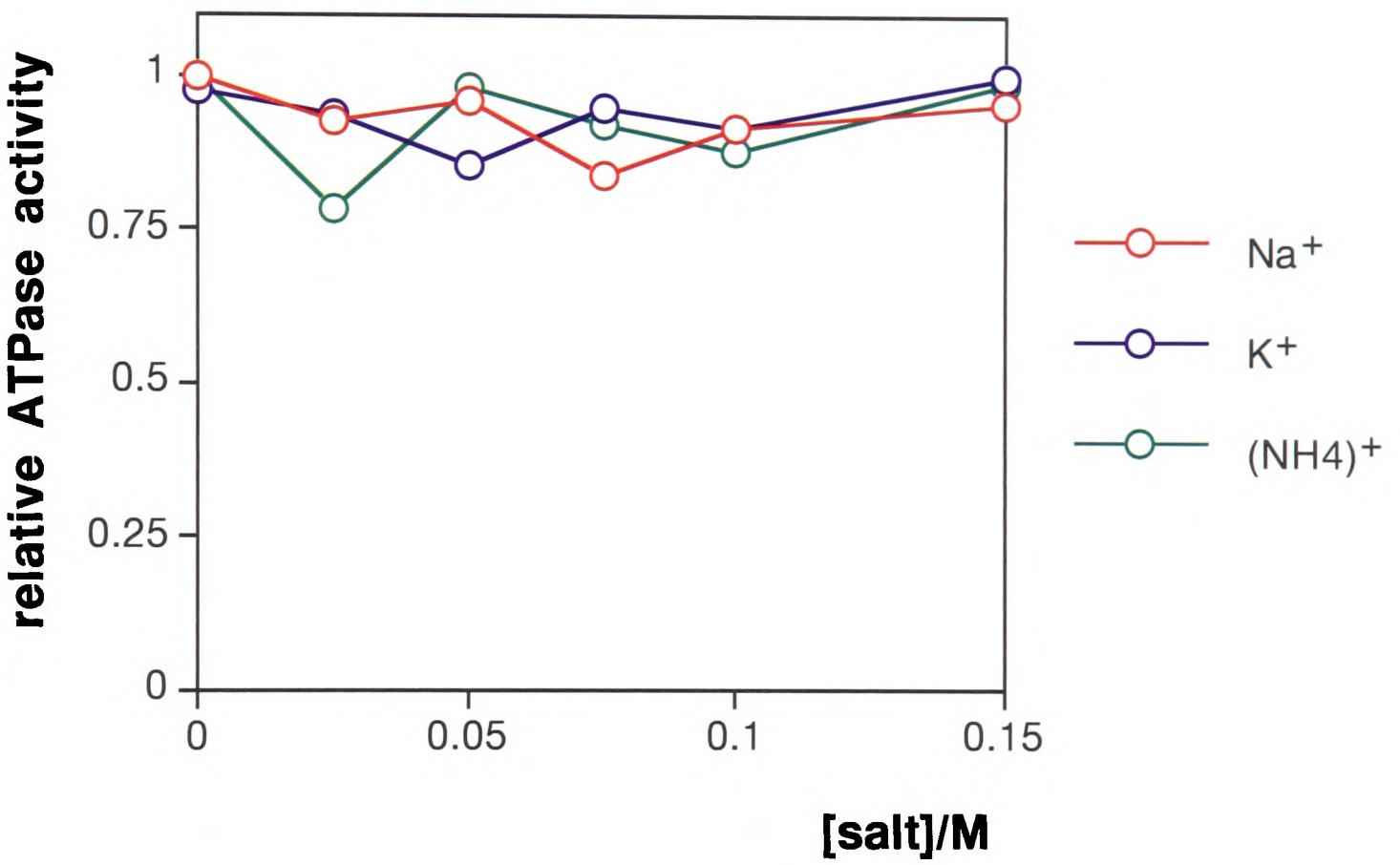


Fig. 3.8. Salt dependence of the ATPase activity of BLM. ATPase activity was measured at different concentrations of NaCl, KCl and NH_4Cl ranging from 0-150 mM. Reactions were incubated for 30 min at 10 nM BLM. A representative example is shown. The maximum ATPase activity in this assay has arbitrarily been assigned a value of 1.

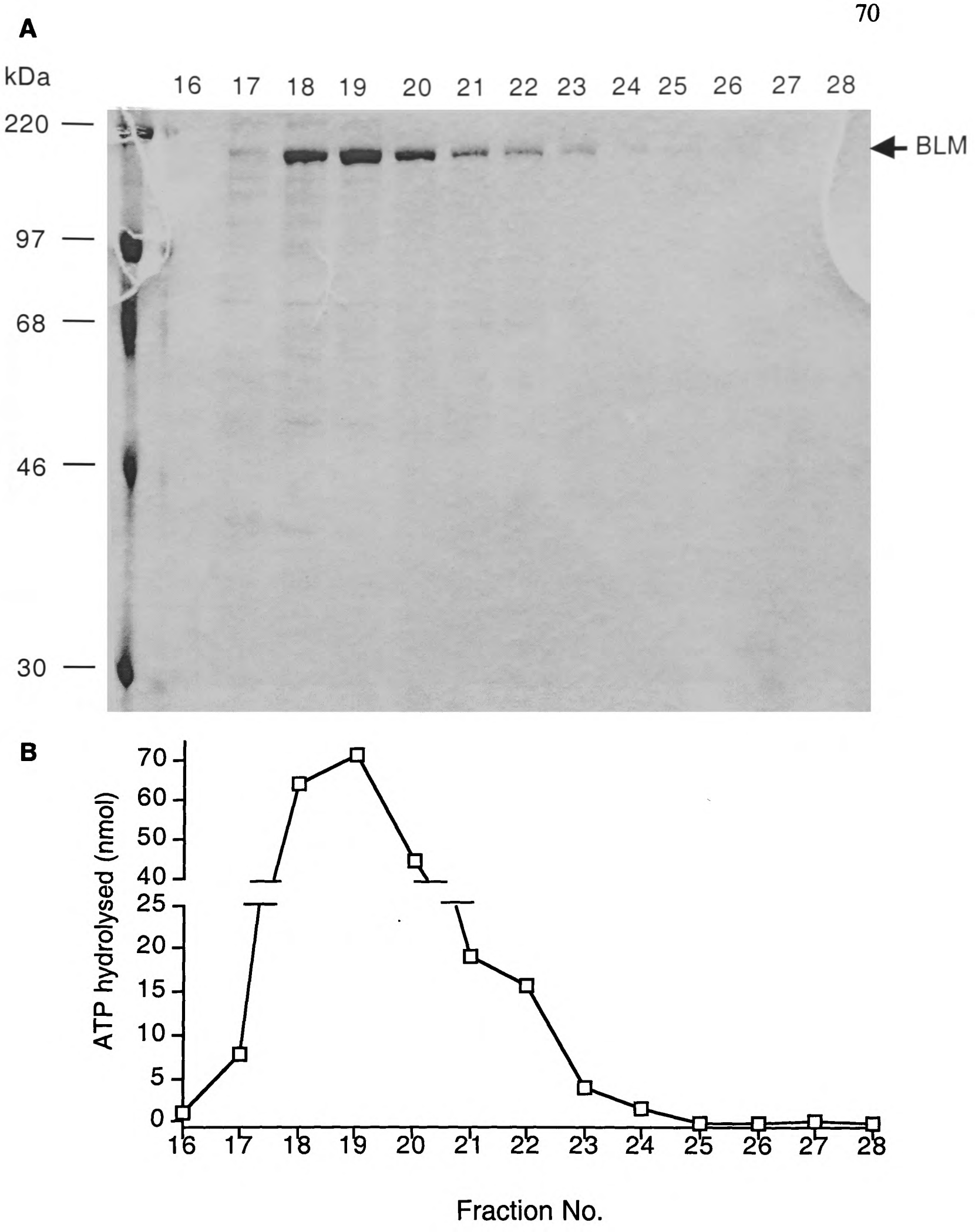


Fig. 3.9. ATPase activity copurifies with BLM protein.
Fractions from a BLM purification using imidazole to elute bound proteins were analysed by SDS-PAGE followed by staining with Coomassie Blue (A) and assayed for ATPase activity (B). Fraction numbers are indicated. Note that the y-axis is broken in B.

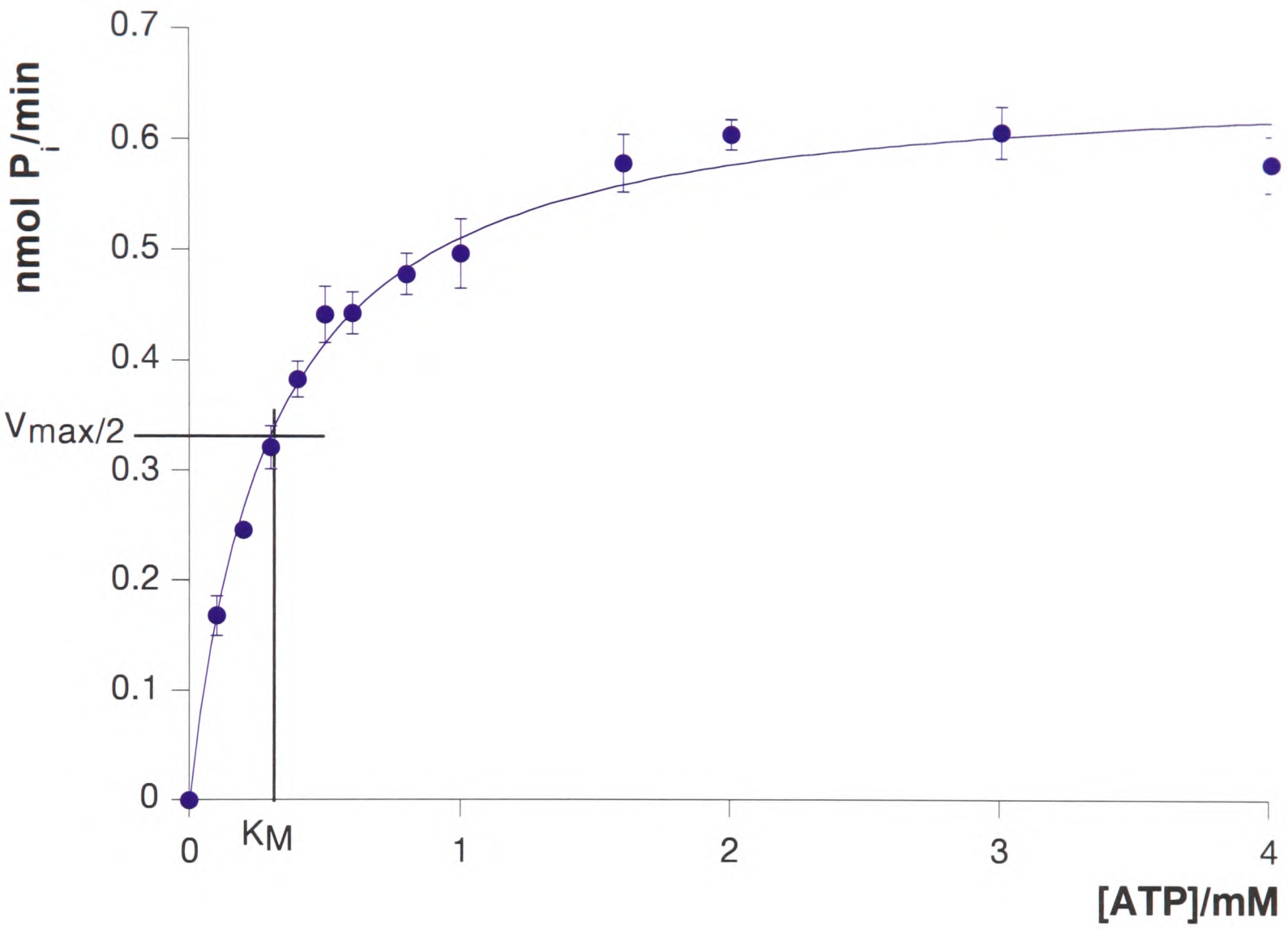


Fig. 3.10. Enzyme kinetics of the ATPase activity of BLM. The release of inorganic phosphate (P_i) was measured as a function of the ATP-concentration. Approximately 3 nM BLM were incubated with 0-4 mM ATP in the presence of 4 mM $MgCl_2$ and 76 μM DNA for 20 min. Each data point represents the mean of three determinations. The K_M is 0.3 mM +/-0.02, V_{max} is 0.67 nmol P_i/min +/-0.01. (The data were fitted to the Michaelis-Menten equation ($v = V_{max} * [ATP]/(K_M+[ATP])$ using Kaleidagraph.)

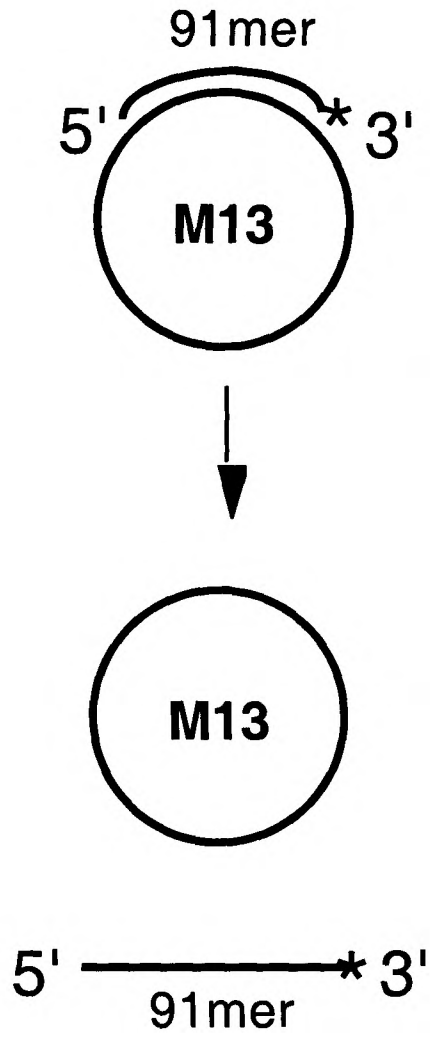
3.2.5 Helicase activity of BLM

The *E. coli* RecQ protein is a 3'-5' DNA helicase. BLM, like RecQ, contains the seven helicase motifs (including a DExH-box) of the SF2 superfamily of helicases, suggesting that BLM is also a helicase. To analyse whether the purified BLM protein possesses DNA unwinding activity, a partially double-stranded substrate was prepared by annealing a 90mer oligonucleotide to single-stranded M13 DNA and radiolabelling it at its 3'-end (Fig. 3.11 A). This substrate was incubated with purified BLM protein, and the reaction products were separated on a polyacrylamide gel and detected by autoradiography. Fig. 3.11 B shows that BLM released the radiolabelled oligonucleotide, a process dependent on the presence of Mg^{2+} and ATP.

3.2.6 Polarity of the helicase activity

Helicases generally possess a polarity of unwinding, which is operationally defined by "the backbone polarity of the flanking single-stranded DNA that facilitates initiation of DNA unwinding *in vitro*" (Lohman and Bjornson 1996). To determine the polarity of the BLM helicase, a substrate consisting of a 90mer oligonucleotide annealed to single-stranded M13 DNA was prepared. This was digested with *Sal*I and the 3'-ends were radiolabelled, creating a linear DNA molecule with 37mer and 55mer double-stranded portions at its ends (Fig. 3.12 A). Following incubation of the substrate with BLM, the 37mer oligonucleotide was completely released whereas no increase of released 55mer over background was observed (Fig. 3.12 B). This reaction was dependent on Mg^{2+} and ATP. According to this result, the direction of DNA unwinding by BLM can be formally defined as 3'-5'. To address the polarity of unwinding further, another substrate was created by annealing radiolabelled 21mer and 30mer oligonucleotides to the ends of a 90mer oligonucleotide (Fig. 3.13 A). In contrast to the substrate described above, here a helicase with 3'-5' polarity would have to unwind the longer of the two oligonucleotides. Increasing concentrations of BLM led to a progressive release of the 30mer oligonucleotide, and, at higher concentrations, of the 21mer oligonucleotide (Fig. 3.13 B).

A



B

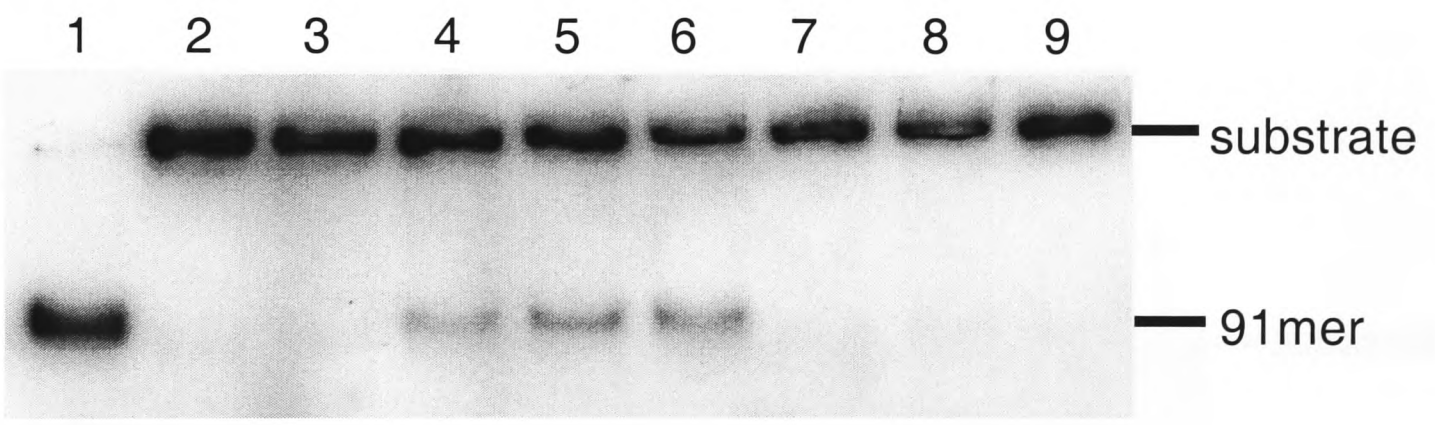


Fig. 3.11. Helicase activity of BLM. (A) scheme for the unwinding assay. A 90mer oligonucleotide was annealed to single-stranded M13 DNA and radiolabelled at its 3'-end. (B) Reactions were incubated for 30 min and run on a 15% polyacrylamide gel. Lanes: 1, heat denatured substrate; 2, native substrate; 3, 1.5 nM BLM; 4, 3 nM BLM; 5, 15 nM BLM; 6, 60 nM BLM; 7, 60 nM BLM, no Mg^{2+}; 8, 60 nM BLM, no ATP; 9, 60 nM heat-inactivated BLM. The positions of the substrate and of the 91mer product are indicated on the right.

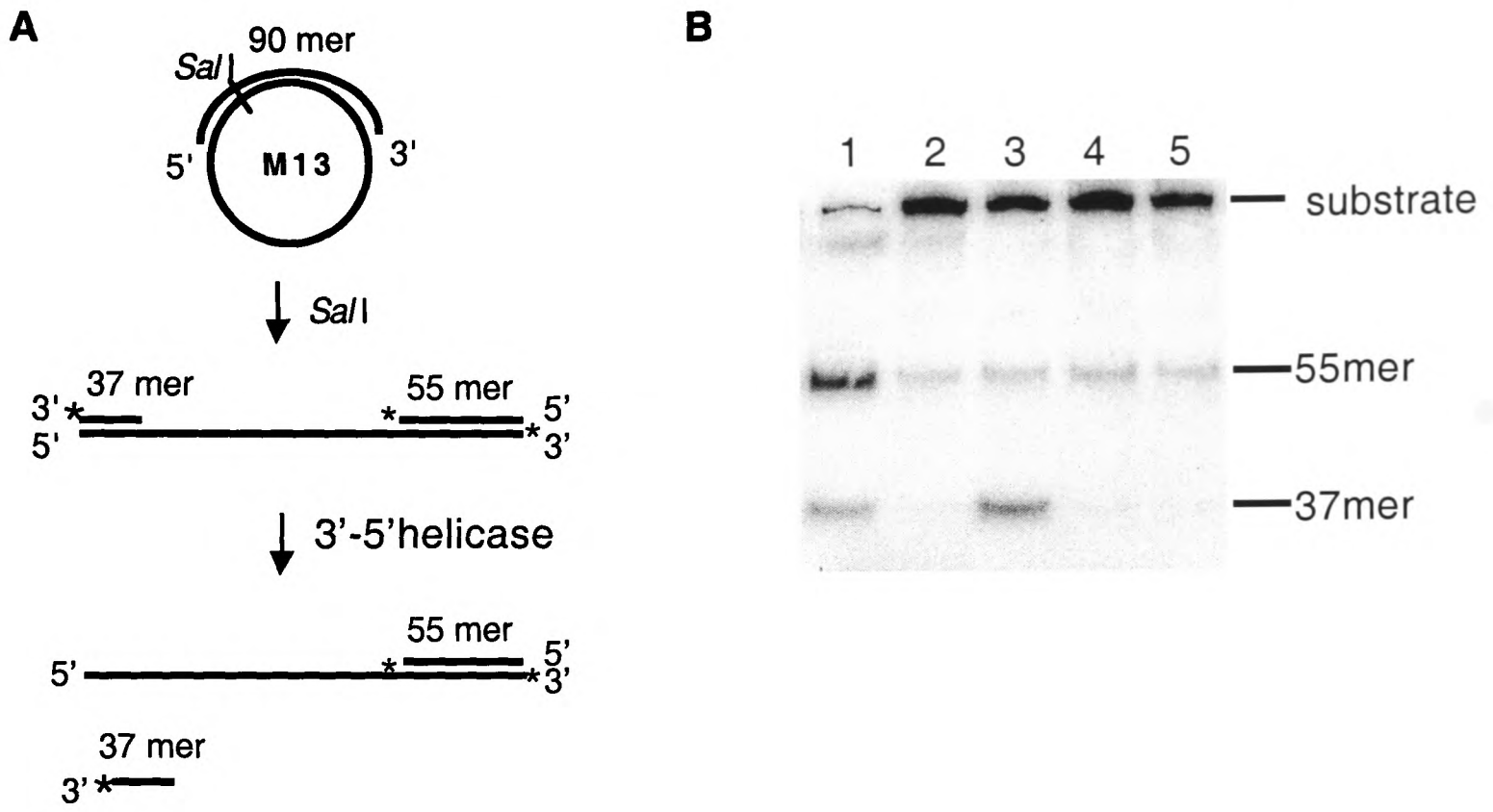


Fig. 3.12. Polarity of the BLM helicase activity I. (A) Scheme for the unwinding assay. A 90mer oligonucleotide was annealed to single-stranded M13 DNA and digested with *Sal*I to yield a partially double-stranded substrate . All 3'-ends were radiolabelled. (B) Reactions were incubated for 30 min and run on a 15% polyacrylamide gel. Lanes: 1, heat-denatured substrate; 2, native substrate; 3, 30 nM BLM; 4, 30 nM BLM, no Mg^{2+} ; 5, 30 nM BLM, no ATP. The positions of the substrate and of the 55mer and 37mer products are indicated on the right.

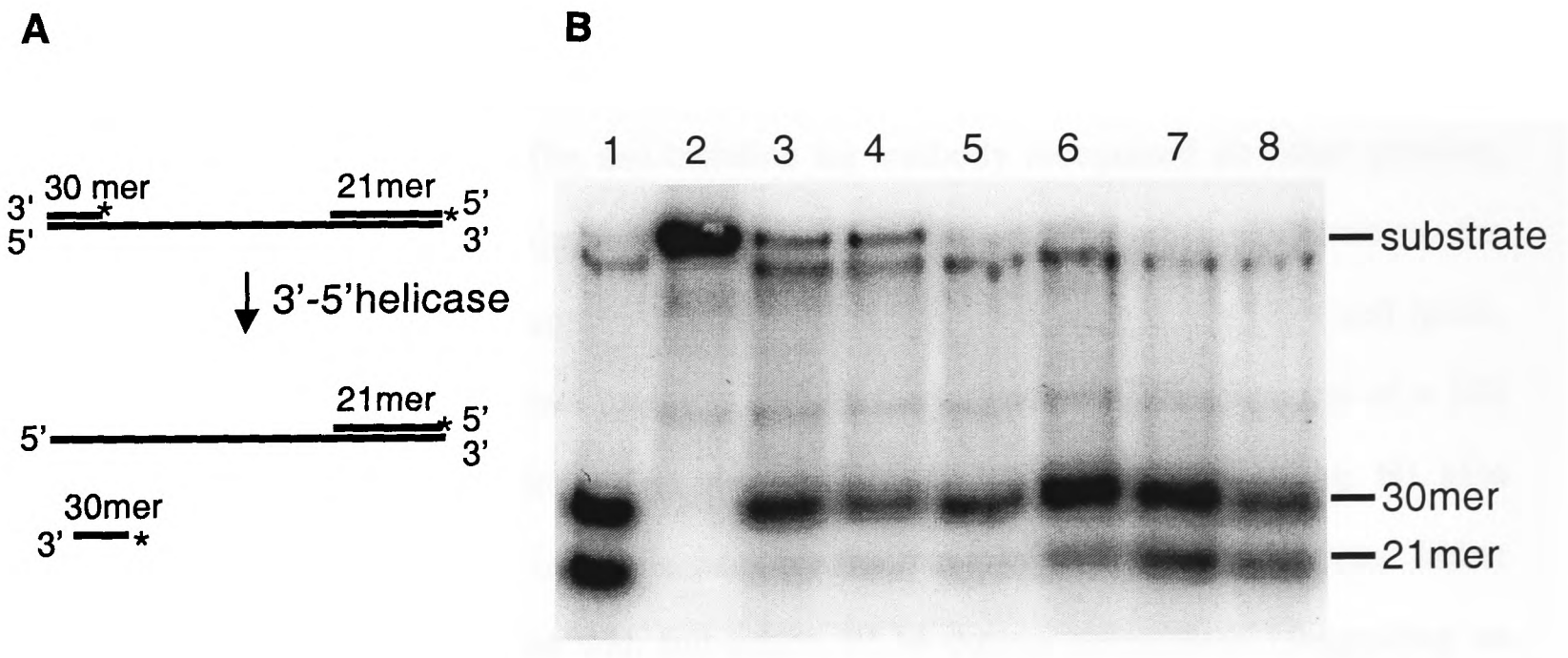


Fig. 3.13. Polarity of the BLM helicase activity II. (A) Scheme for the unwinding assay. A 21mer and a 30mer oligonucleotide were radiolabelled at their 5'-ends and annealed to a 90mer oligonucleotide. (B) Reactions were incubated for 10 min (5 mM $MgCl_2$, 5 mM ATP). Samples were run on an 18% polyacrylamide gel. Lanes: 1, heat-denatured substrate; 2, native substrate; 3, 0.75 nM BLM; 4, 1.5 nM BLM; 5, 3 nM BLM; 6, 6 nM BLM; 7, 15 nM BLM; 8, 30 nM BLM. The positions of the substrate and of the 30mer and 21mer products are indicated on the right.

3.3 Discussion

I have purified recombinant BLM protein to near homogeneity and demonstrated that it possesses DNA-stimulated ATPase activity and helicase activity, unwinding DNA primarily with a 3'-5'-polarity.

The use of a C-terminal hexahistidine tag allowed a one-step purification of BLM to near-homogeneity by metal chelate affinity chromatography. The purified protein was prone to precipitation, especially in the presence of low concentrations of salt. This suggests that its native conformation might be stabilised by hydrophobic interactions that are buried in the presence of high salt and might become exposed at low salt concentrations. However, the ATPase activity of BLM was insensitive to the salt concentration in the buffer over a range of 0-150 mM (Fig. 3.8). The full-length BLM protein migrated at a M_r (relative molecular mass) of 180,000 in SDS-PAGE. This M_r differs from the predicted M_r of 159,000. The reason for this might be some posttranslational modifications in the recombinant protein, like phosphorylation, glycosylation or SUMO-modification, which would increase its relative molecular mass. Both a rabbit polyclonal antibody raised against an N-terminal fragment of BLM and an anti-histidine tag antibody recognised the full-length protein. The anti-histidine tag antibody recognised no other proteins, suggesting that no breakdown products lacking the N-terminus were purified. However, the polyclonal antibody recognised a number of additional bands, especially in the yeast cell lysate, suggesting the presence of breakdown products lacking the C-terminus. The presence of a 100 kDa breakdown product in the eluate but the apparent lack of a corresponding 60 kDa breakdown product with a histidine tag in the same fraction has two possible explanations. Either the 100 kDa product was associated with full-length BLM during purification (suggesting an oligomeric state of BLM), or the missing 60 kDa product was subject to C-terminal degradation, making it "invisible" to the anti-histidine tag antibody.

The ATPase activity of BLM was very low in the absence of DNA and was strongly stimulated by both single-stranded and double-stranded DNA, circular or linear. This is in accordance with the ATPase activity of the budding yeast homologue Sgs1, which was stimulated by a similar range of DNAs, including circular relaxed double-stranded DNA (Bennett *et al.* 1998). However, the human homologue WRN and the *E. coli* homologue RecQ were better stimulated by single-stranded than double-stranded DNA (Orren *et al.* 1999; Umezu *et al.* 1990). The fact that single-stranded DNA activated BLM to a similar extent as double-stranded DNA suggests that the ATPase activity of BLM is independent of any unwinding activity (which is only possible in the presence of at least partially double-stranded DNA). I have shown that BLM is unable to bind or unwind a completely double-stranded blunt-ended substrate (see chapter 5), yet double-stranded DNA stimulated the ATPase activity. However, the supercoiled plasmid DNA used in this experiment might have displayed single-stranded regions due to negative supercoiling of the DNA. Linear and covalently-closed circular DNA stimulated the ATPase activity equally well. This shows that BLM does not need a DNA end to interact with, a property that might have implications for its ability to unwind certain substrates (see chapter 5).

The ATPase activity was strongly promoted by Mg^{2+} and to some extent by Ca^{2+}, but only by low concentrations (<2 mM) of Mn^{2+} ions. This is similar to RecQ that can use Mg^{2+}, Mn^{2+}, Ca^{2+} and to a limited extent (at 2 mM) Zn^{2+} (Umezu *et al.* 1990). ATP and dATP were the most effectively hydrolysed (2'-deoxy)ribonucleoside 5'-triphosphates. They could be partially replaced by CTP or dCTP but not by any other (d)NTP. The WRN helicase was also found to be able to utilise ATP, dATP, CTP and dCTP for its unwinding activity (Shen *et al.* 1998b). RecQ is known to be able to hydrolyse ATP and dATP but not GTP (Umezu 1990). The pH optimum for the ATPase activity of BLM is 7.5-8.5. This is slightly above the physiological pH of 7.2 in the cell. However, there might be a different pH in the nuclear microenvironment

where BLM is normally located. The optimum temperature for the ATPase activity is 42°C. This is above the body temperature of 37°C and probably reflects the general increase of chemical reaction rates with temperature until the enzyme denatures. The protein is active as an ATPase in the presence of NaCl, KCl or NH_4Cl, and the activity does not differ over a salt concentration from 0-150 mM. This is in marked contrast to Sgs1 which was reported to be very sensitive to the salt concentration in the reaction buffer with a 90% reduced helicase activity at 100 mM salt compared to no salt (Bennett *et al.* 1998). The fact that the ATPase activity coeluted with BLM confirms that this activity is associated with BLM rather than with a contaminant, unless this contaminant elutes with the same profile as BLM. In order to confirm the ATPase activity of BLM beyond doubt, it would be necessary to mutate one of the key residues for the ATPase activity (e.g. the invariant K in helicase motif I) and prove that the mutant protein, purified in an identical way, is inactive. The kinetics for the ATPase activity of BLM follows Michaelis-Menten-kinetics. The maximum rate for the release of inorganic phosphate was 0.67 nmol P_i/min, the K_M of the reaction was 0.3 mM ATP, and the k_{cat} was approximately 4000 min^{-1}. This k_{cat} differs from the k_{cat} values published for WRN, which range from 50-200 min^{-1} (Orren *et al.* 1999, Brosh *et al.* 1999) to 1,000,000 min^{-1} (Suzuki *et al.* 1997). However, these values might not be comparable since they were obtained under slightly different reaction conditions. The K_M of 0.3 mM ATP obtained for BLM is slightly higher than that of 51 µM published for WRN (Shen *et al.* 1998b). However, the K_M for WRN refers to the helicase activity, not the ATPase activity. Also, again, different reaction conditions were used for the two proteins.

BLM unwinds a 90mer oligonucleotide annealed to single-stranded M13. This result has two implications. It shows that BLM is a relatively efficient helicase compared to WRN, which cannot even efficiently unwind a substrate of 42 nucleotides unless a single-strand binding

protein is present (Gray *et al.* 1997, Shen *et al.* 1998b, Brosh *et al.* 1999). Secondly, it shows that BLM does not need a free single-stranded DNA tail to start unwinding, suggesting that it is able to load onto covalently-closed single-stranded DNA. The unwinding patterns of two substrates in Fig. 3.12 and Fig. 3.13 suggest BLM has 3'-5' polarity with respect to the single-strand it might interact with first. However, in one of the assays, at high concentrations of BLM (>3 nM) the substrate indicating 5'-3' polarity was also unwound. There are two possible explanations for this: Either BLM can initiate unwinding from a blunt end, or the polarity of BLM is not as strictly defined as is generally assumed. The first explanation can be ruled out since later experiments showed that BLM is unable to unwind a double-stranded, blunt-ended 25mer (data not shown) or 50mer (see chapter 5). Furthermore it was shown later that BLM could unwind both a substrate with a 3'-tail and one with a 5'-tail to a limited extent (see chapter 5). Therefore, BLM might be able to interact with DNA single strands in both directions. This interpretation will have to await more refined structural analysis of DNA-helicase complexes. It should be noted that Sgs1 was also found to unwind a substrate defining 5'-3' activity to a limited extent (Bennett *et al.*1998).

Chapter 4: Structure of BLM

4.1 Introduction

Almost all helicases for which the assembly state has been determined form oligomers, in particular dimers or hexamers (Lohman and Bjornson 1996). Therefore, it seemed interesting to study the potentially oligomeric state of BLM. BLM belongs to the SF2 superfamily (Gorbalenya and Koonin 1993), which contains proteins with seven conserved helicase motifs. None of the known hexameric helicases belongs to this superfamily: DnaB, T7gp4 and T4gp41 are members of the DnaB-like family, Rho belongs to the Rho/proton-translocating ATPase family, SV40 large T antigen is part of superfamily SF3, and RuvB belongs to superfamily 4. However, some members from superfamilies SF1 and SF2 are dimeric: Rep and UvrD belong to SF1 (but UvrD may also form higher oligomers (Runyon *et al.* 1993)), UL9 is a member of SF2. At the beginning of this study, no member of the RecQ family had been studied in terms of their oligomeric state yet. Four techniques have primarily been employed in the past to study the assembly state of helicases: size exclusion chromatography (gel filtration), electron microscopy, density gradient centrifugation and SDS-PAGE after subunit crosslinking. The first two methods were used in this study.

4.2 Results

4.2.1 Size-exclusion chromatography of purified BLM

In order to characterise the quaternary structure of purified BLM protein, I carried out size-exclusion chromatography using a superose 6 column on the FPLC. The vast majority of BLM eluted in a peak covering an elution volume of 11.5-12.5 ml (Fig. 4.1 B, western blot). On the basis of the elution of molecular mass standards, this peak covers a range of molecular masses between 670 kDa (thyroglobulin) and 950 kDa (IgM). Each fraction was also assayed for its ability to catalyse ATP hydrolysis in a DNA-dependent manner. Figure 4.1 A shows that the major peak of ATPase activity coeluted with BLM, indicating that the protein in the complex is enzymatically active. In addition to the major peak of ATPase activity, a lower level of activity was observed between the main peak and a position near the γ-globulin standard (M_r 158,000).

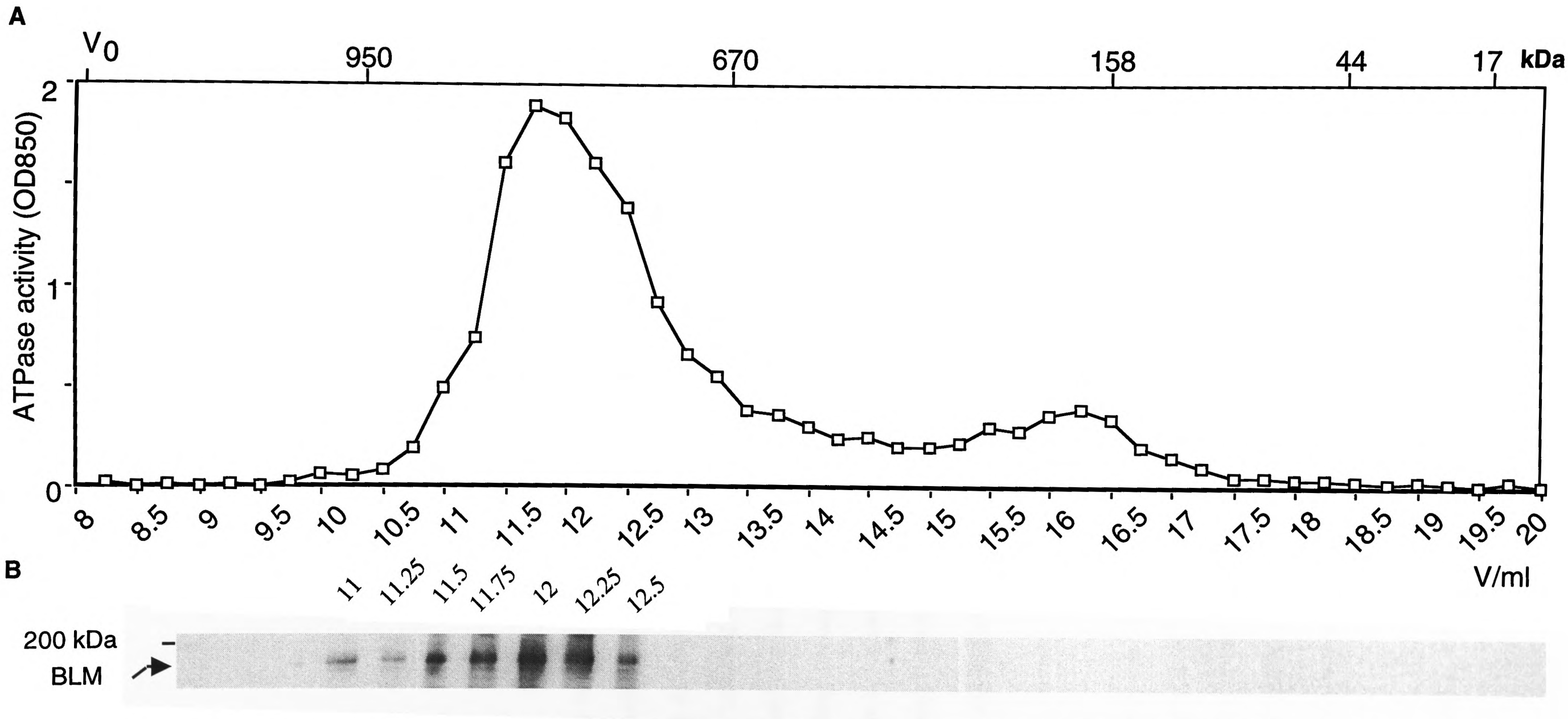


Fig. 4.1. Size-exclusion chromatography (gel filtration) of purified BLM. Approximately 15 µg BLM protein were applied to a superose 6 column. (A) ATPase activity of 0.25 ml elution fractions. The elution positions of the following standards are shown: dextran blue (void volume, V_o), immunglobulin M (950 kDa), thyroglobulin (670 kDa), γ-globulin (158 kDa), ovalbumin (44 kDa) and myoglobin (17 kDa). (B) Western blot of the elution fractions from 10.25 ml to 16.75 ml using IHIC33 (anti-BLM polyclonal antibody). Fractions containing BLM are labelled above the lanes.

4.2.2 Size-exclusion chromatography of extracts from yeast overexpressing BLM

To confirm that the oligomeric BLM complex found is not an artefact of the purified protein but already exists prior to purification, a precleared extract from yeast cells overexpressing BLM was passed over a superose 6 column using the same running conditions as for the purified protein. Western-blotting of the fractions (Fig. 4.2) shows that the majority of BLM eluted in a peak covering an elution volume of 10.5-12.0 ml, placing it between the molecular mass standards of 950 kDa and 670 kDa (see Fig. 4.1).

4.2.3 Size-exclusion chromatography of HeLa cell extracts

In order to find out whether BLM forms a complex of similar size *in vivo*, a HeLa whole cell extract was passed over a superose 6 column using the same running conditions as for purified BLM. The elution fractions were subjected to western-blotting which shows, despite the poor quality of the blot, that the majority of BLM eluted in a peak covering fractions 11.5-12.5, between the molecular mass standards of 950 kDa and 670 kDa. In these fractions, the antibody recognised both full-length BLM and a degradation product of approximately M_r 130,000. Furthermore, a small amount of degraded BLM (two breakdown products of approximately M_r 130,000 and M_r 100,000) eluted in a peak covering fractions 15.5-16.5, close to the molecular mass standard of 158 kDa.

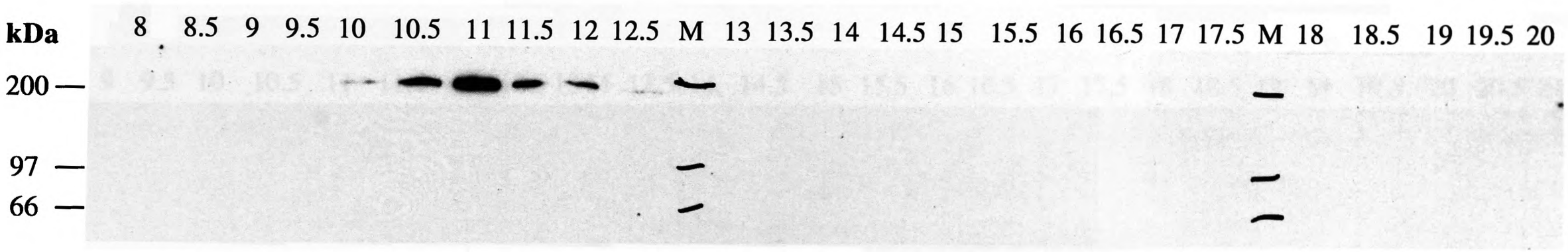


Fig. 4.2. Size-exclusion chromatography (gel filtration) of a lysate from yeast overexpressing *BLM*.
200 µl yeast lysate were applied to a superose 6 column. Western blot of 0.5 ml elution fractions (elution volume 8 ml-20 ml) using IHIC33 (polyclonal anti-BLM antibody).

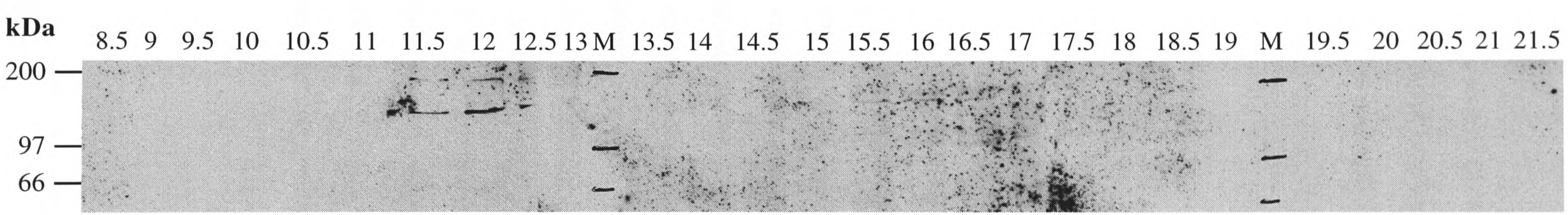


Fig. 4.3. Size-exclusion chromatography (gel filtration) of a HeLa cell extract.
200 µl cell extract were applied to a superose 6 column. Western blot of 0.5 ml elution fractions (elution volume 8.5-21.5 ml) using IHIC33 (polyclonal anti-BLM antibody).

4.2.4 Electron microscopy of BLM

To gain further insight into the oligomeric state of BLM I conducted electron microscopy studies on BLM particles negatively stained with uranyl acetate. The BLM sample used (1 μM) had been incubated with $MgCl_2$ and the essentially non-hydrolysable ATP analogue ATPγS. Fig. 4.4 shows that the sample was enriched with ring-shaped particles.

4.2.5 Image analysis of BLM rings

The detailed analysis of the ring-shaped particles was conducted by Dr. Richard Newman at the ICRF at Lincoln's Inn Field. It is presented here with his permission because important conclusions about the oligomeric state of BLM can be drawn from these results.

In order to determine the structure of the protein, electron micrographs were taken and digitised (Fig. 4.5 A), and raw images of BLM molecules were selected. In total, 537 individual particles were chosen for image averaging using a reference-free alignment method of van Heel (1989, and van Heel and Frank 1981). The algorithm sorts images into class averages. 50 class averages containing a minimum of 8 images were created. During this process, the main sources of inter-image variation were assessed using eigenvector analysis. Subsequently, automatic multivariate classification procedures were applied to find the rotational orientations of the original images relative to the common symmetry pattern (so-called "alignment by classification"). For each of the data sets created by these reference-free techniques, an average was produced that represents a continuum of different rotational orientations (Fig. 4.5 B). Among these, we observed sixfold symmetric ring structures (Fig. 4.5 B, top panels) and fourfold symmetric square structures (Fig. 4.5 B, bottom panel). The sixfold symmetric structures had a maximum outer diameter of ≈13 nm and a central pore of ≈3.5 nm. The fourfold symmetric structures had sides of ≈11 nm and a central pore of ≈4 nm. The deviations of the averages from perfect sixfold or fourfold symmetry were almost certainly due to the

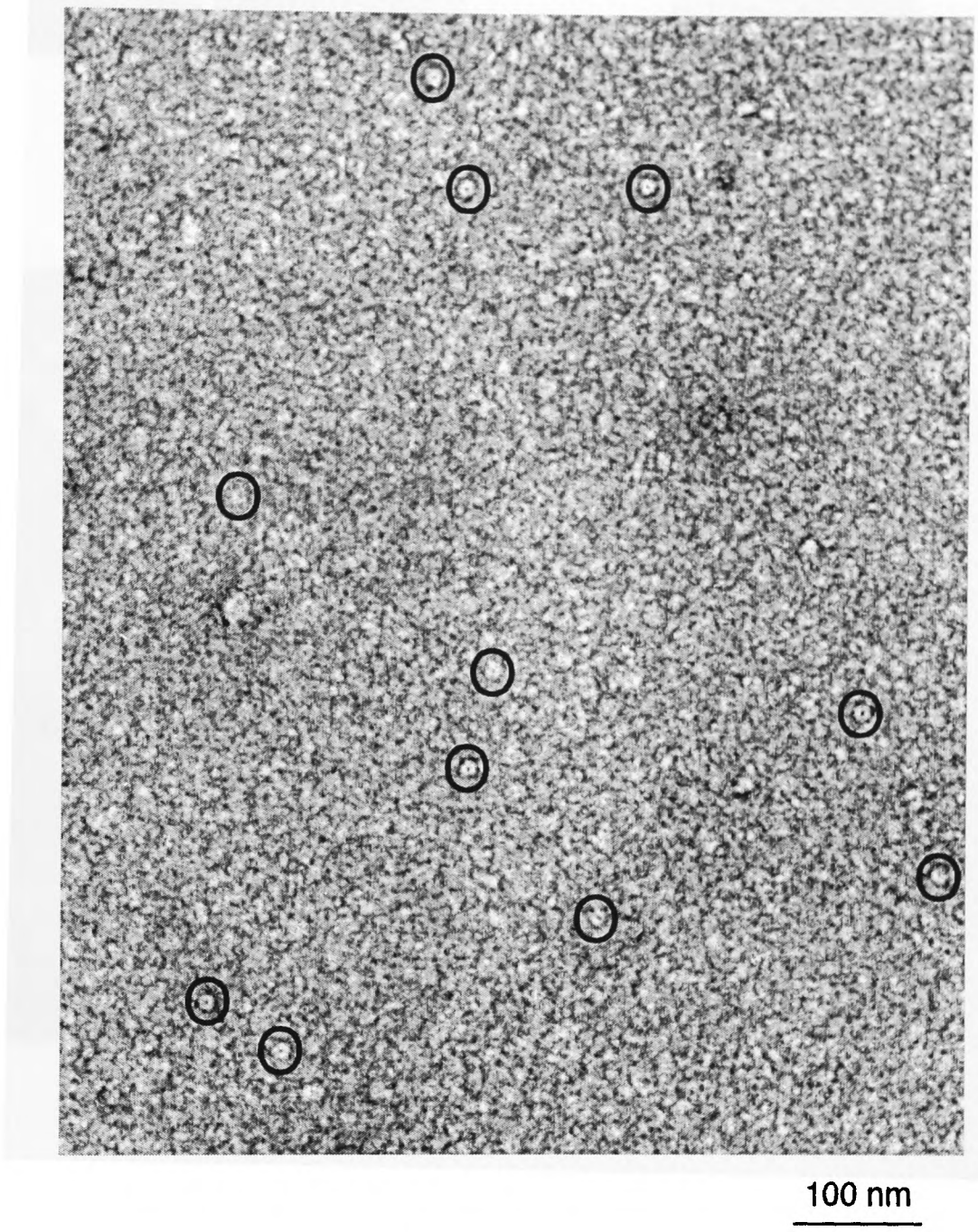


Fig. 4.4. Survey electron micrograph of purified BLM. The protein is negatively stained with 1% uranyl acetate. Circles denote representative particles chosen for averaging.

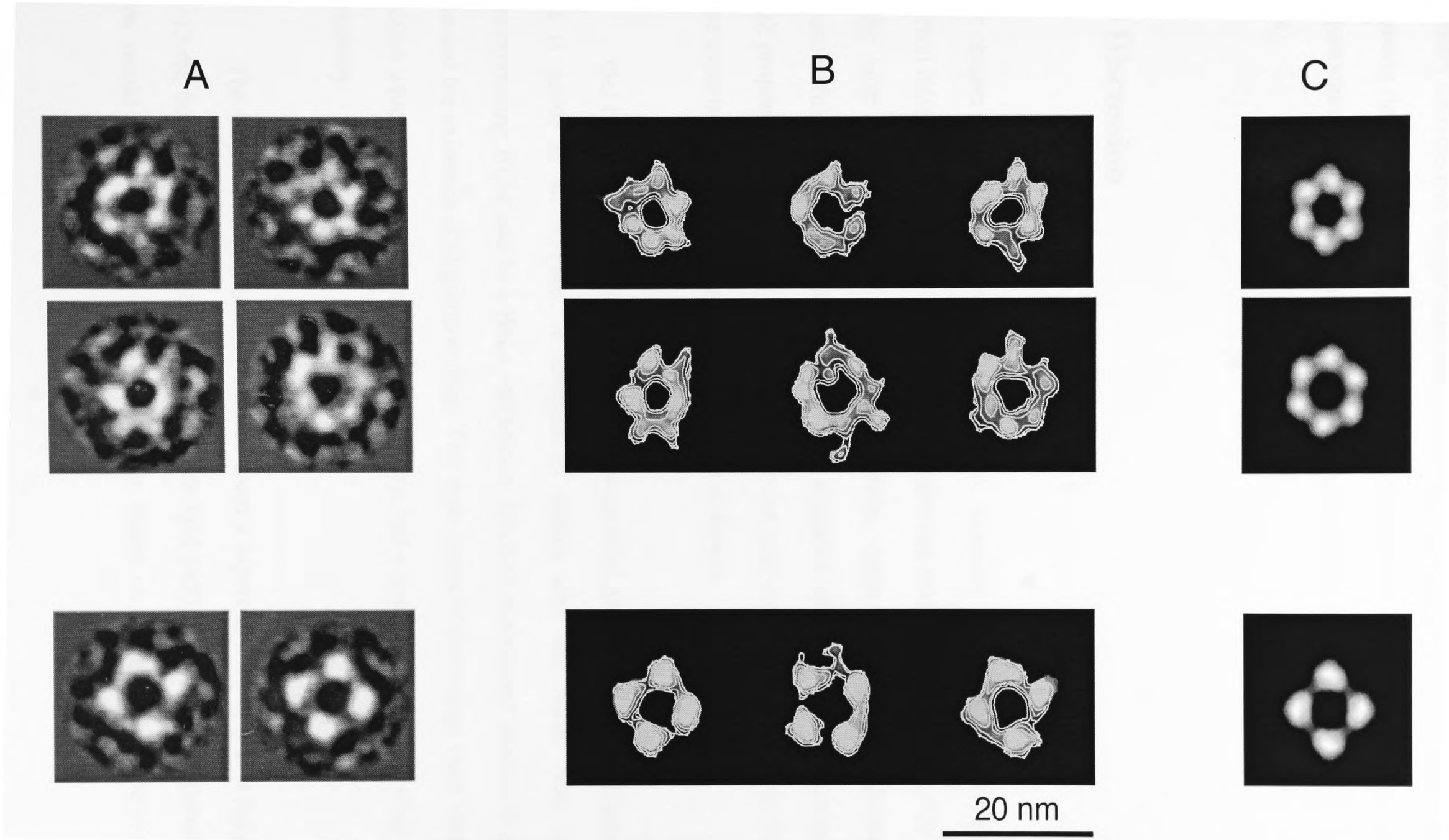


Fig. 4.5. Image analysis of BLM particles. (A) Typical raw images chosen from an electron micrograph for averaging. (B) Using a reference-free algorithm, 537 particles were aligned, sorted into data sets according to their similarity and averaged. Six such class averages depicting sixfold symmetry (top) and three depicting fourfold symmetry (bottom) are shown. No symmetry has been imposed during the averaging process. (C) Exact sixfold symmetry (top) and fourfold symmetry (bottom) has been imposed on the three largest data sets.
(B and C courtesy of Dr. Richard Newman.)

distortions arising from the negative-staining procedure. We therefore imposed sixfold symmetry onto the two largest data sets (containing 27 individual images each) of the apparently hexameric ring structures (Fig. 4.5 C, upper panels) and fourfold symmetry onto the largest data set (containing 18 individual images) of the apparently tetrameric structures (Fig. 4.5 C, bottom panel).

4.3 Discussion

This chapter describes studies of the oligomeric assembly state of BLM by gel filtration and electron microscopy. Attempts to crosslink subunits and resolve them by SDS-PAGE failed due to the large subunit size of 160 kDa. Similarly, density gradient centrifugation remained unsuccessful since the majority of BLM was degraded after the runs. On some occasions, a small proportion of full-length BLM appeared to run near the 158 kDa molecular mass marker in these experiments, indicating a monomer (data not shown).

Gel filtration experiments showed that the purified protein formed an oligomeric complex that is active as an ATPase. A complex of similar size was found both in yeast cells overexpressing BLM and in a HeLa cell extract. Electron microscopy studies of purified BLM revealed the existence of oligomeric rings. Two main forms of these rings were observed: A large fraction which showed apparent sixfold symmetry, and a smaller fraction showing clear fourfold symmetry.

The majority of purified BLM eluted from a superose 6 column in a tight peak around 12-13 ml, between the molecular mass standards IgM (950 kDa) and thyroglobulin (670 kDa). This would define this complex as a pentamer, based on the predicted subunit mass of M_r

159,000 for BLM. On the other hand, the elution position is determined both by the molecular mass and the shape of a protein. Since IgM (950 kDa), the highest molecular mass standard used, has a shape very different from a globular protein, it might elute earlier than a more compact complex of the same molecular mass. Therefore, it is conceivable that the BLM complex found corresponds to a hexamer (predicted M_r 960,000) eluting later than IgM. However, BLM had been found to migrate at approximately 180 kDa in SDS-PAGE (see chapter 3), which might be due to posttranslational modifications (although this higher M_r has not been proven yet). Assuming a M_r of 180,000, the elution position found would correspond to a tetramer. Finally, the resolution of the column in the 1000 kDa area is poor. Therefore, the only conclusion to be drawn from this experiment is that active BLM eluted in a high molecular mass complex that is consistent with either a tetramer, pentamer or hexamer. A low level of ATPase activity was found between this peak and a second peak near the γ-globulin standard (158 kDa), suggesting the presence of other oligomeric forms of BLM at a low concentration that cannot be detected by western blotting. Interestingly, the large BLM complex observed formed in the absence of ATP, $MgCl_2$ or DNA. This is in contrast to other oligomeric helicases, which form complexes that need to be stabilised by one or more of these factors. (Fouts *et al.* 1999, San Martin *et al.* 1997, Bujalowski *et al.* 1994, Dong *et al.* 1995, Patel *et al.* 1993). It should also be noted that a high salt concentration of around 0.5 M KCl was used in the gel filtration experiments. Only at this concentration, BLM was consistently found to elute in a tight peak. At lower salt concentrations (0.1-0.25 M), BLM either eluted in a very broad peak covering a wide range of molecular masses (data not shown) or was undetectable in the eluate. These results confirm the earlier observation (see chapter 3) that BLM seems to be stabilised in solution by a high salt concentration. It also appears that a high salt concentration stabilises a particular oligomeric form of BLM. Physiological salt concentration is assumed to be 0.15 M NaCl. However, in the nuclear environment where BLM is located, a higher ionic strength might prevail. Also, BLM might require protein-protein interactions to form a stable complex in

the cell, which are not present *in vitro*. Thus, it is possible that the BLM complex found in gel filtration under the experimental conditions used also occurs in the cell.

Under the same experimental conditions, a similar size complex of BLM was found in both an extract from yeast cells overexpressing BLM and in a HeLa cell extract. The high ionic strength of the running buffer probably broke up any complexes with other proteins which are dependent on ionic interactions. Such complexes could have been expected especially in the HeLa cell extract, where BLM was not overexpressed, given that BLM is known to physically interact with other proteins, e.g. topoisomerase 3α. (Wu *et al.* 1999, submitted). In the yeast extract, BLM eluted slightly earlier (peak at 11 ml) than in the HeLa cell extract (peak at 12 ml), suggesting a slightly larger size complex of BLM in the yeast extract. However, some variation between experiments of the peak in HeLa cells was observed (data not shown), with the peak ranging from 11 ml to 12 ml.

In electron microscopy experiments, ring-shaped particles were observed at a low frequency compared to other ring helicases studied at a similar concentration (e.g. T7 helicase/primase 1.5 μM (Egelman *et al.* 1995), *E. coli* DnaB 0.7 μM (Yu *et al.* 1995), SV 40 large T antigen 0.7 μM (San Martin *et al.* 1997). The background of amorphous proteinaceous material was high. This might reflect degradation of BLM between its purification and the preparation of the grid for electron microscopy. During this period of at least 24 h, the protein was stored at 4°C. Alternatively, the ring particles may have been unstable under the buffer conditions used. Notably, the salt concentration was 250 mM KCl rather than 500 mM KCl used in gel filtration. However, a lower salt concentration was desirable for electron microscopy to help prevent salt crystal formation on the grid. The ring-shaped particles observed had a diameter of 11-13 nm and a central hole of 3.5-4 nm. These dimensions are very similar to those observed for other ring helicases (San Martin *et al.* 1997, Egelman *et al.* 1995). Given that the predicted subunit size of BLM (M_r 159,000) is considerably larger than that of other ring

helicases (SV40 large T antigen, M_r 82,500; T7gp4, M_r 63,000 or 56,000 (truncated form)), the BLM subunits might form ring structures that are elongated rather than globular. In a top-down view, the diameter of such a structure would be similar to that of a structure consisting of smaller subunits. The central hole of the observed particles has the right dimensions to accommodate DNA. This has been demonstrated for other ring helicases like T7gp4 (Egelman *et al.* 1995) and the *E. coli* branch migration protein RuvB (Stasiak *et al.* 1994) and awaits further experimental investigation. The majority of individual ring-shaped particles somewhat deviated from perfect symmetry (Fig. 4.5 A, top panels). This was probably due to a distortion of the subunits by the uranyl acetate staining. Therefore, it was impossible to determine the apparent number of subunits in each ring or its symmetry with certainty. A small fraction of the particles (10-15%) appeared to have clearly fourfold symmetry (Fig. 4.5 A, bottom panel).

Sixfold symmetry was imposed on the two largest data sets appearing to contain six-subunit-structures. The resulting images (Fig. 4.5 C, top panels) have six subunits of similar size but differ in their outer diameter and the size of the central hole. This might reflect two different conformational states of the rings. However, such conformational changes are normally triggered by ATP hydrolysis, which was impossible in the presence of the ATPγS used. Alternatively, the two classes of sixfold symmetric structures might have opposite hands, possibly indicating that they repesent rings lying on the carbon support film in opposite orientations related by a 180° rotation. Fourfold symmetry was imposed on the largest data set appearing to contain four-subunit-structures. The resulting image seems to consist of four subunits which are larger than the subunits in the sixfold symmetric structures. The central hole has a dimension similar to that of the larger sixfold symmetric structure. This apparently tetrameric structure might either represent an oligomeric form distinct from the hexameric ring

(such as a tetramer or a double-tetramer seen top-down) or a side-view of a two-tiered hexameric barrel structure (as in the case of bacteriophage T7gp4 (Egelman *et al.* 1995)). However, it seems

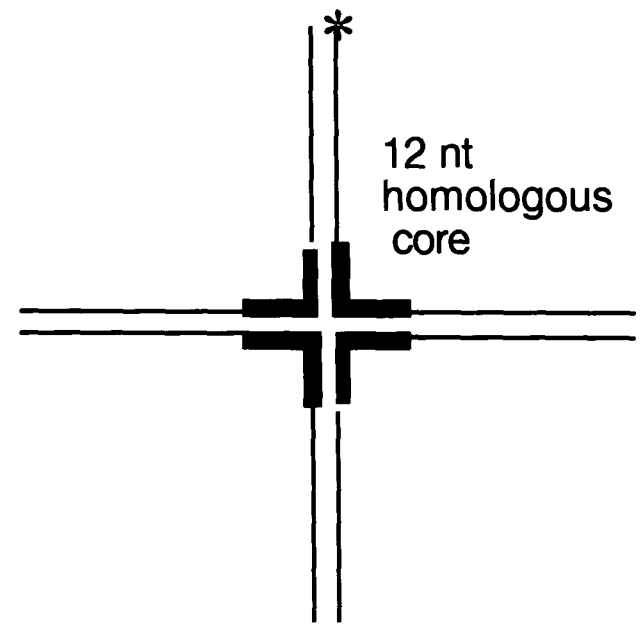
difficult to imagine how a central hole of the size observed could be accommodated in a side-view of a hexamer.

It is not clear at this stage whether BLM can adopt more than one active oligomeric form. Interestingly, it was recently reported that a truncated form of BLM (comprising amino acid residues 1-431) forms hexamers and dodecamers, suggesting that the oligomerisation domain resides in the N-terminus (Beresten *et al.* 1999). Given that the majority of helicases characterised so far appear to form either dimers or hexamers, a tetrameric or octameric structure of BLM would seem unusual. Further analysis with more concentrated full-length BLM preparations is required to answer this question.

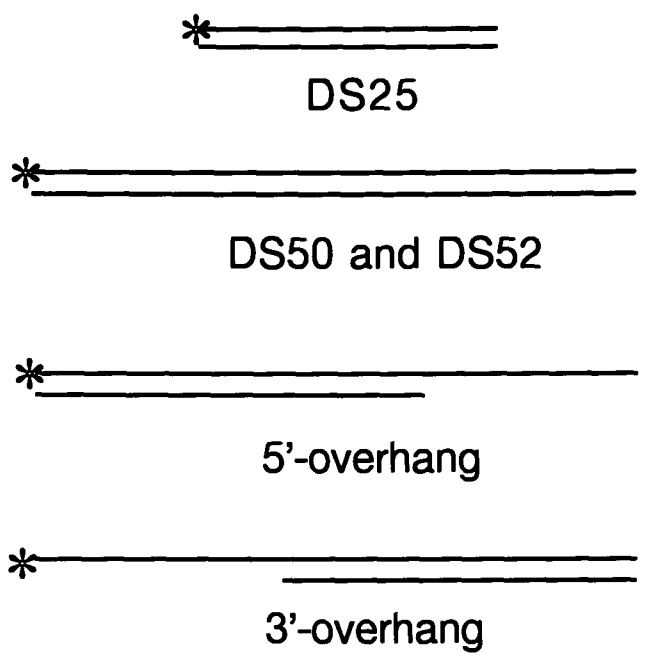
Chapter 5: Interaction of BLM with Holliday junctions

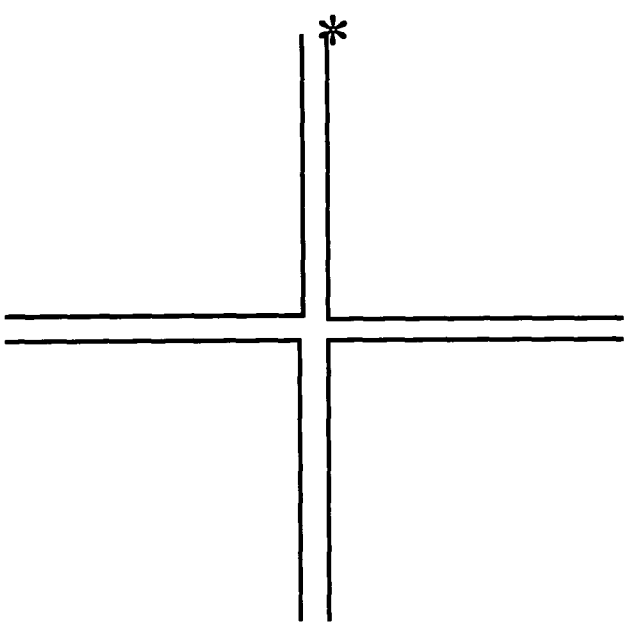
5.1 Introduction

Cells from Bloom's syndrome (BS) patients show a number of chromosomal and replication abnormalities implicating BLM in processes of DNA metabolism. The hallmark of BS cells is an increase in sister chromatid exchanges and the occurrence of quadriradial chromosomes (German 1998). This points to a role for BLM in preventing homologous recombination events. Also, replication in BS cells is retarded (Ockey and Saffhill 1986), and unusual replication intermediates occur (Lönn 1990), suggesting that BLM has a role in DNA replication. One way to investigate the function of a helicase in a pathway of DNA metabolism is to study its specificity for DNA structures occuring in replication, recombination or during repair events. Fortuitously, I discovered that BLM dissociated a synthetic four-way junction (a model for a Holliday junction, a key intermediate in recombination) in an unwinding reaction. In an attempt to understand how this substrate is recognised, I then compared the unwinding of a Holliday junction with that of a number of other synthetic DNA substrates, which are related to the Holliday junction in primary sequence, but not in structure. These included blunt-ended substrates, bubbles of various sizes, a nicked substrate, G4-DNA and substrates with 3' or 5' tails. Furthermore, I studied the specificity for Holliday junction unwinding and binding by direct competition experiments. All substrates used in these assays are listed in Fig. 5.1 and Table 5.1. Finally, in collaboration with Dr. Angelos Constantinou from Dr. Steve West's laboratory at ICRF Clare Hall, a possible branch migration activity of BLM was investigated.

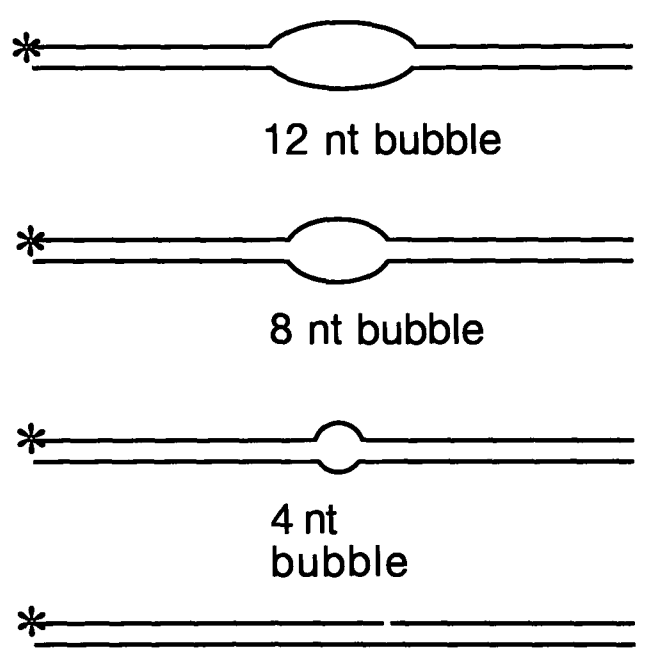


HJX12



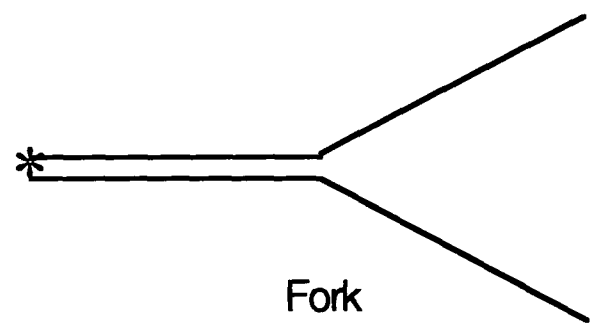


HJX0





G4-TP



Fork

Fig. 5.1. Synthetic DNA substrates used in binding and unwinding assays.

Table 5.1: DNA substrates

Name	Description	Oligonucleotides
G4-TP	G4-DNA including 3' single-stranded tail, based on consensus repeat from the murine immunoglobulin Sγ2b switch region (G-nucleotides participating in G-quartets boxed)	**TP**: 5'TGGACCAGACCTAGCAGCTAT**GGGGG**AGCT**GGGG**AA**GG**T**GGG**AATGTGA3'
HJ-X12	Mobile 50 nt Holliday junction with 12 nt homologous core (boxed)	**X12-1**: 5'GACGCTGCCGAATTCTGGC**TTGCTAGGACAT**CTTTGCCCACGTTGACCCG3' **X12-2**: 5'CGGGTCAACGTGGGCAAAG**ATGTCCTAGCAA**TGTAATCGTCTATGACGTC3' **X12-3**: 5'GACGTCATAGACGATTACA**TTGCTAGGACAT**GCTGTCTAGAGACTATCGC3' **X12-4**: 5'GCGATAGTCTCTAGACAGC**ATGTCCTAGCAA**GCCAGAATTCGGCAGCGTC3'
Fork	Fork consisting of 2 strands of HJ-X12	**X12-1**: 5'GACGCTGCCGAATTCTGGCTTGCTAGGACATCTTTGCCCACGTTGACCCG3' **X12-2**: 5'CGGGTCAACGTGGGCAAAGATGTCCTAGCAATGTAATCGTCTATGACGTC3'
HJ-X0	Static 50 nt Holliday junction	**X0-1**: 5'GACGCTGCCGAATTCTGGCTTGCTCGGACATCTTTGCCCACGTTGACCCG3' **X0-2**: 5'CGGGTCAACGTGGGCAAAGATGTCCCACGATTGTAATCGTCTATGACGTC3' **X0-3**: 5'GACGTCATAGACGATTACAATCGTGCACAGGGCTGTCTAGAGACTATCGC3' **X0-4**: 5'GCGATAGTCTCTAGACAGCCCTGTGGAGCAAGCCAGAATTCGGCAGCGTC3'
12 nt bubble	50 nt double-strand with 12 nt internal bubble (non-homologous region in bold)	**X0-1**: 5'GACGCTGCCGAATTCTGGC**TTGCTCGGACAT**CTTTGCCCACGTTGACCCG3' **BU12**:5'CGGGTCAACGTGGGCAAAG**CCAATGCGATCG**GCCAGAATTCGGCAGCGTC3'
8 nt bubble	50 nt double-strand with 8 nt internal bubble (non-homologous region boxed)	**X0-1**: 5'GACGCTGCCGAATTCTGGCTT**GCTCGGAC**ATCTTTGCCCACGTTGACCCG3' **BU8**: 5'CGGGTCAACGTGGGCAAAGAT**AATGCGAT**AAGCCAGAATTCGGCAGCGTC3'
4 nt bubble	50 nt double-strand with 4 nt internal bubble (non-homologous region boxed)	**X0-1**: 5'GACGCTGCCGAATTCTGGCTTGC**TCGG**ACATCTTTGCCCACGTTGACCCG3' **BU4**: 5'CGGGTCAACGTGGGCAAAGATGT**TGCG**GCAAGCCAGAATTCGGCAGCGTC3'
Nick50	50 nt double-strand with internal nick	**X0-1**: 5'GACGCTGCCGAATTCTGGCTTGCTCGGACATCTTTGCCCACGTTGACCCG3' **Ni30**: 5'CGGGTCAACGTGGGCAAAGATGTCCGAGCA3' **Ni20**: 5'AGCCAGAATTCGGCAGCGTC3'
DS50	50 nt double-strand, based in sequence on two HJ-X12 arms	**X12-1**: 5'GACGCTGCCGAATTCTGGCTTGCTAGGACATCTTTGCCCACGTTGACCCG3' **DS50**: 5'CGGGTCAACGTGGGCAAAGATGTCCTAGCAAGCCAGAATTCGGCAGCGTC3'
DS25	25 nt double-strand, based in sequence on one HJ-X12 arm	**DS25-1**: 5'GACGCTGCCGAATTCTGGCTTGCTA3' **DS25-2**: 5'TAGCAAGCCAGAATTCGGCAGCGTC3'
DS52	52 nt double-strand	**BL3**: 5'AAAATGAGAAAATTCGACCTATCCTTGCGCAGCTCGAGAAGCTCTTACTTTG3' **BL4**: 5'CAAAGTAAGAGCTTCTCGAGCTGCGCAAGGATAGGTCGAATTTTCTCATTTT3'
3'-overhang	31 nt double-strand with 19 nt 3'-overhang	**X12-1**: 5'GACGCTGCCGAATTCTGGCTTGCTAGGACATCTTTGCCCACGTTGACCCG3' **3'OH**: 5'ATGTCCTAGCAAGCCAGAATTCGGCAGCGTC3'
5'-overhang	31 nt double-strand with 19 nt 5'-overhang	**X12-1**: 5'GACGCTGCCGAATTCTGGCTTGCTAGGACATCTTTGCCCACGTTGACCCG3' **5'OH**: 5'CGGGTCAACGTGGGCAAAGATGTCCTAGCAA3'
SS69	69 nt oligonucleotide	**C22**: 5'AATTCGTTACTGAAGACAACTGGAAAAATATGGTGCGGAAGTGATTTCAGTA TTACAGAAATACTGAC3'

5.2 Results

5.2.1 Unwinding of DNA substrates

5.2.1.1 HJ-X12

HJ-X12 contains a four-way junction mimicking a Holliday junction with 25 nt arms and a 12 bp homologous core; its sequence is based on a previous publication (Lloyd *et al.*1993). My initial observation was that a similar Holliday junction with a slightly different sequence was dissociated by BLM in a standard unwinding reaction (Fig. 5.2). The main products of the reaction were two-stranded "half-junctions" and single strands; a three-stranded product occurred at later time points and at a low concentration. Based on this result, I measured the unwinding rate of HJ-X12. Fig. 5.3 A and B shows a representative unwinding experiment in which BLM efficiently dissociated HJ-X12 with an initial unwinding rate of 98 nmol substrate/μmol BLM/min. In the following quantifications (Fig. 5.4-5.13), graphs with identical axes will be used to allow comparisons between substrates.

5.2.1.2 DS50 and DS52

In principle, there are two ways in which BLM can recognise a synthetic Holliday junction. It might either interact with the centre of the junction, or it might recognise its double-stranded portions, either at the ends or along the molecule. To address the latter possibility, the unwinding of two double-stranded molecules was tested. DS50 and DS52 are both fully double-stranded blunt-ended molecules of 50 nt and 52 nt length, respectively. DS50 is based in sequence on two arms of HJ-X12. Fig. 5.4 A and B and Fig. 5.5 A and B show representative examples of unwinding experiments of DS50 and DS52, respectively. Neither substrate was unwound by BLM.

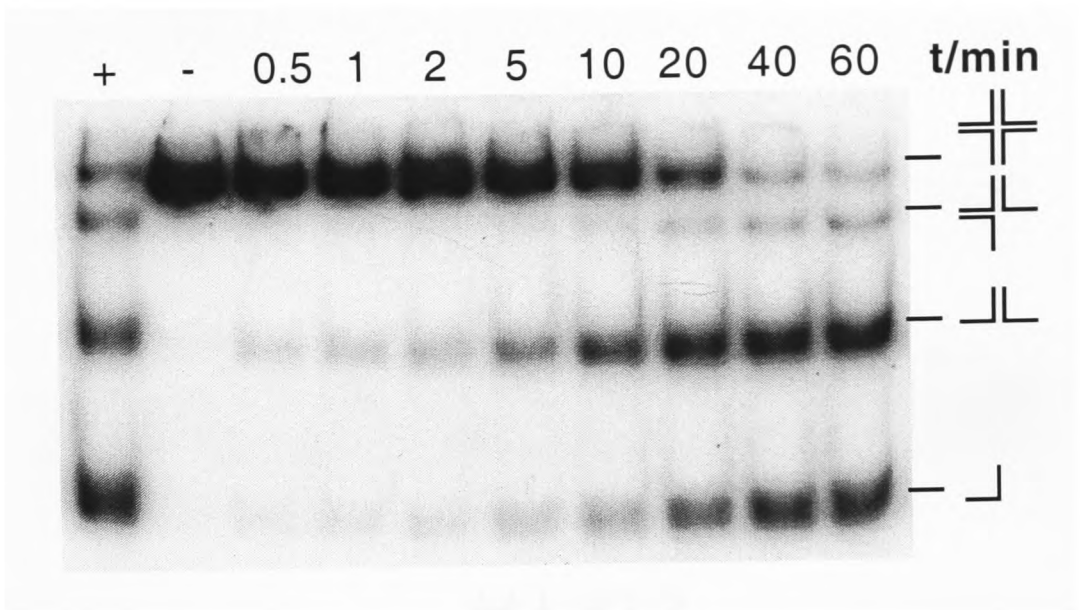
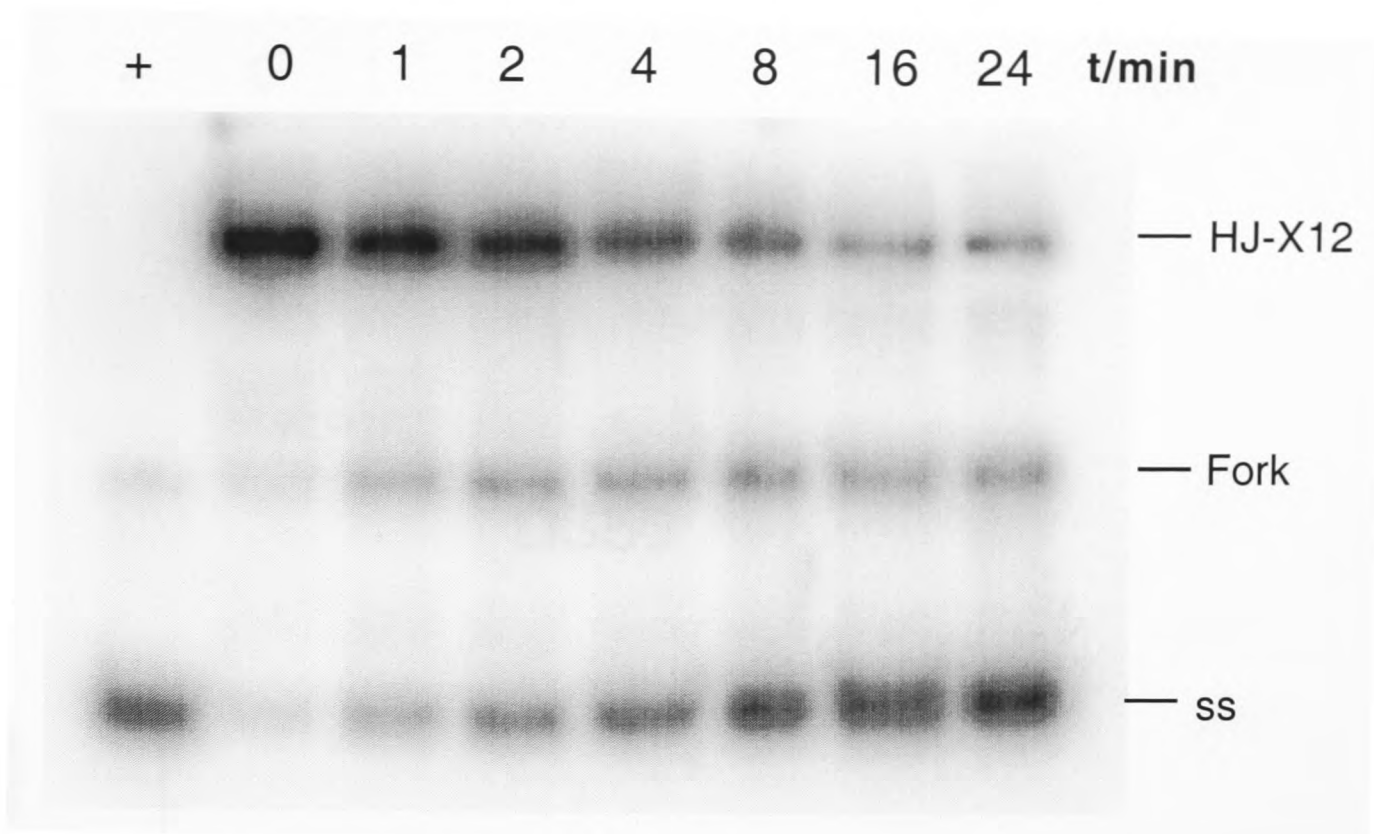


Fig. 5.2. Unwinding of Holliday junction substrate HJ-X12A by BLM. 1 nM BLM was incubated with 1 nM ^{32}P-labelled HJ-X12A in buffer containing 5 mM $MgCl_2$ and 5 mM ATP. Samples were taken at the indicated times and separated by gel electrophoresis using a 10% polyacrylamide gel. Lane 1, heat-denatured substrate; lane 2, native substrate. HJ-X12A was a generous gift from Dr. Alain van Gool.

A



B

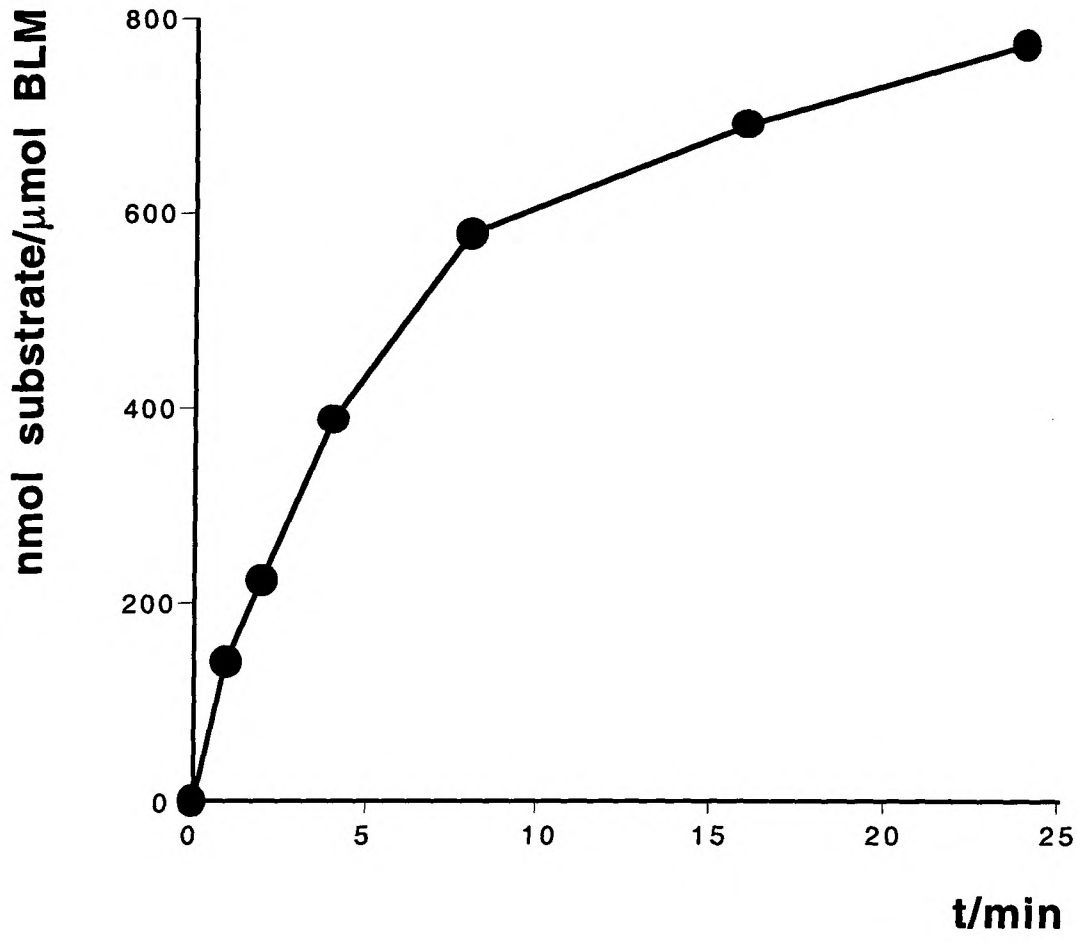


Fig. 5.3. Unwinding of HJ-X12.

1 nM BLM was incubated with 1 nM ^{32}P-labelled HJ-X12 in buffer containing 2 mM $MgCl_2$ and 2 mM ATP. (A) Samples were taken at the indicated times and separated by gel electrophoresis using a 10% polyacrylamide gel. The positions of the substrate and the products are indicated on the right. (B) Quantification of the unwinding reaction.

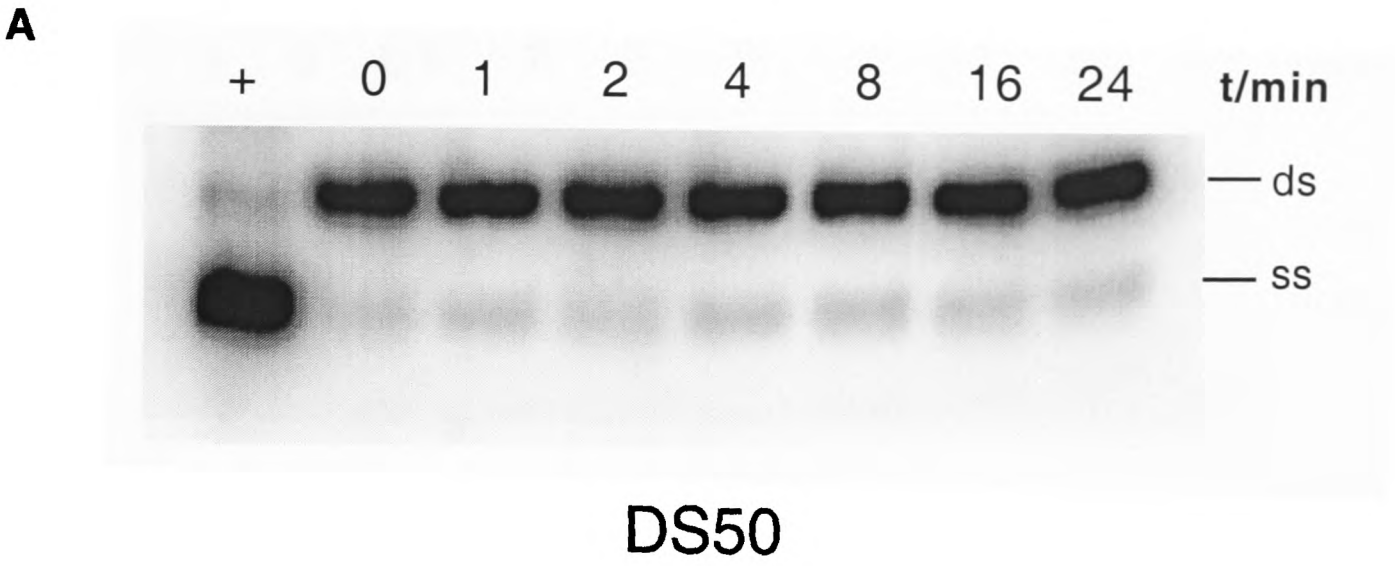


Fig. 5.4. Unwinding of DS50.
1 nM BLM was incubated with 1 nM ^{32}P-labelled DS50 in buffer containing 2 mM $MgCl_2$ and 2 mM ATP. (A) Samples were taken at the indicated times and separated by gel electrophoresis using a 10% polyacrylamide gel. The positions of the substrate and the product are indicated on the right. (B) Quantification of the unwinding reaction.

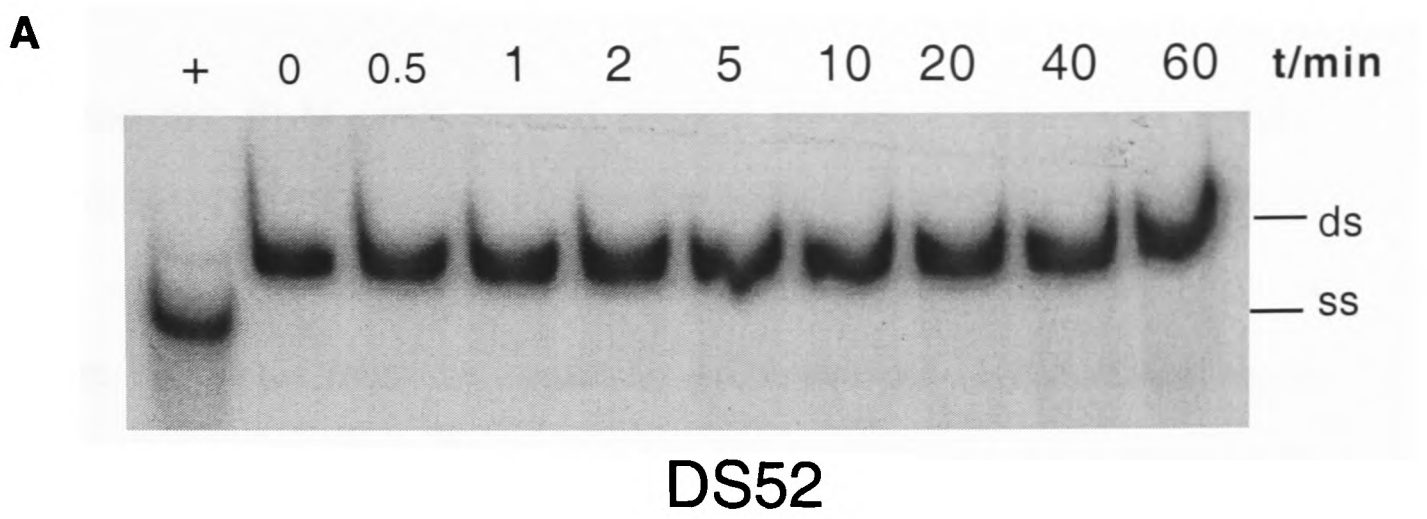


Fig. 5.5. Unwinding of DS52.
1 nM BLM was incubated with 1 nM ^{32}P-labelled DS52 in buffer containing 2 mM $MgCl_2$ and 2 mM ATP. (A) Samples were taken at the indicated times and separated by gel electrophoresis using a 10% polyacrylamide gel. The positions of the substrate and the product are indicated on the right. (B) Quantification of the unwinding reaction.

5.2.1.3 HJ-X0

Having established that BLM could unwind HJ-X12 but not a blunt-ended double-stranded molecule based on the sequence of two of its arms, it seemed possible that BLM recognised the junction at the centre. However, since HJ-X12 contains a 12 nt homologous core, its strands might be transiently single-stranded in this central region when hydrogen bonds are broken and reestablished. BLM might recognise these single strands rather than the junction itself. Therefore, unwinding of a second Holliday junction called HJ-X0 was tested. HJ-X0 is a non-mobile (static) Holliday junction with 25 nt arms. Its sequence is based on a publication by Whitby *et al.* (1996). Fig. 5.6 A and B shows a representative unwinding experiment in which BLM efficiently dissociated HJ-X0 with an initial unwinding rate of 71 nmol substrate/µmol BLM/min.

5.2.1.4 "Bubbles" and nicked substrate

To establish if it is junctions only that BLM recognises in the centre of a double-stranded molecule or if it is also able to interact with other DNA structures within such a double-stranded molecule, I tested four further substrates for unwinding: a 4 nt bubble, an 8 nt bubble , a 12 nt bubble and a nick. They are all based on a double-stranded molecule of 50 nt length but contain an internal stretch of mismatches ("bubbles") of 4 nt, 8 nt and 12 nt, or a nick, respectively. All substrates are based in sequence on two arms of HJ-X0. Fig. 5.7 A and B shows a representative unwinding experiment in which BLM efficiently dissociated the 12 nt bubble with an initial unwinding rate of 58 nmol substrate/µmol BLM/min. Fig. 5.8 A and B shows a representative unwinding experiment in which BLM inefficiently dissociated the 8 nt bubble with an initial unwinding rate of 9.4 nmol substrate/µmol BLM/min. Fig. 5.9 A and B shows a representative unwinding experiment in which the 4 nt bubble was hardly dissociated by BLM with an initial unwinding rate of 1.2 nmol substrate/µmol BLM/min.

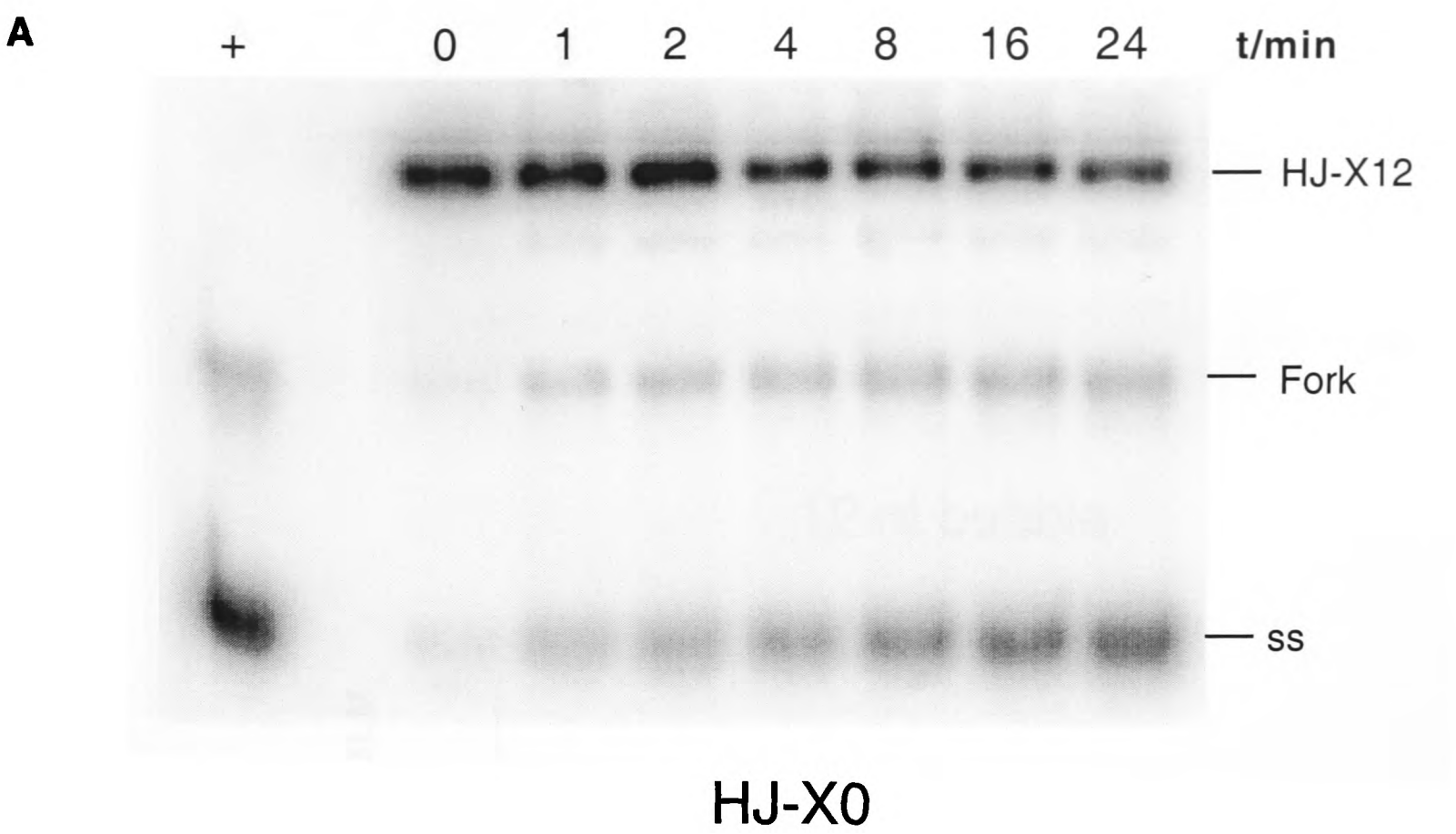


Fig. 5.6. Unwinding of HJ-X0.

1 nM BLM was incubated with 1 nM ^{32}P-labelled HJ-X0 in buffer containing 2 mM $MgCl_2$ and 2 mM ATP. (A) Samples were taken at the indicated times and separated by gel electrophoresis using a 10% polyacrylamide gel. The positions of the substrate and the products are indicated on the right. (B) Quantification of the unwinding reaction.

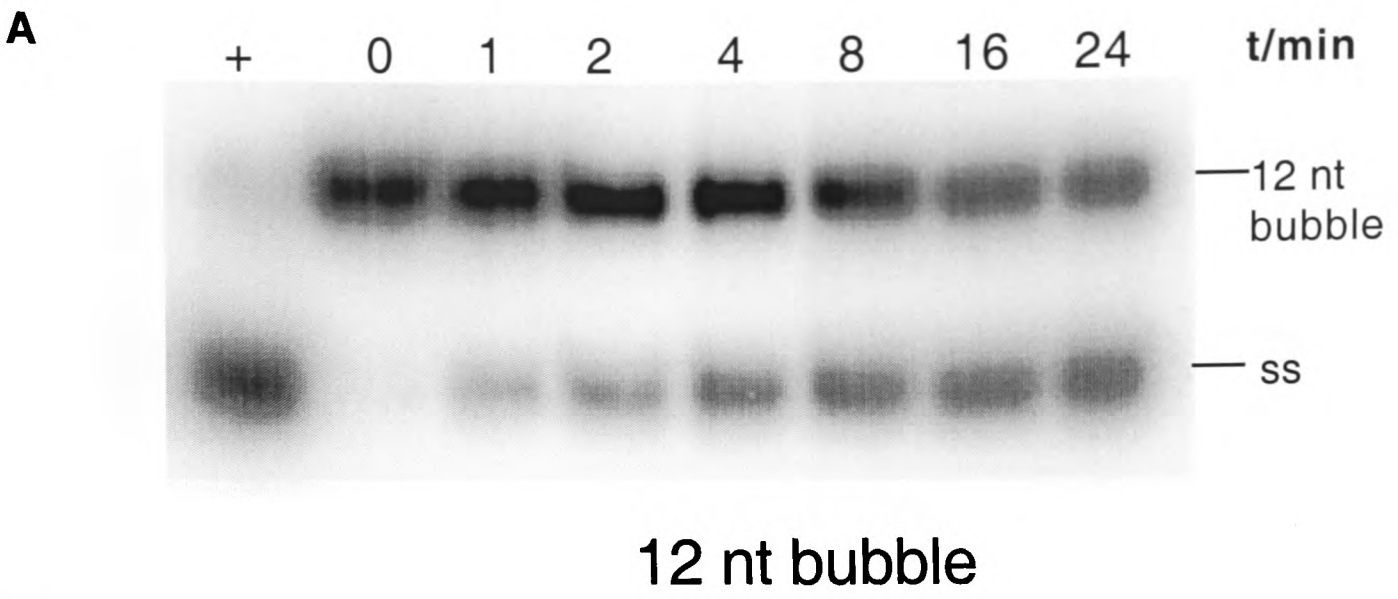


Fig. 5.7. Unwinding of the 12 nt bubble.
1 nM BLM was incubated with 1 nM ^{32}P-labelled 12 nt bubble in buffer containing 2 mM $MgCl_2$ and 2 mM ATP. (A) Samples were taken at the indicated times and separated by gel electrophoresis using a 10% polyacrylamide gel. The positions of the substrate and the product are indicated on the right. (B) Quantification of the unwinding reaction.

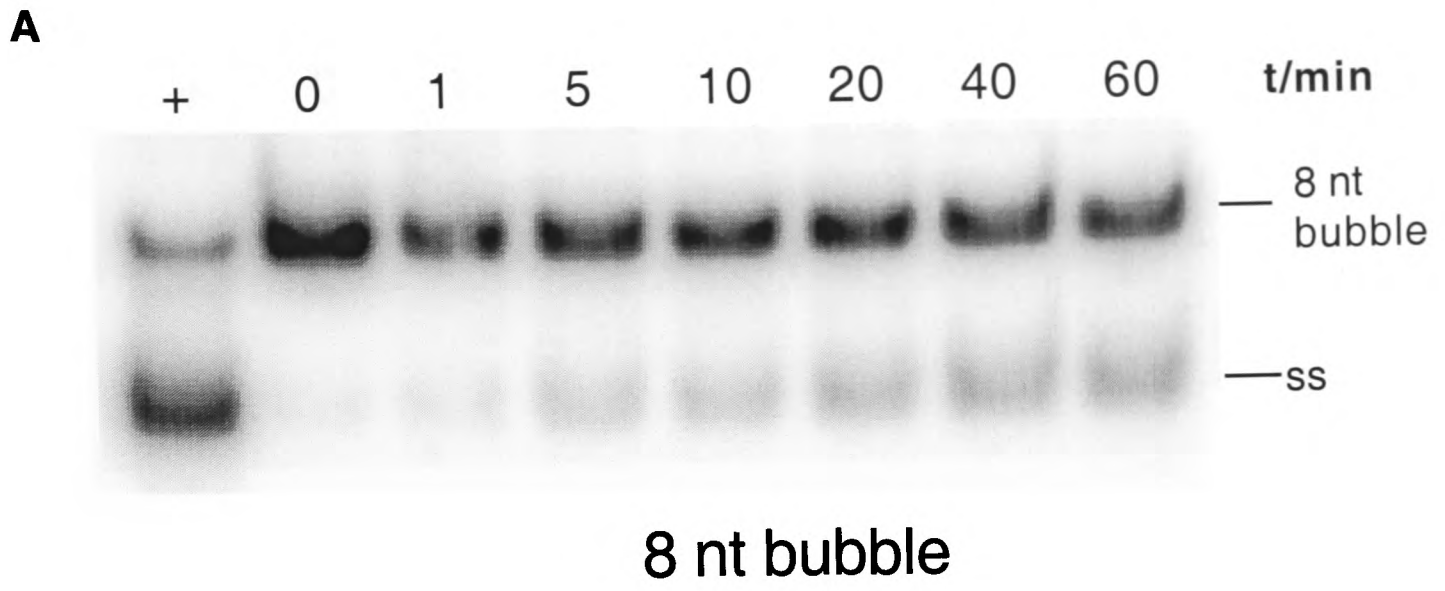


Fig. 5.8. Unwinding of the 8 nt bubble.
1 nM BLM was incubated with 1 nM ^{32}P-labelled 8 nt bubble in buffer containing 2 mM $MgCl_2$ and 2 mM ATP. (A) Samples were taken at the indicated times and separated by gel electrophoresis using a 10% polyacrylamide gel. The positions of the substrate and the product are indicated on the right. (B) Quantification of the unwinding reaction.

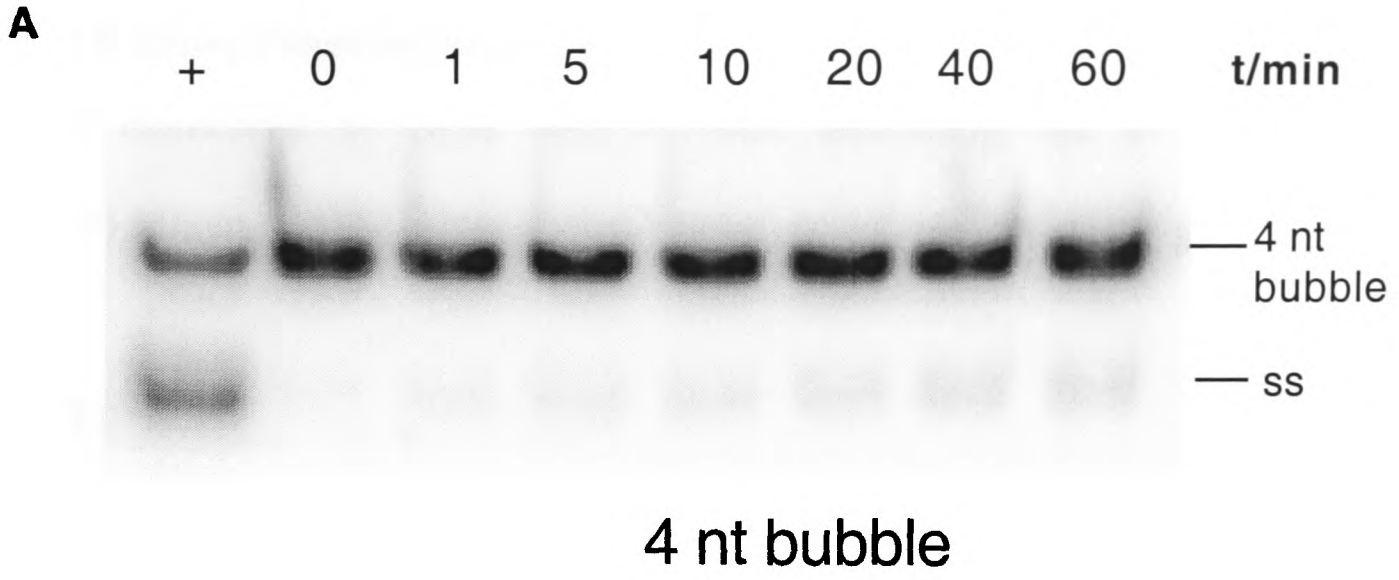


Fig. 5.9. Unwinding of the 4 nt bubble.
1 nM BLM was incubated with 1 nM ^{32}P-labelled 4 nt bubble in buffer containing 2 mM $MgCl_2$ and 2 mM ATP. (A) Samples were taken at the indicated times and separated by gel electrophoresis using a 10% polyacrylamide gel. The positions of the substrate and the product are indicated on the right. (B) Quantification of the unwinding reaction.

Fig. 5.10 A and B shows a representative unwinding experiment in which substrate Nick 50 was hardly dissociated by BLM with an initial unwinding rate of 2 nmol substrate/μmol BLM/min.

5.2.1.5 G4-TP

G-quartet, G-tetraplex or G-quadruplex (G4) DNA contains structures formed by four guanine bases hydrogen-bonded (Hoogsteen bonding) in a square planar array (Williamson *et al.* 1989). It arises spontaneously *in vitro*, at physiological salt concentration, within or between single-stranded DNA containing short guanine-rich motifs. Such guanine-rich sequences occur in immunoglobulin switch-regions, gene promoters, rDNA and telomeres (Sen *et al.* 1988). However, it is not certain yet if G4-DNA also forms *in vivo*. G4-TP is a 49 nt G4-DNA substrate containing 14 guanines participating in Hoogsteen bonding, as well as a 7 nt 3'tail. It is based on a consensus repeat from the murine immunoglobulin Sγ2b switch region. Sun *et al.* had previously shown that BLM very efficiently unwinds G4-TP but essentially fails to unwind the same substrate lacking a 3'-tail (Sun *et al.* 1998). Known at the time of this study to be the substrate most efficiently unwound by BLM, G4-TP served as a control in this series of experiments to compare it with the Holliday junction. Fig. 5.11 A and B shows a representative unwinding experiment in which BLM efficiently dissociated G4-TP with an initial unwinding rate of 89.5 nmol substrate/μmol BLM/min.

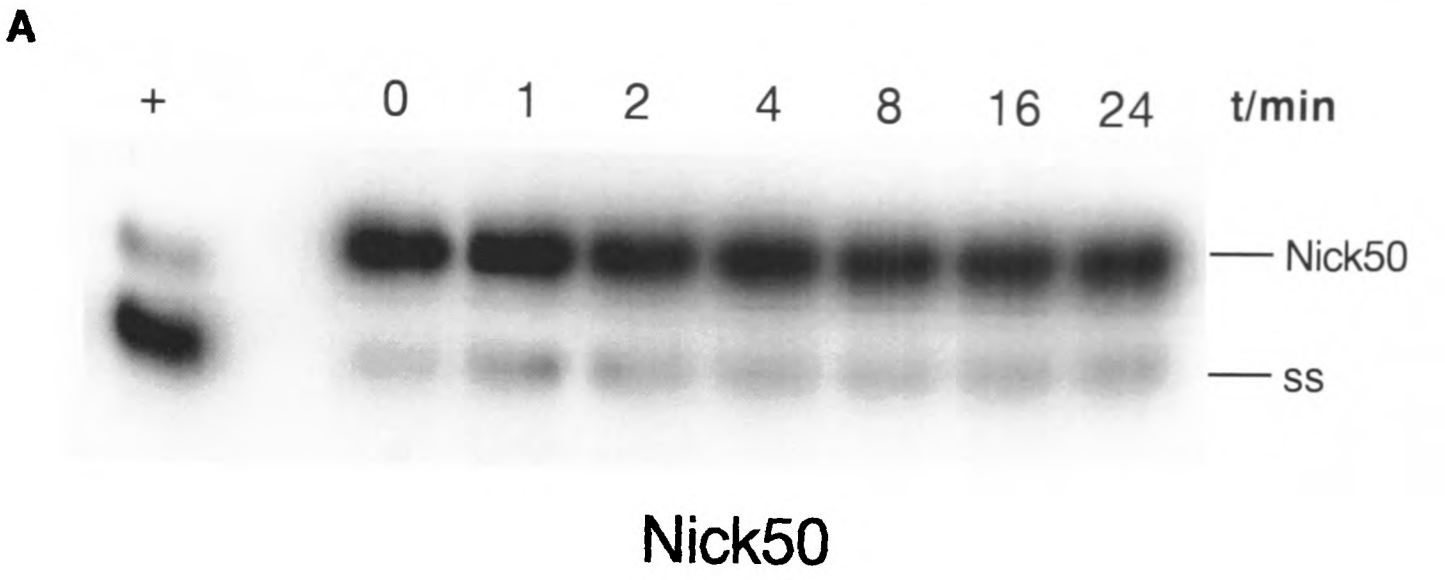


Fig. 5.10. Unwinding of Nick50.
1 nM BLM was incubated with 1 nM ^{32}P-labelled Nick50 in buffer containing 2 mM $MgCl_2$ and 2 mM ATP. (A) Samples were taken at the indicated times and separated by gel electrophoresis using a 10% polyacrylamide gel. The positions of the substrate and the product are indicated on the right. (B) Quantification of the unwinding reaction.

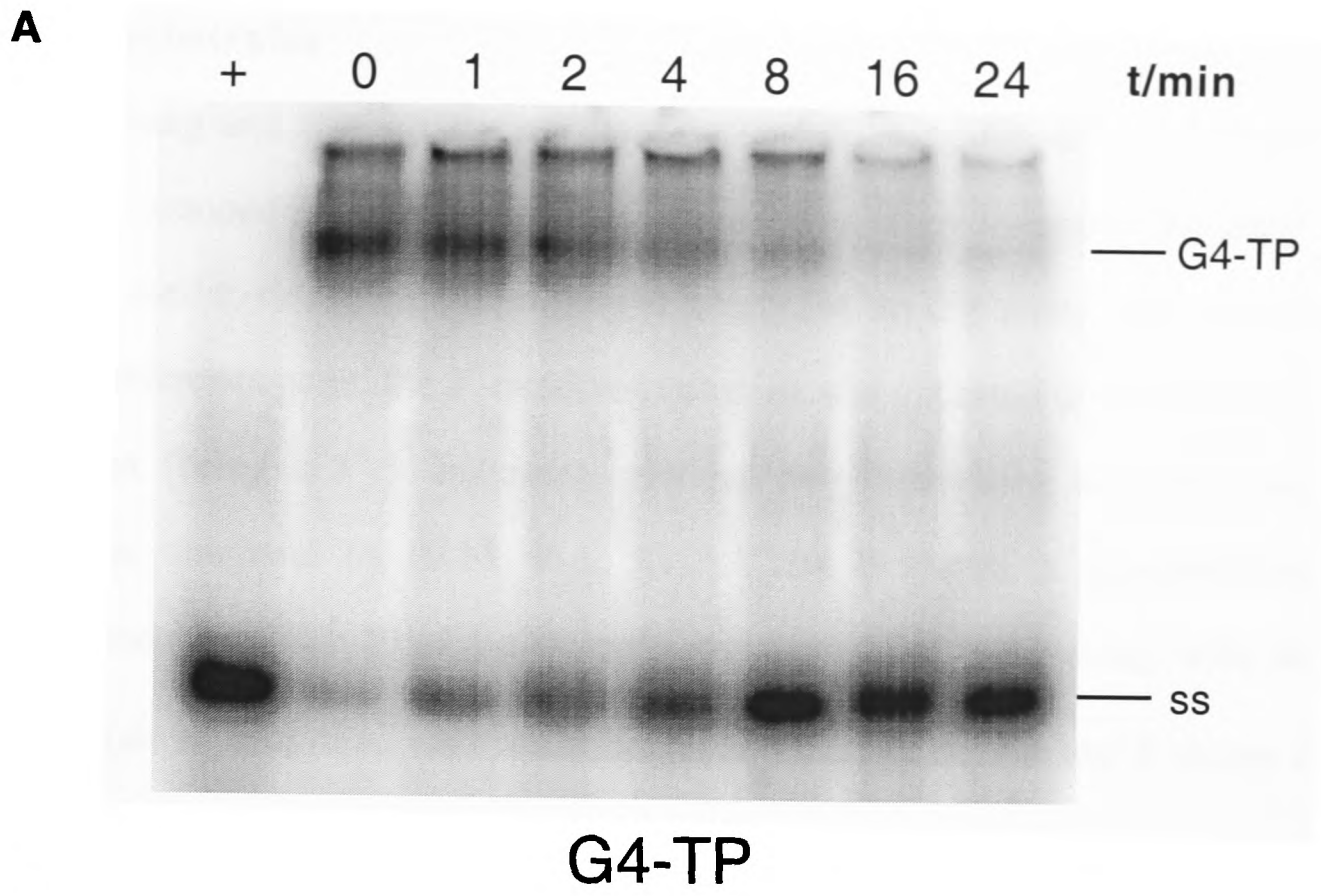
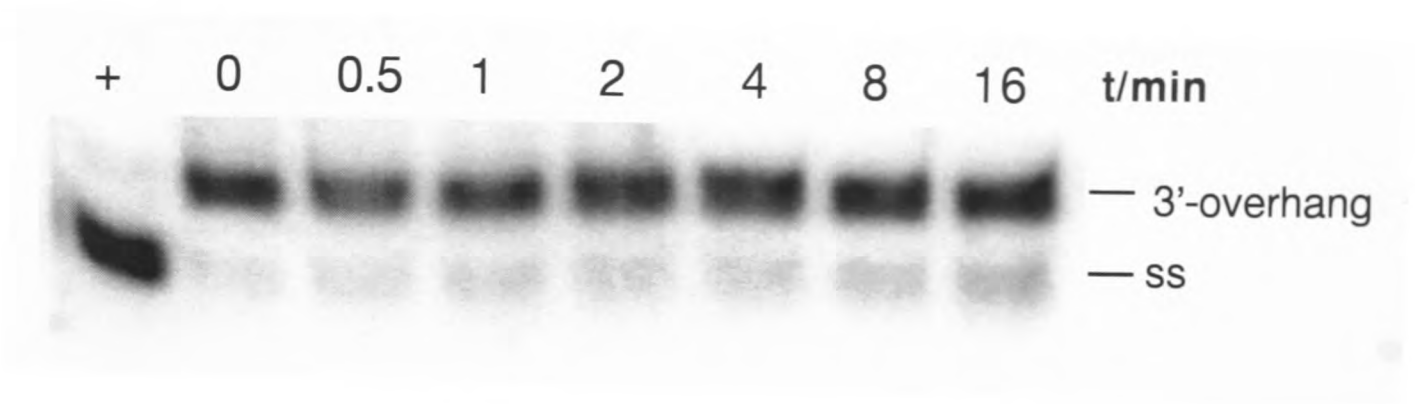


Fig. 5.11. Unwinding of G4-TP.
1 nM BLM was incubated with 1 nM ^{32}P-labelled G4-TP in buffer containing 2 mM $MgCl_2$ and 2 mM ATP. (A) Samples were taken at the indicated times and separated by gel electrophoresis using a 10% polyacrylamide gel. The positions of the substrate and the product are indicated on the right. (B) Quantification of the unwinding reaction.

5.2.1.6 Tailed substrates

Substrates 3'-overhang and 5'-overhang are double-stranded molecules of 31 nt length with a 19 nt single-stranded 3'- and 5'-overhang, respectively. They resemble "standard" helicase substrates used to determine the polarity of a helicase. In this study, they served as a control and a reference point: the 3'-overhang substrate was expected to be efficiently unwound by BLM (being a 3'-5' helicase), whereas the 5'-overhang substrate was expected not to be unwound by BLM. Fig. 5.12 A and B shows a representative unwinding experiment in which BLM inefficiently dissociated the 3'-overhang with an initial unwinding rate of 13.8 nmol substrate/μmol BLM/min. Fig. 5.13 A and B shows a representative unwinding experiment in which the 5'-overhang was very inefficiently dissociated by BLM with an initial unwinding rate of 5.8 nmol substrate/μmol BLM/min.

A



B

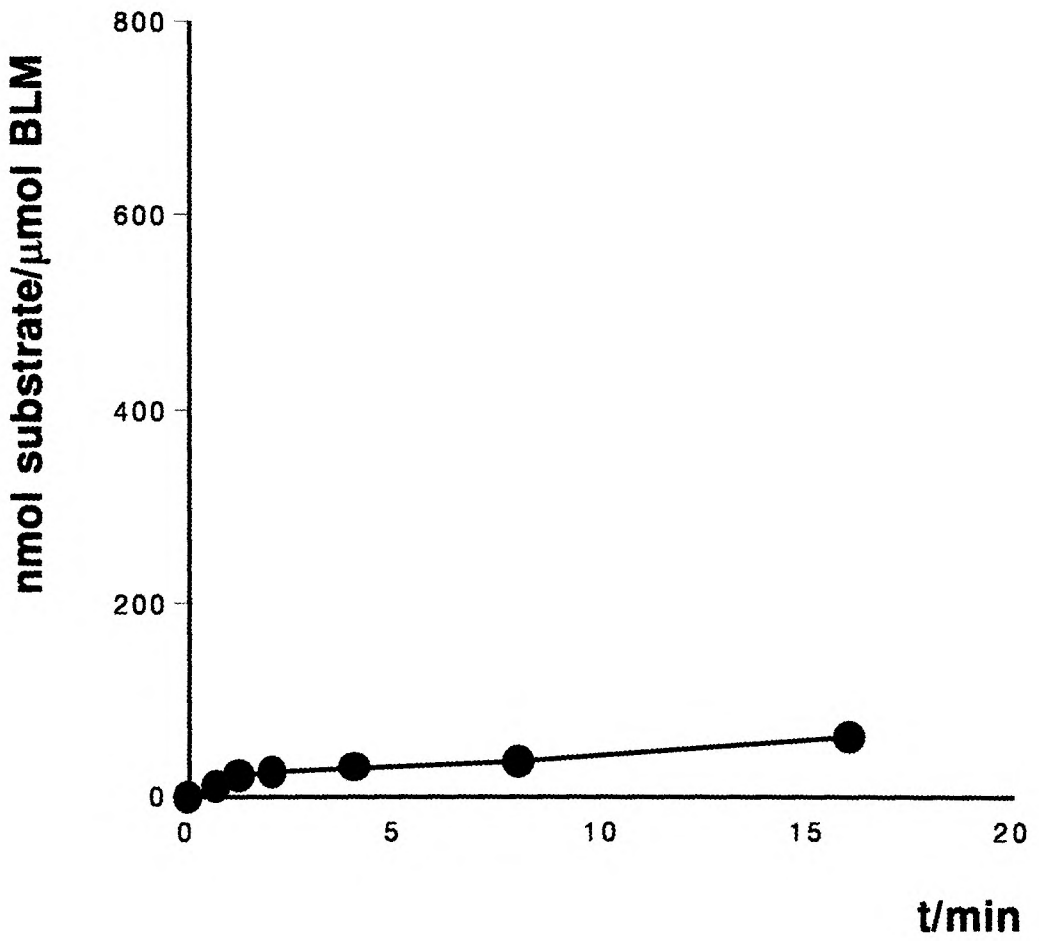


Fig. 5.12. Unwinding of 3'-overhang.
1 nM BLM was incubated with 1 nM ^{32}P-labelled 3'-overhang in buffer containing 2 mM $MgCl_2$ and 2 mM ATP. (A) Samples were taken at the indicated times and separated by gel electrophoresis using a 10% polyacrylamide gel. The positions of the substrate and the product are indicated on the right. (B) Quantification of the unwinding reaction.

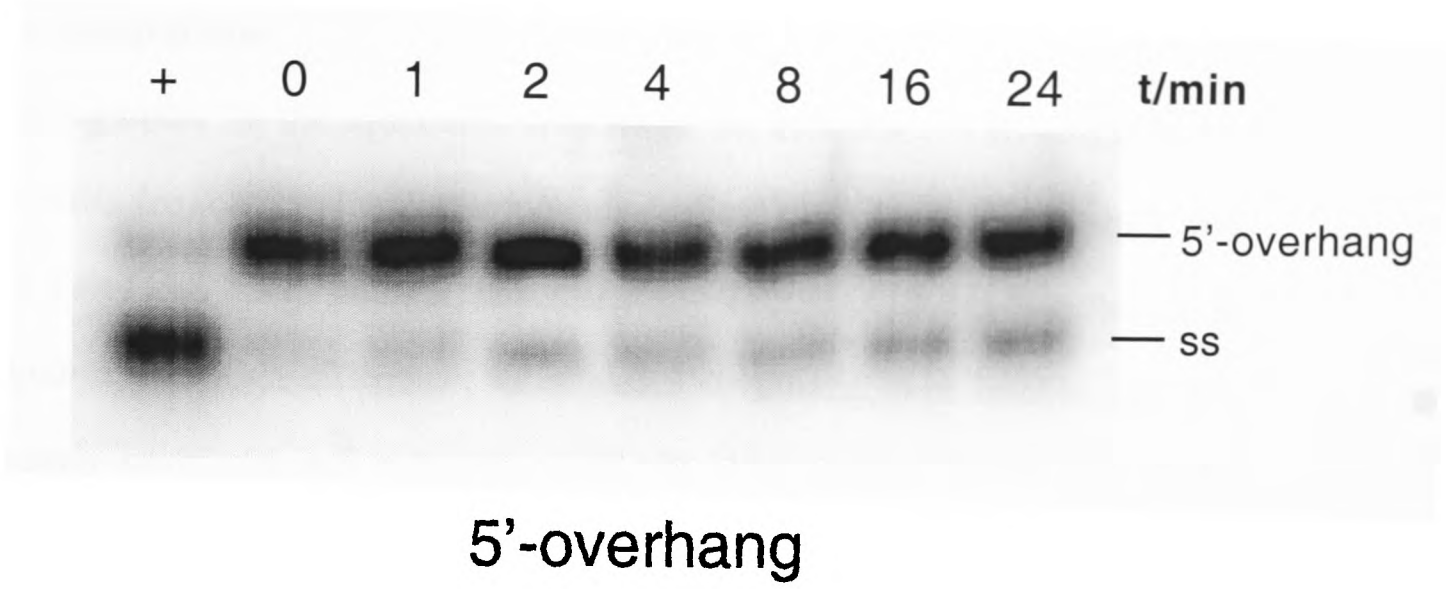


Fig. 5.13. Unwinding of 5'-overhang.
1 nM BLM was incubated with 1 nM ^{32}P-labelled overhang in buffer containing 2 mM $MgCl_2$ and 2 mM ATP. (A) Samples were taken at the indicated times and separated by gel electrophoresis using a 10% polyacrylamide gel. The positions of the substrate and the product are indicated on the right. (B) Quantification of the unwinding reaction.

5.2.1.7 Substrate comparison

To establish a ranking order for the substrates in terms of the efficiency with which BLM unwound them, results from several independent unwinding assays were combined and averaged (Table 5.2 and Fig. 5.14). Overall, substrates G4-TP, HJ-X12, HJ-X0 and 12 nt bubble were unwound with high efficiency, substrates 3'-overhang, 8 nt bubble and 5'-overhang were poorly unwound, and substrates Nick 50, 4 nt bubble, DS50 and DS52 were very poorly unwound with no unwinding at all in some experiments.

Table 5.2: Unwinding of substrates by BLM

Substrate	nmol*/μmol BLM/min	Standard dev.	No. of determ.
G4-TP	92.6	2.2	3
HJ-X12	63.7	38.1	10
HJ-X0	50.9	31.9	5
12 nt bubble	38.2	19.1	9
3'overhang	10.6	5.5	6
8 nt bubble	8	2.8	3
5'overhang	4.5	2.7	4
Nick50	2.3	2.9	4
4 nt bubble	1.6	1.4	5
DS50	0	0	6
DS52	0	n.a.	2

*(substrate molecules)

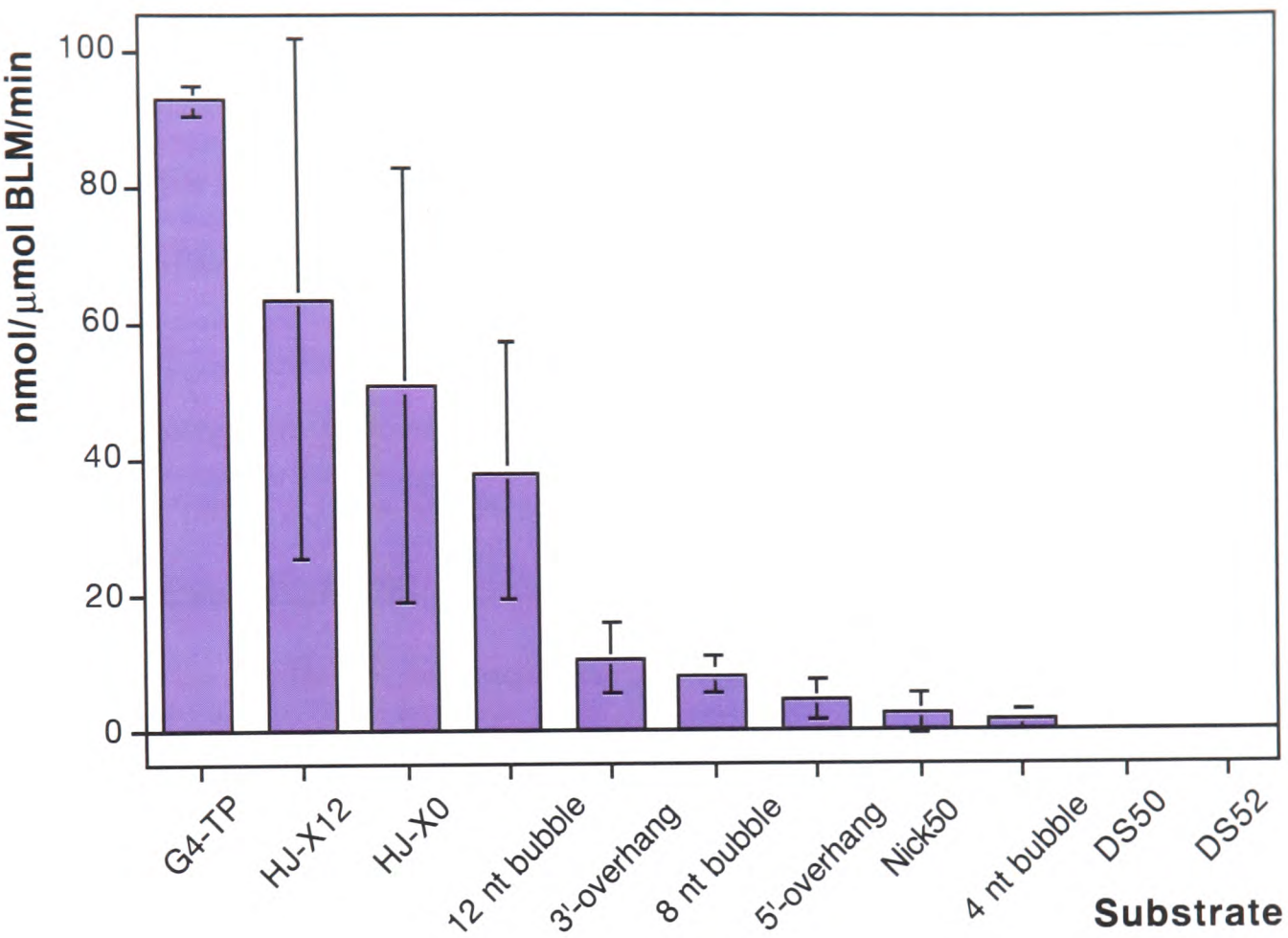


Fig. 5.14. Comparison of the unwinding efficiency of substrates.
Data from several unwinding experiments were combined (see also Table 5.2). Error bars represent standard deviations from the means.

5.2.2 Specificity of the BLM-Holliday junction interaction

Based on the result that BLM was able to efficiently unwind a synthetic Holliday junction (HJ-X12) but completely failed to unwind a blunt-ended linear double-stranded molecule (DS50) identical in sequence to two of the arms of the junction, I further investigated the specificity of BLM for Holliday junctions by undertaking direct competition experiments between HJ-X12 and several other substrates.

In an unwinding competition assay (Fig. 5.15), increasing concentrations of both unlabelled HJ-X12 (panel A) and RuvA (panel B), a Holliday junction specific protein from *E. coli,* prevented BLM from unwinding the labelled Holliday junction. RuvA seemed to compete by binding to the junction, forming a high molecular mass complex that was retarded in the gel. In contrast, neither a double-stranded blunt-ended 25mer (DS25, based in sequence one arm of HJ-X12) (panel C) nor a 69mer oligonucleotide (panel D) prevented Holliday junction unwinding to a significant extent.

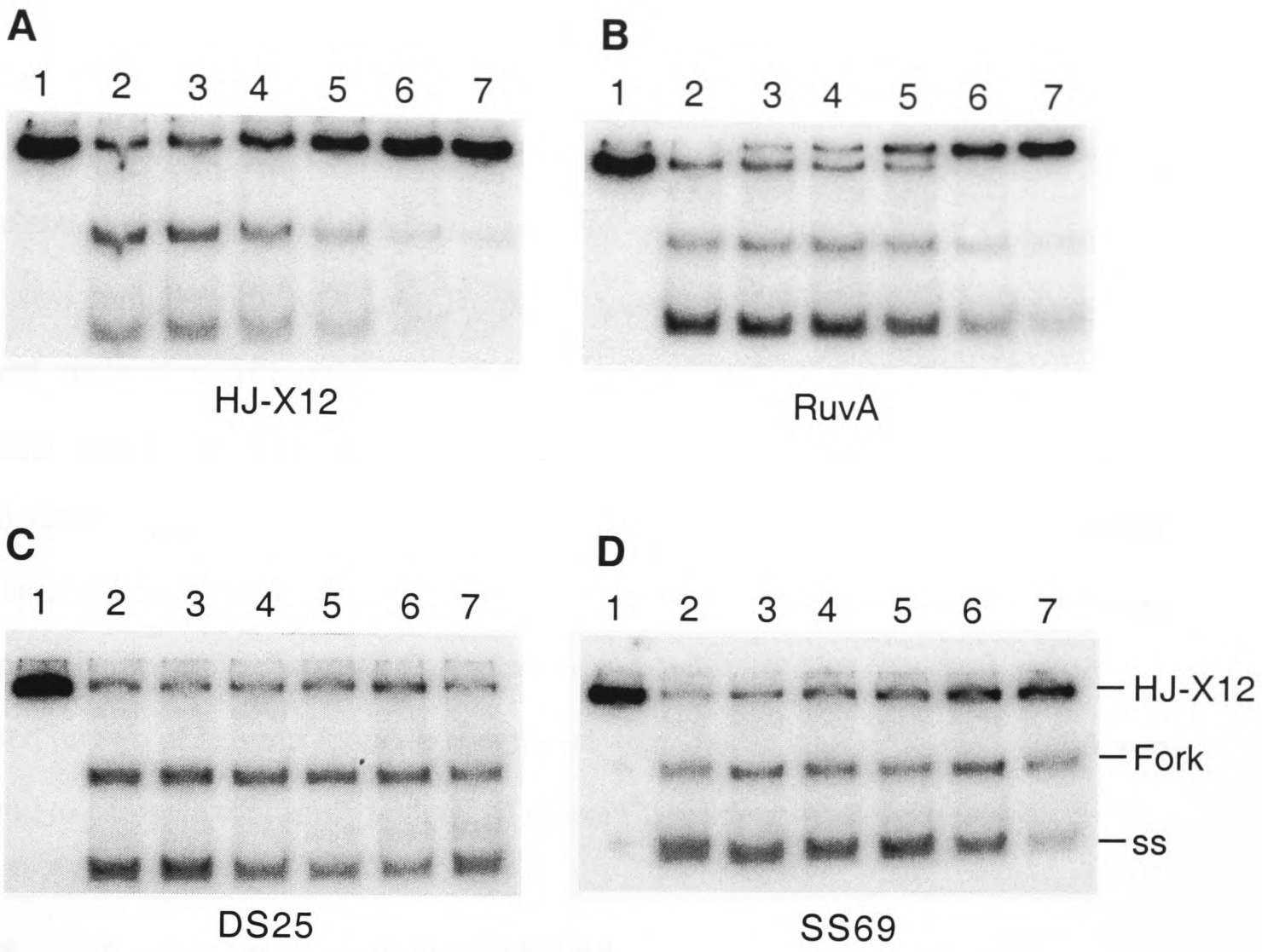


Fig. 5.15. Competition for unwinding of HJ-X12 by BLM.
1 nM BLM was incubated with 1 nM ^{32}P-labelled HJ-X12 in buffer containing 2 mM $MgCl_2$ and 2 mM ATP in the presence of increasing amounts of unlabelled competitor. Competitors: (A) HJ-X12, (B) RuvA, (C) DS25, (D) 69mer oligonucleotide (SS69). Lane 1, no BLM; lanes 2-7, 0, 0.2, 1, 5, 25, 100 nM competitor.

Subsequently, I used bandshift assays to study the binding specificity of BLM for HJ-X12. BLM bound to HJ-X12 in a protein concentration-dependent manner, forming two complexes (Fig. 5.16 A). Under the same conditions, BLM failed to form a complex with blunt-ended, linear duplex DNA (DS50) (panel B). BLM also bound to a 50mer oligonucleotide (panel C) and to a fork consisting of two strands of HJ-X12 (panel D), forming two complexes in each case. Based on this result, I tested direct competition of unlabelled molecules with BLM binding to labelled HJ-X12 (Fig. 5.17). In this experiment, BLM only formed one stable complex with HJ-X12. Neither a single-stranded 50mer (panel E) nor a double-stranded 52mer (panel D) competed substantially for the binding of BLM to the Holliday junction. A 3'-tailed substrate (3'-overhang) competed only incompletely (panel C). However, unlabelled HJ-X12 (panel A) and a fork based on two of its arms (panel B) competed with similar high efficiency. RuvA was also found to compete efficiently with BLM (panel F), yielding a distinct product.

5.2.3 Branch migration activity of BLM

Based on the observation that BLM bound and unwound synthetic Holliday junctions with some specificity, it seemed promising to study whether BLM has branch migration activity. Therefore, I approached Dr. Angelos Constantinou from Dr. Steve West's group at ICRF Clare Hall and provided him with purified BLM for *in vitro* branch migration assays. The following data, except for Fig. 5.18 c, were obtained by Dr. Constantinou and are presented here with his permission. They show a new and potentially important enzymatic activity of BLM.

α-structures containing Holliday junctions were prepared by RecA-mediated DNA strand exchange between gapped circular and partially homologous ^{32}P-labelled linear duplex DNA (Fig. 5.18 A) (see Eggleston *et al.* 1997). Using these substrates, strand exchange proceeds for 2765 bp but is prevented from reaching completion by the presence of a 1670 bp region of sequence heterology at the distal end of the linear DNA.

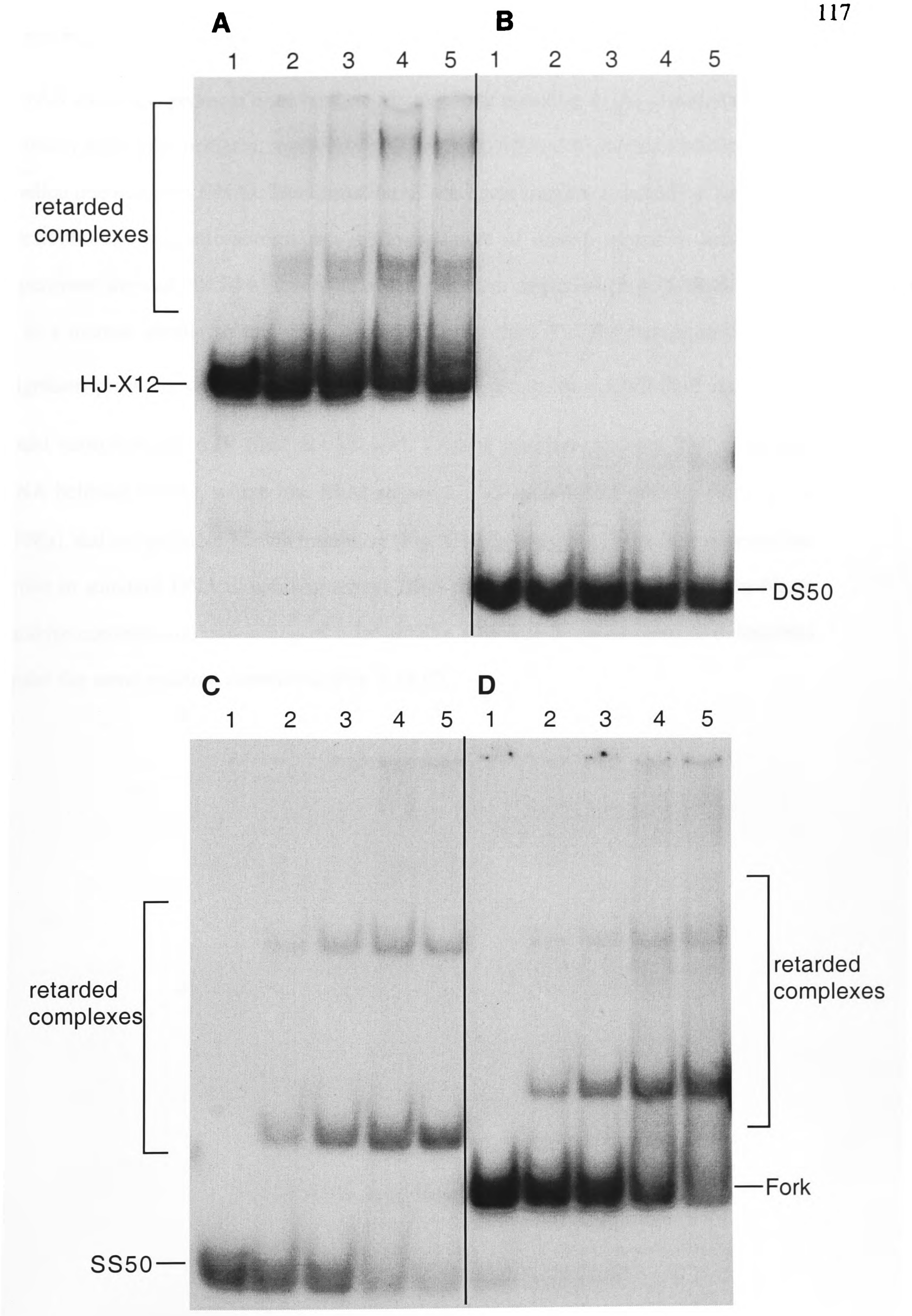


Fig. 5.16. Binding of BLM to substrates. BLM was incubated with (A) HJ-X12, (B) DS50, (C) SS50, (D) Fork for 30 min at room temperature. Products were separated on a 5% polyacrylamide gel. Bandshift assays were carried out using 0.5 nM ^{32}P-labelled substrate and 0 nM (1), 17 nM (2), 34 nM (3), 68 nM (4), 136 nM (5) BLM.

RuvAB and RecG promote branch migration reactions resulting in the dissociation of the recombination intermediates, regenerating the starting substrates (gapped circular and ^{32}P-labelled linear duplex DNA). The formation of the linear duplex, detected by agarose gel electrophoresis and autoradiography, is the signature of branch migration activity. The experiment showed that BLM catalysed efficient branch migration (Fig. 5.18 B, lanes 1-6) in a manner similar to that promoted by RuvAB (lane 7). The formation of branch migration products was dependent on ATP hydrolysis; neither AMP-PNP nor ATPγS could substitute for ATP (data not shown). Control reactions showed that a different DNA helicase (PcrA), which like BLM shows a 3'-5' unwinding polarity (Bird *et al.* 1998a), did not promote branch migration (Fig. 5.18 B, lanes 8-11) but was nevertheless active in standard DNA unwinding assays (data not shown). Also, BLM was unable to catalyse conventional unwinding of a far smaller (0.5 kb) 3'-tailed restriction fragment under the same reaction conditions (Fig. 5.18 C).

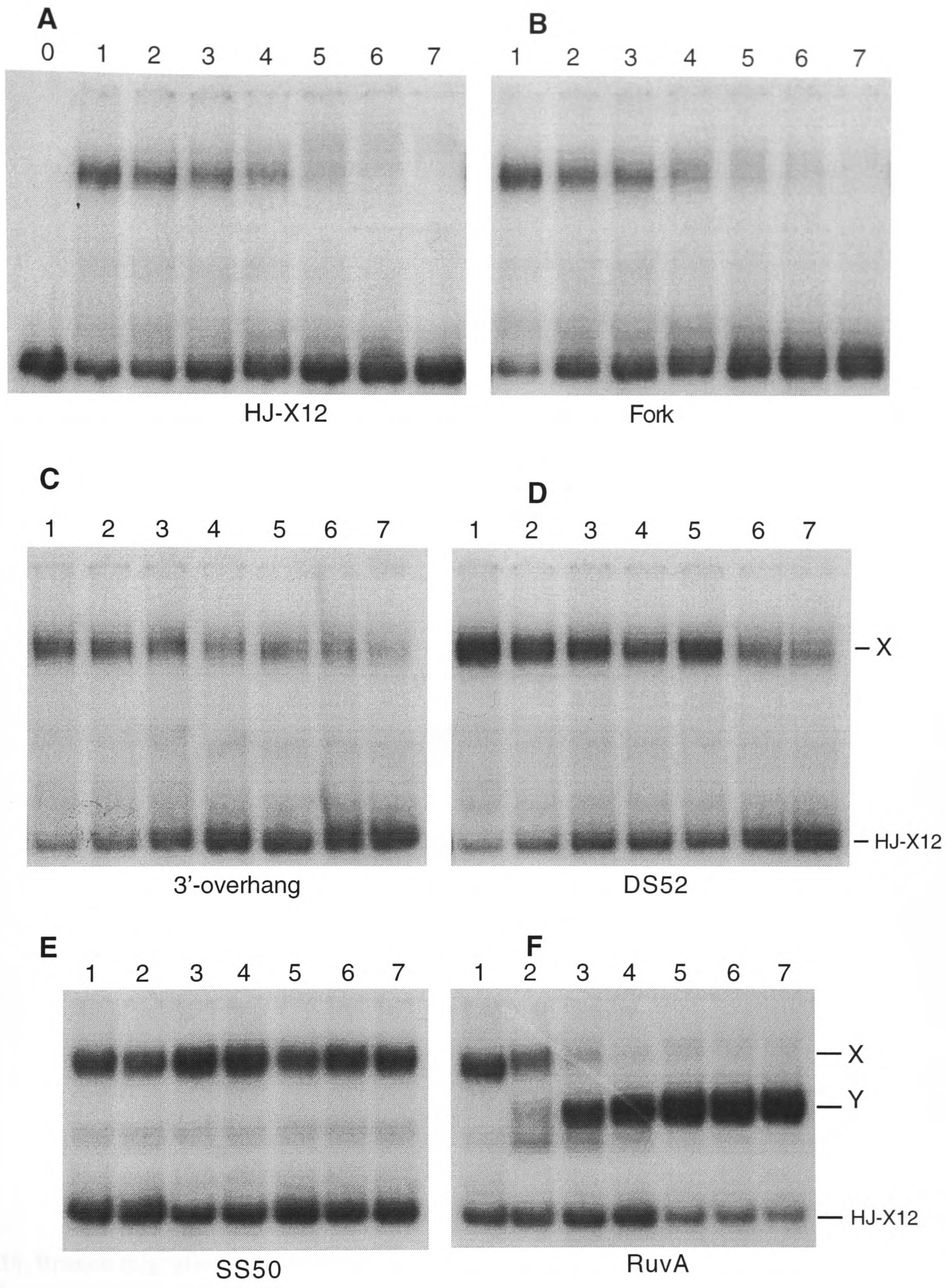


Fig. 5.17. Competition for binding of BLM to HJ-X12.
Bandshift competition assays were carried out using 68 nM BLM and 0.5 nM ^{32}P-labelled HJ-X12. Competitors: (A) HJ-X12, (B) Fork, (C) 3'-overhang, (D) DS52, (E) SS50, (F) RuvA. Lanes: 1, no competitor; 2, 3.1 nM; 3, 6.2 nM, 4, 12.5 nM, 5, 25 nM, 6, 50 nM, 7, 100 nM competitor. The position of HJ-X12 is indicated. X denotes a BLM-HJ-X12-complex, Y a RuvA-HJ-X12 complex.

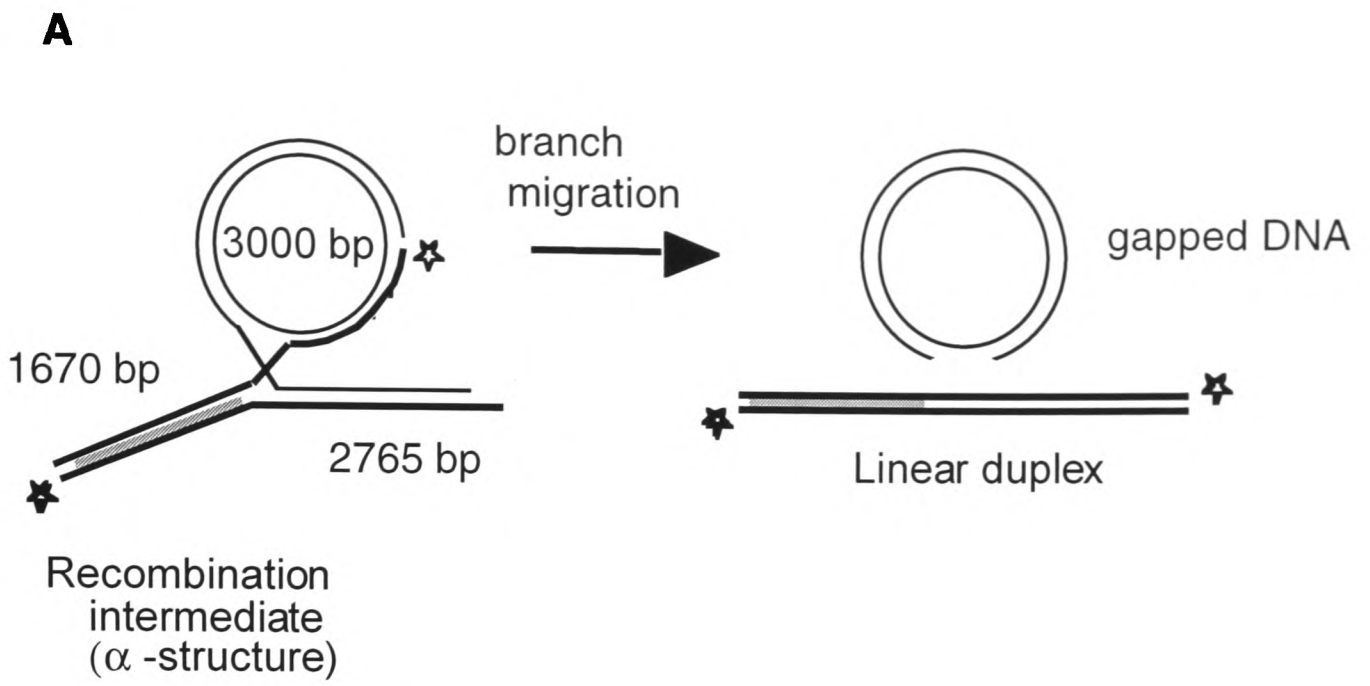


Fig. 5.18. Branch migration activity of BLM.
(A) Schematic diagram of the assay. A branch migration protein acts on a Rec-A-preformed recombination intermediate (α-structures) and reconstitutes the starting substrates (gapped DNA and linear duplex DNA). Asterisks denote ^{32}P-labels. (B) α -structures were incubated with BLM, RuvAB or PcrA, as indicated, and the ^{32}P-labelled products were analysed by agarose gel electrophoresis. The linear duplex product of branch migration (L) is indicated. (C) Time course showing that BLM (20 nM) is unable to unwind a 0.5 kb linear duplex (1 nM).

5.3 Discussion

The purpose of the studies presented in this chapter was to determine the significance of the interaction of BLM with Holliday junctions, key intermediates in recombination. My initial observation was that BLM dissociated a small synthetic Holliday junction with a 12 nt homologous core (HJ-X12) (Fig. 15.2). Interestingly, the products of this reaction differed from those obtained with the *E. coli* branch migration proteins, RuvB and RecG (Lloyd and Sharples 1993b). Whereas these proteins exclusively generate half-junctions or "splayed arms", BLM mainly created half-junctions and single strands which appeared at about the same time and in roughly equal amounts. In addition, a three-stranded product appeared at later time points. Two mechanisms for the generation of these products can be envisaged: BLM could, like RuvB, first dissociate the junction into two halves by binding to the branch point and extruding the splayed arms, followed by unwinding of the half junctions by virtue of its helicase activity. In this case, the half-junction should appear earlier in time than the single-stranded product, and no three-stranded product should be present. However, the three-stranded product could result from reannealing of half-junctions and single-strands. Alternatively, BLM might unwind the junction conventionally, starting at the branchpoint or the ends and moving along any of the arms. However, if this was the case, more of the three-stranded product would be expected, unless this is a very short-lived intermediate that is immediately converted into a half-junction. A more detailed analysis of the early stages of the dissociation reaction would be required to answer this question. This could be done by a single-turnover experiment in which any reaction intermediate is trapped by adding a large excess of unlabelled substrate shortly after the start of the reaction.

A double-stranded blunt-ended molecule (DS50) based on the same sequence as two arms of HJ-X12 was not unwound by BLM, suggesting that it can neither open up

double-stranded DNA nor start unwinding from a blunt end. Therefore, BLM must directly interact with the branch point of the junction. BLM dissociated a static Holliday junction (HJ-X0) as efficiently as a mobile junction with a 12 nt homologous core (HJ-X12), which might expose some single-stranded DNA during the movement within the core. This suggests it is not single-stranded DNA that BLM recognises at the centre of the junction but the structure of the junction itself. However, BLM was also able to start unwinding from single-stranded regions within double-stranded DNA. Unwinding from a 12 nt internal bubble was as efficient as that from a Holliday junction, whereas unwinding from an 8 nt bubble was severely reduced. Neither a 4 nt bubble nor an internal nick (Nick50) allowed initiation of any substantial unwinding. This means that BLM is not highly specific for Holliday junctions. It was already known at the time of this study that BLM can unwind a number of DNA substrates (Karow *et al.* 1997, Sun *et al.* 1998). However, the present results show that BLM does not require a DNA end to enter double-stranded DNA. Interestingly, neither a 3'-tailed substrate (3'-overhang) nor a 5'-tailed substrate (5'-overhang) used as controls in this study were efficiently unwound by BLM. This is in accordance with observations by Sun *et al.* who reported that a 21 nt duplex with a 15 nt 3'-tail was essentially not unwound by BLM (Sun *et al.* 1998). The reason might be that a tail of 15-19 nt is too short for the enzyme to bind to. However, a 7 nt 3'-tail was sufficient to allow BLM to unwind G4-DNA (Sun *et al* 1998), and an internal single-stranded region of only 12 nt is readily dissociated. This could mean that BLM preferentially recognises a forked structure. This is present in a "bubble", which can essentially be regarded as a "double-fork". A direct comparison between a forked and a 3'-tailed substrate would be required to confirm this. If BLM preferred forked structures over 3'-tails, this would distinguish it from Sgs1 which was shown to specifically recognise the junction of a double-stranded DNA and its 3'-overhang (Bennett *et al.* 1999). Surprisingly, BLM unwound a 5'-tailed substrate to a limited extent, confirming that its polarity is not absolute (see also chapter 3). G4-DNA with a 7 nt 3'-tail (G4-TP) was very efficiently unwound by BLM, confirming earlier results (Sun *et al* 1998).

However, it should be noted that only 14 guanines per strand take part in the G-quartets of this substrate. These might be more easily disrupted than HJ-X12 (50 nt to generate a half-junction). Therefore, the current study, which compares the number of molecules, not base pairs, dissociated by BLM, might overstate the efficiency of G4 unwinding. Nevertheless, the ability of BLM to unwind G4-DNA is remarkable, and its implications will be discussed in chapter 6.

The method employed for the substrate comparison is open to criticism. The enzyme (monomer):substrate (number of molecules) ratio used was close to 1:1. Even assuming that BLM acts as a hexamer (see chapter 4), this ratio would only be 1:6. Since the substrates used were small (30-100 nt double-stranded regions) and because the subunits of BLM are large (160 kDa), it is unlikely that more than two BLM molecules are able to bind to one substrate molecule at a time. Under these conditions, the substrate concentration will quickly drop to sub-saturating levels during the reaction and decrease the reaction rate. This is probably the reason why for some substrates, the reaction rates were decreasing over the time course. Furthermore, under near equimolar conditions, a minor variation of the substrate concentration would have dramatic effects on the reaction rate. This might explain some of the considerable variations between experiments (Fig. 5.14 and Table 5.2). The reason these reaction conditions were chosen were largely of practical nature. The concentration of the radiolabelled substrates after their preparation was low, and the enzyme concentration I used allowed visualisation of the products after reasonable incubation and exposure times. The problem could probably be circumvented in the future by mixing an excess of unlabelled substrate with the labelled substrate. Although this would decrease the fraction of labelled substrate unwound, it would keep the reaction rate steady for longer periods of time and would prevent fluctuations in the unwinding rate due to small variations in substrate concentrations.

Comparing the initial unwinding rates only, the substrates can be grouped into three classes (Fig. 5.14, Table 5.2): Substrates G4-TP, HJ-X12, HJ-X0 and 12BU were all unwound efficiently, substrates 3'-overhang, 8BU and 5'-overhang were unwound inefficiently, and substrates Nick 50, 4BU, DS50 and DS52 were not unwound (at least in one experiment) or very poorly unwound. Thus, BLM seems to prefer G4-DNA, Holliday junctions and internal bubbles of at least 12 nt over the other substrates tested.

In an unwinding competition assay, neither a 69mer oligonucleotide (SS69) nor a double-stranded 25mer (DS25) substantially inhibited the unwinding of HJ-X12 at 100 x molar excess (Fig. 5.15 C and D). This is not surprising for DS25, since BLM neither bound nor unwound even a double-stranded 50mer (DS50). Short oligonucleotides like SS69 however have been shown to stimulate the ATPase activity of BLM (see chapter 3), so the protein must interact with them. Maybe this interaction is only weak or transient and therefore does not compete with the unwinding of a Holliday junction. RuvA inhibited unwinding of the junction by BLM, probably by competitive binding, visible as a bandshift on the gel (Fig. 5.15.B). Unlabelled Holliday junction also competed efficiently which was to be expected.

Similar results were obtained in bandshift and bandshift competition assays (Fig. 5.16 and Fig. 5.17). In the absence of glutaraldehyde, two complexes of BLM-HJ-X12 were observed (Fig. 15.16 A), suggesting that BLM binds in two oligomeric forms (possibly two hexamers as in the case of the *E. coli* branch migration protein RuvB). However, in the presence of the crosslinking agent (Fig. 5.17), only one complex was present, suggesting that this complex is unstable in the absence of glutaraldehyde and gives rise to the other complex during gel electrophoresis. BLM bound to HJ-X12 and a fork (half-junction), and both competed completely for binding of HJ-X12. Under the same conditions, BLM failed to bind a 50mer duplex (DS50), and a 52mer duplex (DS52) did not compete for HJ-X12 binding. An oligomer was bound by BLM, yet failed

to act as a strong competitor for HJ-X12. This might reflect different affinities of BLM for these two substrates. A 3'-tailed substrate (3'-overhang) did not compete completely even at the highest concentration used, consistent with the observation that it was also poorly unwound by BLM. The affinity of BLM for the junction was much less than that of RuvA, since in the presence of a 5 x excess of BLM over RuvA (based on moles of monomers), RuvA-junction complexes predominated. RuvA serves to target RuvB to the Holliday junction, which only has a limited inherent affinity for junctions. In light of BLM's comparatively low affinity, the question arises if a similar targetting factor exists for BLM. Overall, the results from the unwinding and binding competition experiments corresponded well. Holliday junctions seem to be one but not the only preferred substrate of BLM.

The branch migration activity of BLM is the first activity of this kind reported for a eukaryotic protein. It was dependent on ATP and distinct from the helicase unwinding activity of BLM, since a 3'-tailed restriction fragment of 0.5 kb length failed to be unwound, yet branch migration occurred over 2765 bp. Furthermore PcrA, a helicase with the same polarity as BLM, was unable to perform branch migration under the same conditions. Since recombination is increased in BS cells, one function of BLM might be to act as an anti-recombinase. A model for this will be presented in chapter 6.

Chapter 6: Discussion

6.1 Summary of the key results

In this study, human BLM protein was purified in recombinant form and characterised biochemically. The key results are the following:

1. As predicted from its primary structure, BLM is a DNA dependent ATPase and an ATP dependent DNA helicase. The polarity of unwinding is 3'-5'.
2. Like many replicative helicases and like the *E. coli* branch migration protein RuvB, BLM forms oligomeric rings, with either fourfold or sixfold symmetry.
3. Similar to other RecQ helicases, BLM binds and unwinds a variety of DNA structures with different efficiencies. Of the substrates tested it shows preference for G4-DNA, synthetic Holliday junctions and internal bubbles.
4. BLM has branch migration activity. This is the first time that a eukayotic protein has been shown to migrate a Holliday junction over several hundred base pairs.

6.2 BLM - an "anti-recombinase" during replication?

Several results from this and previous studies indicate that BLM has a role as an "anti-recombinase". Cells from BS individuals are characterised by a marked increase in sister-chromatid exchanges (SCEs), which probably result from homologous recombination events. SCEs are the diagnostic feature of BS and are scored on metaphase chromosomes. SCEs can therefore only arise during S phase, when the two sister chromatids are (at least partially) present, or in G_2. In combination with the decreased replication rate in BS cells and their unusal replication intermediates, this points to a role for BLM in S-phase. Since recombination events are increased in the absence of BLM, its presence must prevent them from occuring by some as yet unknown mechanism.

When do recombination events occur in S phase? When a replication fork encounters DNA damage in the form of a nick, a DSB arises. This is repaired both by end-joining and by homologous recombination in eukaryotes, including humans. A lesion in the DNA can be bypassed by the replication fork, leaving a gap in one of the newly synthesised strands behind. This gap is subsequently repaired by postreplicational repair (Cox 1997). The potential role for BLM as an anti-recombinase is consistent with the findings that its *E. coli* homologue, RecQ, suppresses illegitimate recombination (Hanada *et al.* 1997) and that Sgs1, its budding yeast homologue, suppresses mitotic recombination (Watt *et al.* 1996).

6.2.1 BLM may remove "road blocks" to the replication fork

One way for BLM to prevent the necessity for recombinational repair would be to remove obstacles in the DNA that would make a replication fork stall or bypass it (Fig. 6.1). Since BS cells are generally not hypersensitive to DNA damaging agents, it is unlikely that BLM plays a part in one of the major DNA repair pathways that remove DNA adducts, crosslinks, missing bases or mismatches. However, another potential "roadblock" to replication might be DNA secondary structure, for example G4-DNA. Although its existence *in vivo* has not yet been proven, sequences throughout the genome can potentially form G4-DNA, and it is highly stable *in vitro*. It has been shown that BLM very efficiently unwinds G4-DNA (Sun *et al.* 1998 and chapter 5 of this thesis), which would be consistent with a function for BLM to remove these structures.

Furthermore, in eukaryotes, one of the major obstacles to replication are nucleosomes. In this respect it is noteworthy that RuvAB, one of the branch migration proteins in *E. coli*, has recently been shown to be able to disrupt nucleosomes from the DNA during branch migration (Grigoriev and Hsieh 1998). Given that BLM also has branch migration activity (as well as helicase activity), it is tempting to speculate that it also shares the ability to disrupt DNA-histone interactions with RuvAB, even when acting as a helicase.

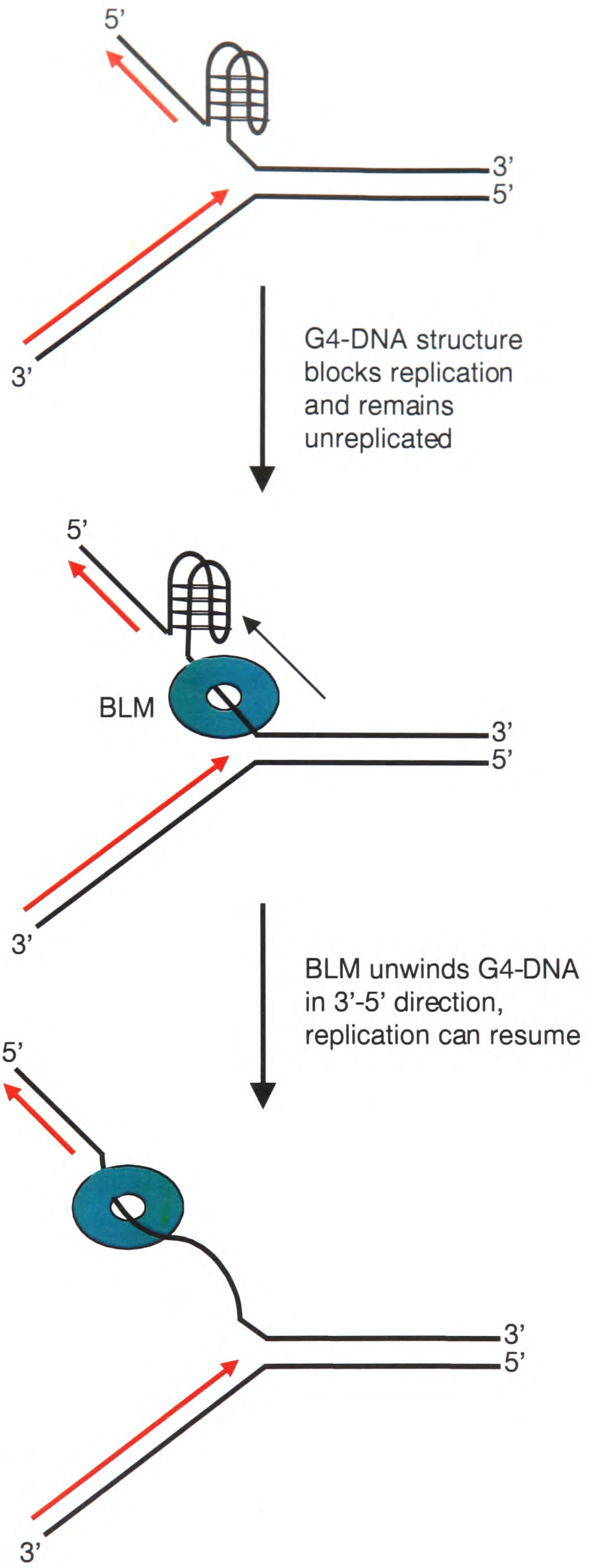


Fig. 6.1. Model 1: BLM removes "roadblocks" to the replication fork.

6.2.2 BLM may help stabilise stalled replication forks

Another possibility for BLM to prevent recombination might be to stabilise a stalled replication fork (Fig. 6.2). This assumes that DNA damage is not repaired by recombinational repair when (or shortly after) the replication fork has encountered it, but that the fork gets stalled and replication restarts once the damage has been removed by other repair pathways. A model for this was recently suggested by Courcelle and Hanawalt (1999) who found that RecQ, the *E. coli* homologue of BLM, and RecJ, a 5'single-stranded exonuclease, process nascent DNA (with preference for the lagging strand) prior to the resumption of replication in UV-irradiated *E. coli.* According to this model, RecQ and RecJ unwind and degrade the nascent lagging strand at a stalled replication fork, increasing the single-stranded region at the fork. The triple-stranded structure thus arising can then be maintained by RecA which presumably binds them simultanously until the lesion is repaired and replication can resume. This would prevent the free 3'end of the leading strand from initiating unwanted recombination at a site of near homology. However, the role of RecA in this model is one of maintaining a triplex structure rather than promoting strand exchange like in homologous recombination. By analogy, BLM could perform a similar role to RecQ in conjunction with hRAD51 and a yet unidentified single-strand specific exonuclease. This is supported by a physical interaction found in our laboratory between BLM and hRAD51, the human homologue of RecA (Leonard Wu, unpublished results). Furthermore, it is consistent with a stimulatory activity of RPA on BLM (Robert Brosh, personal communication), since RPA might target BLM to single-stranded regions at the replication fork.

Alternatively, if a nascent DNA strand has already initiated an unwanted recombination event, BLM might disrupt this, possibly together with topoisomerase III. The two enzymes might unlink plectonemically wound mispaired strands after heteroduplex formation, requiring both helicase unwinding and topoisomerase strand passage activity (Wu *et al.* 1999) (Fig. 6.3). This model is consistent with the strand passage activity of RecQ and topoisomerase III

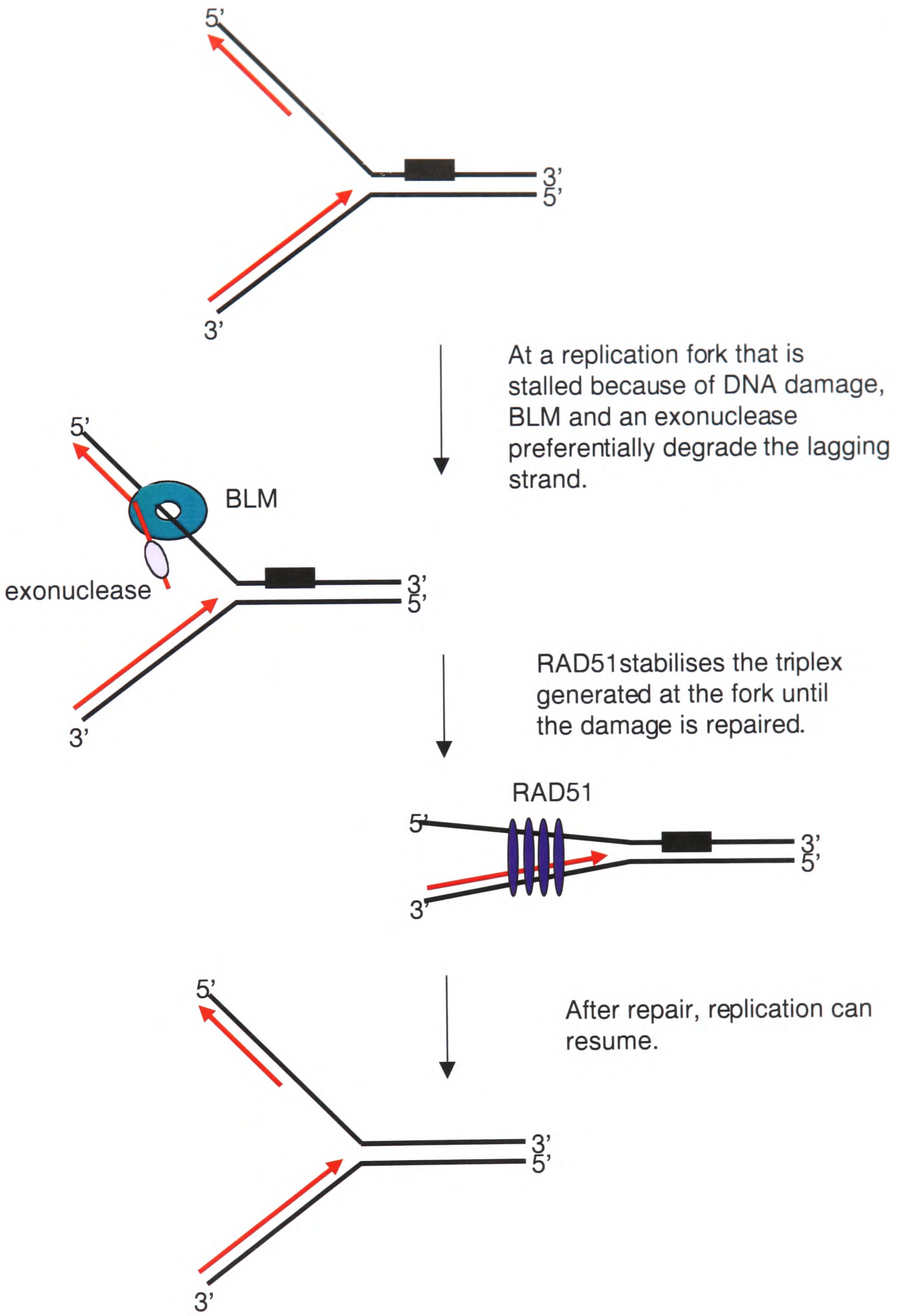


Fig. 6.2. Model 2: BLM and an exonuclease stabilise a collaped replication fork by degrading nascent DNA.

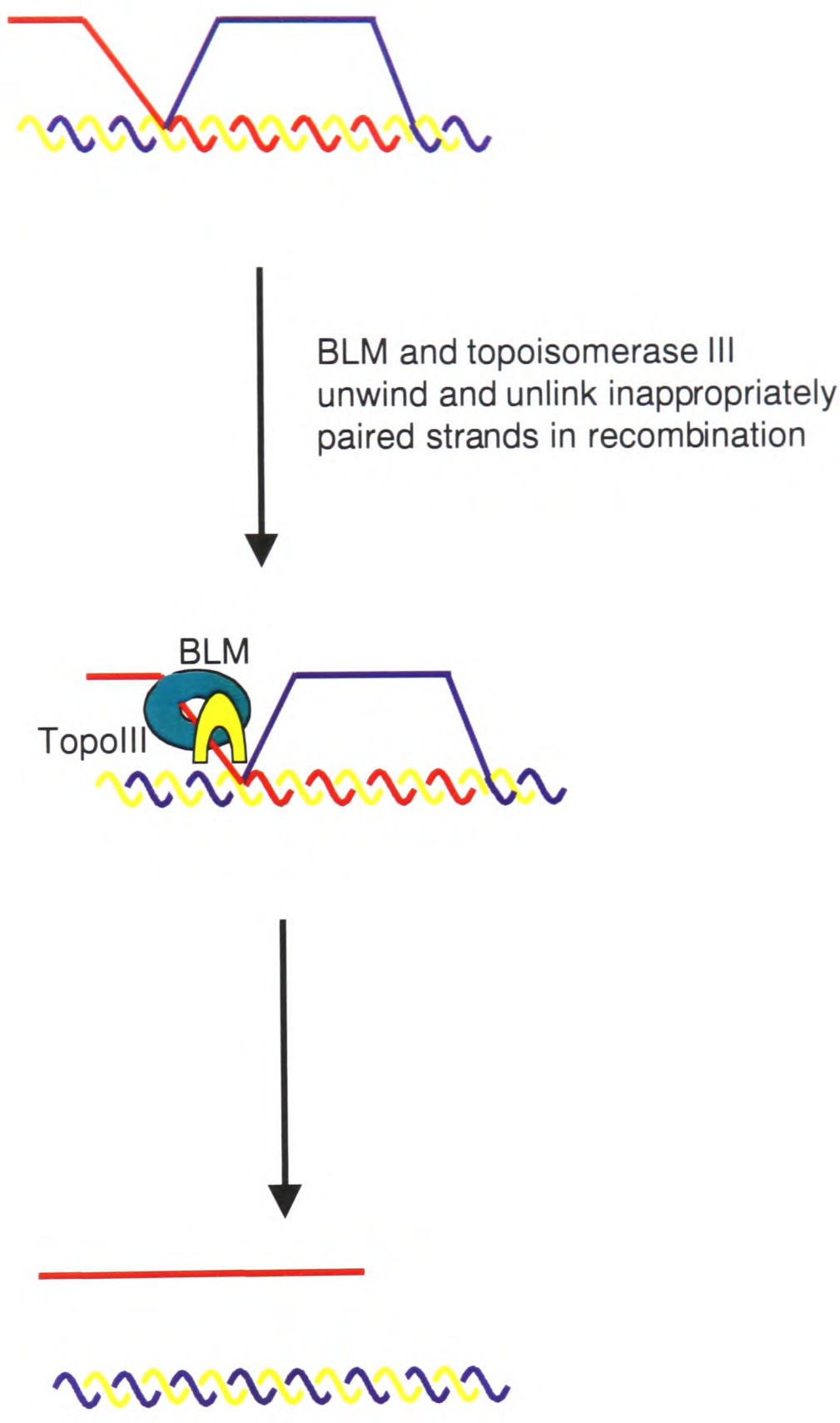


Fig. 6.3. Model 3: BLM dissociates paired DNA strands in recombination events.

(from *E. coli* or yeast) reported by Harmon *et al.* (1999). Also, our laboratory has found that BLM, like Sgs1 (Gangloff *et al.* 1996) and Rqh1 (Goodwin *et al.* 1999), physically interacts with human topoisomerase IIIα (Wu *et al.*, submitted), although no functional interaction has been shown yet.

Besides initiating unwanted recombination, nascent strands at a stalled replication fork could potentially fold back, anneal and form a so-called "chicken foot" structure (Postow *et al.* 1999) resembling a Holliday junction (Fig. 6.4). This structure could stabilise a collapsed replication fork on the one hand but also represents a target for a Holliday junction resolvase like RuvC in *E. coli* that would create a double-strand break. To prevent the latter and for replication to resume after the damage in front of the fork has been repaired, the Holliday-junction-like structure would have to be reverted by the branch migration activity of BLM. This model fits with the branch migration activity of BLM we observed, and with the ability of BLM to bind to and unwind Holliday junctions with some specificity. The ability to disrupt synthetic junctions was also found for two other RecQ members implicated in the negative regulation of recombination, Sgs1 (Bennett *et al.* 1999) and RecQ (Harmon *et al.* 1998). However, one has to assume that an additional factor, such as RPA, can impose directionality on the branch migration process to drive the "chicken foot" back to the starting point.

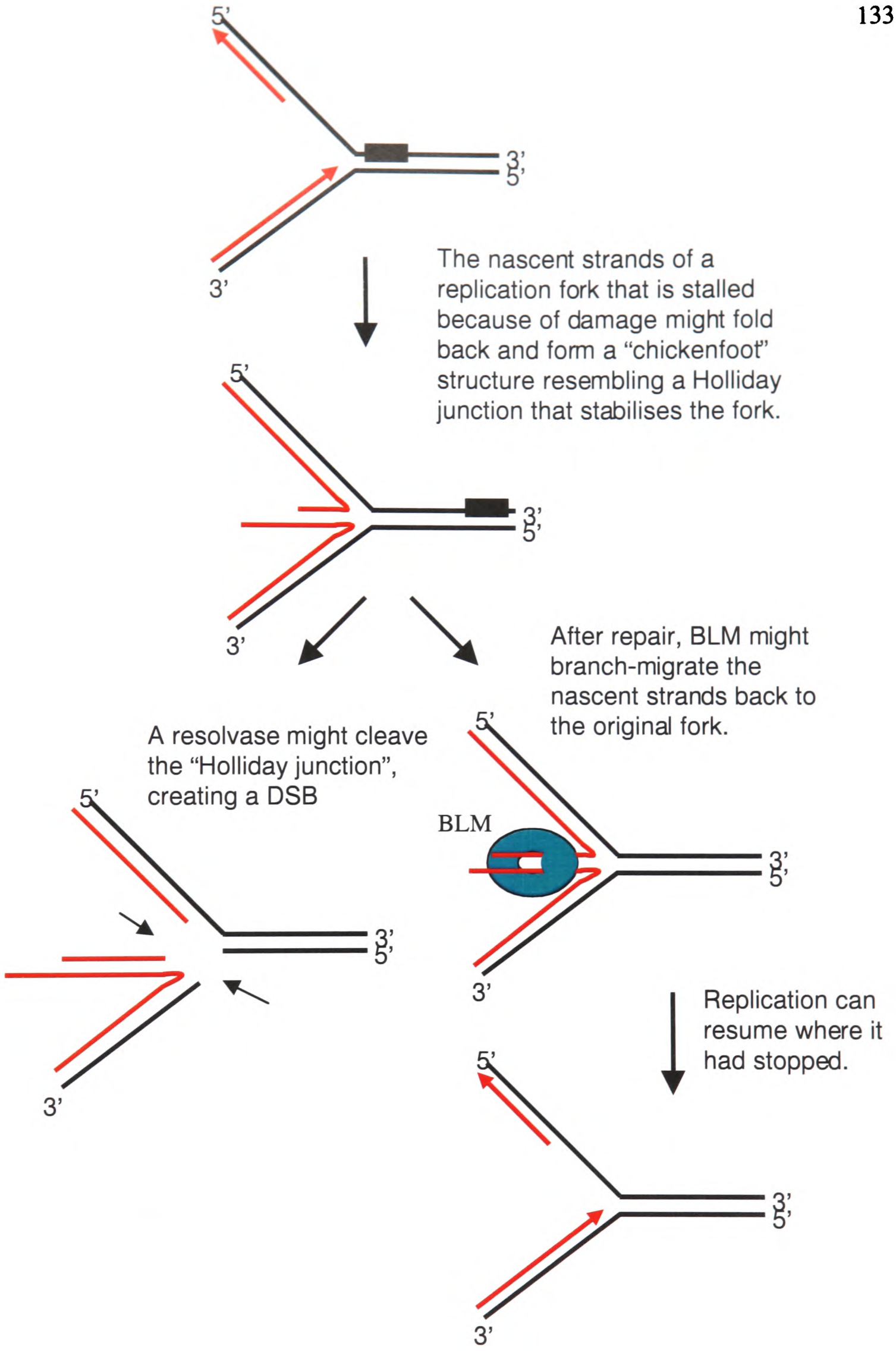


Fig. 6.4 Model 4: BLM acts as a reverse branch migrator at a "chickenfoot" structure

6.3 BLM - a role in chromosome separation?

The frequent chromosomal breaks observed in BS cells point to a defect in chromosome segregation. This could be due to a failure to complete chromosome separation during replication, a putative function of a helicase and topoisomerase (Duguet 1997, Wang 1996). When two replication forks approach each other, positive supercoils build up in front of them, inhibiting the final stages of replication. According to a recent model (Watt and Hickson 1996), Sgs1, the budding yeast homologue of BLM, could unwind the DNA in the unreplicated region, and topoisomerase II or III could decatenate the two daughter molecules. By analogy, BLM and human topoisomerase(s) III could perform a similar role (Fig. 6.5). This model is supported by the decatenation activity of *E. coli* RecQ and topoisomerase III (Harmon *et al.* 1999) and by the physical interaction between BLM and human topoisomerase IIIα. It is also consistent with the chromosome segregation defect seen in *sgs1*, *rqh1* and *top3* mutants.

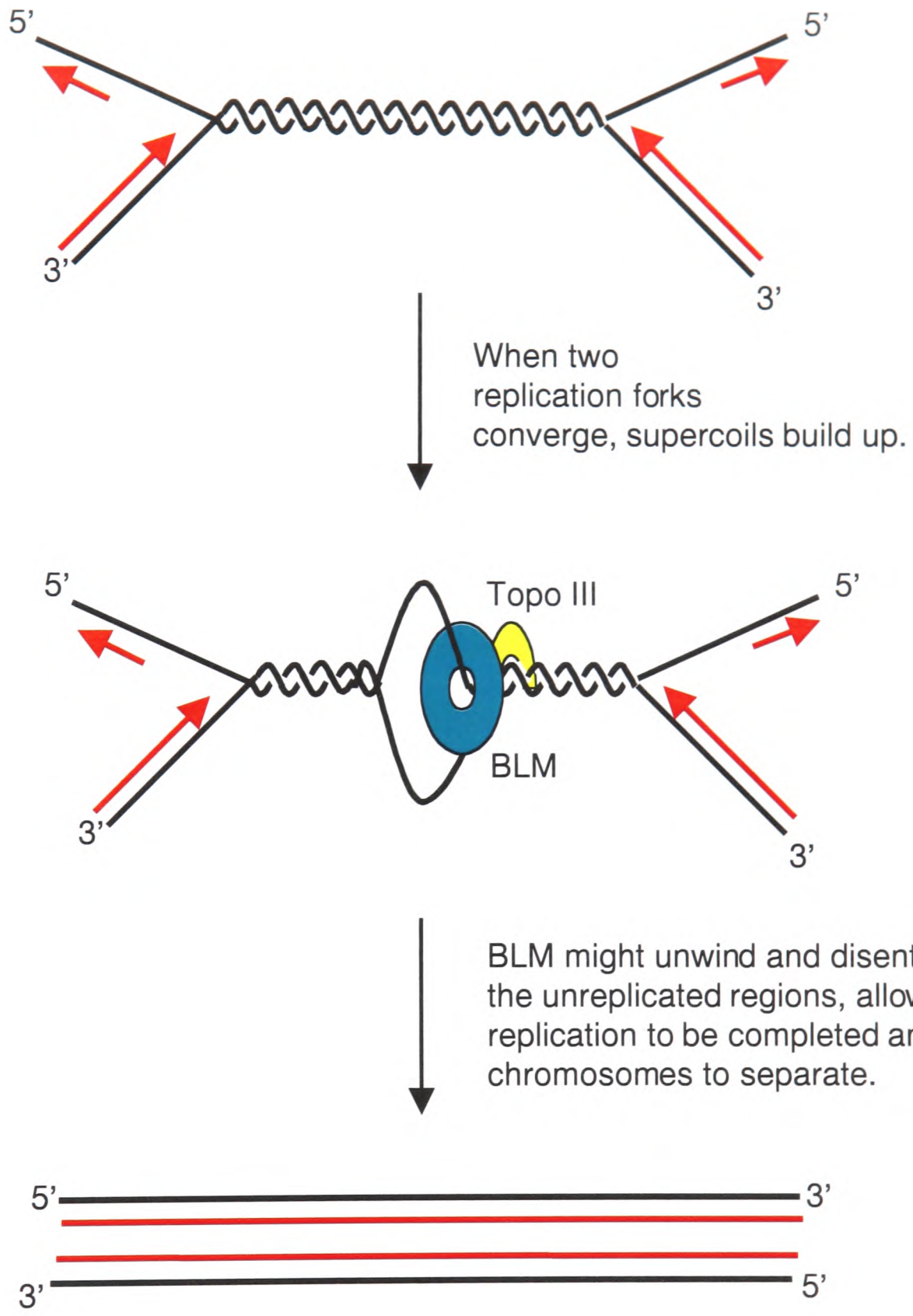


Fig. 6.5. Model 5: BLM helps segregate chromosomes at the merging point of two replication forks.

6.4 Outlook

This study has revealed some of the enzymatic and structural properties of BLM. Since it is unlikely that BLM acts on its own, it will be particularly important in the future to identify its partners in the cell and to address its function(s) in conjunction with these other proteins, including RPA, topoisomerase III and RAD51. Some of these studies are already ongoing and have been mentioned above. In particular, it would be interesting to see if BLM and human topoisomerase IIIα display a similar decatenation activity as their *E. coli* counterparts. Moreover, the substrate specificity and enzymatic properties of BLM should be further explored using more physiological DNA substrates, e.g. nucleosomal DNA. This might alter the rather broad specificity found so far and reveal new properties of the enzyme, e.g. the ability to remove nucleosomes. Furthermore, it would increase our understanding of the mechanism of unwinding if BLM was found to form rings encircling DNA (as a number of replicative helicases have been shown to). Finally, the role of BLM in the cell could be addressed by plasmid recombination assays or by its colocalisation with other proteins or with G4-DNA.

These approaches should eventually reveal what process(es) BLM is involved in that prevent genome instability, the accumulation of mutations and the formation of cancer in Bloom's syndrome patients.

Bibliography

Ariyoshi, M., Vassylyev, D. G., Iwasaki, H., Nakamura, H., Shinagawa, H., and Morikawa, K. (1994). Atomic structure of the RuvC resolvase: a Holliday junction-specific endonuclease from *E. coli*. Cell *78*, 1063-72.

Austin, C. A., Marsh, K. L., Wasserman, R. A., Willmore, E., Sayer, P. J., Wang, J. C., and Fisher, L. M. (1995). Expression, domain structure, and enzymatic properties of an active recombinant human DNA topoisomerase IIβ. J Biol Chem *270*, 15739-46.

Bahr, A., De Graeve, F., Kedinger, C., and Chatton, B. (1998). Point mutations causing Bloom's syndrome abolish ATPase and DNA helicase activities of the BLM protein. Oncogene *17*, 2565-71.

Baker, T. A., and Bell, S. P. (1998). Polymerases and the replisome: machines within machines. Cell *92*, 295-305.

Balajee, A. S., Machwe, A., May, A., Gray, M. D., Oshima, J., Martin, G. M., Nehlin, J. O., Brosh, R., Orren, D. K., and Bohr, V. A. (1999). The Werner syndrome protein is involved in RNA polymerase II transcription. Mol Biol Cell *10*, 2655-68.

Bambara, R. A., Murante, R. S., and Henricksen, L. A. (1997). Enzymes and reactions at the eukaryotic DNA replication fork. J Biol Chem *272*, 4647-50.

Bennett, R. J., Dunderdale, H. J., and West, S. C. (1993). Resolution of Holliday junctions by RuvC resolvase: cleavage specificity and DNA distortion. Cell *74*, 1021-31.

Bennett, R. J., Keck, J. L., and Wang, J. C. (1999). Binding specificity determines polarity of DNA unwinding by the Sgs1 protein of *S. cerevisiae*. J Mol Biol *289*, 235-48.

Bennett, R. J., Sharp, J. A., and Wang, J. C. (1998). Purification and characterization of the Sgs1 DNA helicase activity of *Saccharomyces cerevisiae*. J Biol Chem *273*, 9644-50.

Beresten, S. F., Stan, R., van Brabant, A. J., Ye, T., Naureckiene, S., and Ellis, N. A. (1999). Purification of overexpressed hexahistidine-tagged BLM N431 as oligomeric complexes. Protein Expr Purif *17*, 239-48.

Bird, L. E., Brannigan, J. A., Subramanya, H. S., and Wigley, D. B. (1998). Characterisation of *Bacillus stearothermophilus* PcrA helicase: evidence against an active rolling mechanism. Nucleic Acids Res *26*, 2686-93.

Bird, L. E., Subramanya, H. S., and Wigley, D. B. (1998). Helicases: a unifying structural theme? Curr Opin Struct Biol *8*, 14-8.

Blander, G., Kipnis, J., Leal, J. F., Yu, C. E., Schellenberg, G. D., and Oren, M. (1999). Physical and functional interaction between p53 and the Werner's syndrome protein. J Biol Chem *274*, 29463-9.

Bloom, D. (1954). Congenital telangiectatic erythema resembling lupus erythematosus in dwarfs. Am. J. Dis. Child. *88*, 754-758.

Bootsma, D., Kraemer, K. H., Cleaver, J. E., and Hoeijmakers, J. H. J. (1998). Nucleotide excision repair syndromes: xeroderma pigmentosum, Cockayne syndrome, and trichothiodystrophy. In: The genetic basis of human cancer, ed. Vogelstein, B. and Kinzler, K. W., McGraw-Hill, New York.

Brosh, R. M., Jr., Orren, D. K., Nehlin, J. O., Ravn, P. H., Kenny, M. K., Machwe, A., and Bohr, V. A. (1999). Functional and physical interaction between WRN helicase and human replication protein A. J Biol Chem *274*, 18341-50.

Broughton, B. C., Steingrimsdottir, H., Weber, C. A., and Lehmann, A. R. (1994). Mutations in the xeroderma pigmentosum group D DNA repair/transcription gene in patients with trichothiodystrophy. Nat Genet *7*, 189-94.

Camerini-Otero, R. D., and Hsieh, P. (1993). Parallel DNA triplexes, homologous recombination, and other homology- dependent DNA interactions. Cell *73*, 217-23.

Camerini-Otero, R. D., and Hsieh, P. (1995). Homologous recombination proteins in prokaryotes and eukaryotes. Annu Rev Genet *29*, 509-52.

Campbell, J. L. (1993). Yeast DNA replication. J Biol Chem *268*, 25261-4.

Chakraverty, R. (1998). A yeast model of Bloom's syndrome. PhD thesis.

Chester, N., Kuo, F., Kozak, C., O'Hara, C. D., and Leder, P. (1998). Stage-specific apoptosis, developmental delay, and embryonic lethality in mice homozygous for a targeted disruption in the murine Bloom's syndrome gene. Genes Dev *12*, 3382-93.

Chifflet, S., Torriglia, A., Chiesa, R., and Tolosa, S. (1988). A method for the determination of inorganic phosphate in the presence of labile organic phosphate and high concentrations of protein: application to lens ATPases. Anal Biochem *168*, 1-4.

Cho, H. S., Ha, N. C., Kang, L. W., Chung, K. M., Back, S. H., Jang, S. K., and Oh, B. H. (1998). Crystal structure of RNA helicase from genotype 1b hepatitis C virus. A feasible mechanism of unwinding duplex RNA. J Biol Chem *273*, 15045-52.

Cooper, P. K., Nouspikel, T., Clarkson, S. G., and Leadon, S. A. (1997). Defective transcription-coupled repair of oxidative base damage in Cockayne syndrome patients from XP group G. Science *275*, 990-3.

Courcelle, J., and Hanawalt, P. C. (1999). RecQ and RecJ process blocked replication forks prior to the resumption of replication in UV-irradiated *Escherichia coli*. Mol Gen Genet *262*, 543-51.

Cox, M. M. (1997). Recombinational crossroads: eukaryotic enzymes and the limits of bacterial precedents. Proc Natl Acad Sci USA *94*, 11764-6.

Davey, S., Han, C. S., Ramer, S. A., Klassen, J. C., Jacobson, A., Eisenberger, A., Hopkins, K. M., Lieberman, H. B., and Freyer, G. A. (1998). Fission yeast *rad12+* regulates cell cycle checkpoint control and is homologous to the Bloom's syndrome disease gene. Mol Cell Biol *18*, 2721-8.

Dillingham, M. S., Soultanas, P., and Wigley, D. B. (1999). Site-directed mutagenesis of motif III in PcrA helicase reveals a role in coupling ATP hydrolysis to strand separation. Nucleic Acids Res *27*, 3310-7.

Dong, F., Gogol, E. P., and von Hippel, P. H. (1995). The phage T4-coded DNA replication helicase (gp41) forms a hexamer upon activation by nucleoside triphosphate. J Biol Chem *270*, 7462-73.

Duguet, M. (1997). When helicase and topoisomerase meet! J Cell Sci *110*, 1345-50.

Dunderdale, H. J., and West, S. C. (1994). Recombination genes and proteins. Curr Opin Genet Dev *4*, 221-8.

Dutta, A., and Bell, S. P. (1997). Initiation of DNA replication in eukaryotic cells. Annu Rev Cell Dev Biol *13*, 293-332.

Egelman, H. H., Yu, X., Wild, R., Hingorani, M. M., and Patel, S. S. (1995). Bacteriophage T7 helicase/primase proteins form rings around single-stranded DNA that suggest a general structure for hexameric helicases. Proc Natl Acad Sci USA *92*, 3869-73.

Eggleston, A. K., Mitchell, A. H., and West, S. C. (1997). *In vitro* reconstitution of the late steps of genetic recombination in *E. coli*. Cell *89*, 607-17.

Ellis, N. A. (1997). DNA helicases in inherited human disorders. Curr Opin Genet Dev *7*, 354-63.

Ellis, N. A., Groden, J., Ye, T. Z., Straughen, J., Lennon, D. J., Ciocci, S., Proytcheva, M., and German, J. (1995). The Bloom's syndrome gene product is homologous to RecQ helicases. Cell *83*, 655-66.

Ellis, N. A., Proytcheva, M., Sanz, M. M., Ye, T. Z., and German, J. (1999). Transfection of BLM into cultured Bloom syndrome cells reduces the sister-chromatid exchange rate toward normal. Am J Hum Genet *65*, 1368-1374.

Enoch, T., Carr, A. M., and Nurse, P. (1992). Fission yeast genes involved in coupling mitosis to completion of DNA replication. Genes Dev *6*, 2035-46.

Feaver, W. J., Svejstrup, J. Q., Bardwell, L., Bardwell, A. J., Buratowski, S., Gulyas, K. D., Donahue, T. F., Friedberg, E. C., and Kornberg, R. D. (1993). Dual roles of a multiprotein complex from *S. cerevisiae* in transcription and DNA repair. Cell *75*, 1379-87.

Foucault, F., Vaury, C., Barakat, A., Thibout, D., Planchon, P., Jaulin, C., Praz, F., and Amor-Gueret, M. (1997). Characterization of a new BLM mutation associated with a topoisomerase IIα defect in a patient with Bloom's syndrome. Hum Molec Genet *6*, 1427-34.

Fouts, E. T., Yu, X., Egelman, E. H., and Botchan, M. R. (1999). Biochemical and electron microscopic image analysis of the hexameric E1 helicase. J Biol Chem *274*, 4447-58.

Friedberg, E. C. (1996). Relationships between DNA repair and transcription. Annu Rev Biochem *65*, 15-42.

Fry, M., and Loeb, L. A. (1999). Human Werner syndrome DNA helicase unwinds tetrahelical structures of the fragile X syndrome repeat sequence $d(CGG)_n$. J Biol Chem *274*, 12797-802.

Fujiwara, Y., Higashikawa, T., and Tatsumi, M. (1977). A retarded rate of DNA replication and normal level of DNA repair in Werner's syndrome fibroblasts in culture. J Cell Physiol *92*, 365-74.

Fukuchi, K., Martin, G. M., and Monnat, R. J., Jr. (1989). Mutator phenotype of Werner syndrome is characterized by extensive deletions. Proc Natl Acad Sci USA *86*, 5893-7.

Fukuchi, K., Tanaka, K., Nakura, J., Kumahara, Y., Uchida, T., and Okada, Y. (1985). Elevated spontaneous mutation rate in SV40-transformed Werner syndrome fibroblast cell lines. Somat Cell Mol Genet *11*, 303-8.

Gangloff, S., McDonald, J. P., Bendixen, C., Arthur, L., and Rothstein, R. (1994). The yeast type I topoisomerase Top3 interacts with Sgs1, a DNA helicase homolog: a potential eukaryotic reverse gyrase. Mol Cell Biol *14*, 8391-8.

Gebhart, E., Bauer, R., Raub, U., Schinzel, M., Ruprecht, K. W., and Jonas, J. B. (1988). Spontaneous and induced chromosomal instability in Werner syndrome. Hum Genet *80*, 135-9.

German, J. (1969). Bloom's syndrome. I. Genetical and clinical observations in the first twenty-seven patients. Am J Hum Genet *21*, 196-227.

German, J. (1993). Bloom syndrome: a Mendelian prototype of somatic mutational disease. Medicine *72*, 393-406.

German, J., Archibald, R., and Bloom, D. (1965). Chromosomal breakage in a rare and probably genetically determined syndrome of man. Science *148*, 506-507.

German, J., and Ellis, N. A. (1998). Bloom syndrome. In: The genetic basis of human cancer, ed. Vogelstein, B. and Kinzler, K. W., McGraw-Hill, New York.

German, J., Roe, A. M., Leppert, M. F., and Ellis, N. A. (1994). Bloom syndrome: an analysis of consanguineous families assigns the locus mutated to chromosome band 15q26.1. Proc Natl Acad Sci USA *91*, 6669-73.

Gibbons, R. J., and Higgs, D. R. (1996). The α-thalassemia/mental retardation syndromes. Medicine *75*, 45-52.

Gibbons, R. J., Picketts, D. J., Villard, L., and Higgs, D. R. (1995). Mutations in a putative global transcriptional regulator cause X-linked mental retardation with α-thalassemia (ATR-X syndrome). Cell *80*, 837-45.

Gogol, E. P., Seifried, S. E., and von Hippel, P. H. (1991). Structure and assembly of the *Escherichia coli* transcription termination factor rho and its interaction with RNA. I. Cryoelectron microscopic studies. J Mol Biol *221*, 1127-38.

Goodwin, A., Wang, S. W., Toda, T., Norbury, C., and Hickson, I. D. (1999). Topoisomerase III is essential for accurate nuclear division in *Schizosaccharomyces pombe*. Nucleic Acids Res *27*, 4050-4058.

Gorbalenya, A. E., and Koonin, E. V. (1993). Helicases: amino acid sequence comparisons and structure-function relationships. Curr Opin Struct Biol *3*, 419-429.

Gray, M. D., Shen, J. C., Kamath-Loeb, A. S., Blank, A., Sopher, B. L., Martin, G. M., Oshima, J., and Loeb, L. A. (1997). The Werner syndrome protein is a DNA helicase. Nat Genet *17*, 100-3.

Gray, M. D., Wang, L., Youssoufian, H., Martin, G. M., and Oshima, J. (1998). Werner helicase is localized to transcriptionally active nucleoli of cycling cells. Exp Cell Res *242*, 487-94.

Grigoriev, M., and Hsieh, P. (1998). Migration of a Holliday junction through a nucleosome directed by the *E. coli* RuvAB motor protein. Mol Cell *2*, 373-81.

Groden, J., Nakamura, Y., and German, J. (1990). Molecular evidence that homologous recombination occurs in proliferating human somatic cells. Proc Natl Acad Sci USA *87*, 4315-9.

Hanada, K., Ukita, T., Kohno, Y., Saito, K., Kato, J., and Ikeda, H. (1997). RecQ DNA helicase is a suppressor of illegitimate recombination in *Escherichia coli.* Proc Natl Acad Sci USA *94*, 3860-5.

Hanaoka, F., Takeuchi, F., Matsumura, T., Goto, M., Miyamoto, T., and Yamada, M. (1983). Decrease in the average size of replicons in a Werner syndrome cell line by Simian virus 40 infection. Exp Cell Res *144*, 463-7.

Hand, R., and German, J. (1975). A retarded rate of DNA chain growth in Bloom's syndrome. Proc Natl Acad Sci USA *72*, 758-62.

Harmon, F. G., DiGate, R. J., and Kowalczykowski, S. C. (1999). RecQ helicase and topoisomerase III comprise a novel DNA strand passage function: a conserved mechanism for control of DNA recombination. Mol Cell *3*, 611-20.

Harmon, F. G., and Kowalczykowski, S. C. (1998). RecQ helicase, in concert with RecA and SSB proteins, initiates and disrupts DNA recombination. Genes Dev *12*, 1134-44.

Heyer, W. D., and Kohli, J. (1994). Homologous recombination. Experientia *50*, 189-91.

Higgins, D. G., and Sharp, P. M. (1989). Fast and sensitive multiple sequence alignments on a microcomputer. Comput Appl Biosci *5*, 151-3.

Holliday, R. (1964). A mechanism for gene conversion in fungi. Genet Res *5*, 282-304.

Holm, C. (1994). Coming undone: how to untangle a chromosome. Cell *77*, 955-7.

Huang, S., Li, B., Gray, M. D., Oshima, J., Mian, I. S., and Campisi, J. (1998). The premature ageing syndrome protein, WRN, is a 3'-->5' exonuclease. Nat Genet *20*, 114-6.

Huberman, J. A. (1995). Prokaryotic and eukaryotic replicons. Cell *82*, 535-42.

Imamura, O., Ichikawa, K., Yamabe, Y., Goto, M., Sugawara, M., and Furuichi, Y. (1997). Cloning of a mouse homologue of the human Werner syndrome gene and assignment to 8A4 by fluorescence *in situ* hybridization. Genomics *41*, 298-300.

Irino, N., Nakayama, K., and Nakayama, H. (1986). The *recQ* gene of *Escherichia coli* K12: primary structure and evidence for SOS regulation. Mol Gen Genet *205*, 298-304.

Kamath-Loeb, A. S., Shen, J. C., Loeb, L. A., and Fry, M. (1998). Werner syndrome protein. II. Characterization of the integral 3' --> 5' DNA exonuclease. J Biol Chem *273*, 34145-50.

Kanaar, R., and Hoeijmakers, J. H. (1997). Recombination and joining: different means to the same ends. Genes Funct *1*, 165-74.

Kaneko, H., Matsui, E., Fukao, T., Kasahara, K., Morimoto, W., and Kondo, N. (1999). Expression of the BLM gene in human haematopoietic cells. Clin Exp Immunol *118*, 285-9.

Kaneko, H., Orii, K. O., Matsui, E., Shimozawa, N., Fukao, T., Matsumoto, T., Shimamoto, A., Furuichi, Y., Hayakawa, S., Kasahara, K., and Kondo, N. (1997). BLM (the causative gene of Bloom syndrome) protein translocation into the nucleus by a nuclear localization signal. Biochem Biophys Res Comm *240*, 348-53.

Karow, J. K., Chakraverty, R. K., and Hickson, I. D. (1997). The Bloom's syndrome gene product is a 3'-5' DNA helicase. J Biol Chem *272*, 30611-4.

Karow, J. K., Newman, R. H., Freemont, P. S., and Hickson, I. D. (1999). Oligomeric ring structure of the Bloom's syndrome helicase. Curr Biol *9*, 597-600.

Kim, J. L., Morgenstern, K. A., Griffith, J. P., Dwyer, M. D., Thomson, J. A., Murcko, M. A., Lin, C., and Caron, P. R. (1998). Hepatitis C virus NS3 RNA helicase domain with a bound oligonucleotide: the crystal structure provides insights into the mode of unwinding. Structure *6*, 89-100.

Kitao, S., Lindor, N. M., Shiratori, M., Furuichi, Y., and Shimamoto, A. (1999a). Rothmund-Thomson syndrome responsible gene, RECQL4: genomic structure and products. Genomics *61*, 268-76.

Kitao, S., Ohsugi, I., Ichikawa, K., Goto, M., Furuichi, Y., and Shimamoto, A. (1998). Cloning of two new human helicase genes of the RecQ family: biological significance of multiple species in higher eukaryotes. Genomics *54*, 443-52.

Kitao, S., Shimamoto, A., Goto, M., Miller, R. W., Smithson, W. A., Lindor, N. M., and Furuichi, Y. (1999b). Mutations in *RECQL4* cause a subset of cases of Rothmund-Thomson syndrome. Nat Genet *22*, 82-4.

Kogoma, T. (1997). Stable DNA replication: interplay between DNA replication, homologous recombination, and transcription. Microbiol Mol Biol Rev *61*, 212-38.

Korolev, S., Hsieh, J., Gauss, G. H., Lohman, T. M., and Waksman, G. (1997). Major domain swiveling revealed by the crystal structures of complexes of *E. coli* Rep helicase bound to single-stranded DNA and ADP. Cell *90*, 635-47.

Korolev, S., Yao, N., Lohman, T. M., Weber, P. C., and Waksman, G. (1998). Comparisons between the structures of HCV and Rep helicases reveal structural similarities between SF1 and SF2 superfamilies of helicases. Protein Sci *7*, 605-10.

Kuhn, E. M., and Therman, E. (1986). Cytogenetics of Bloom's syndrome. Cancer Genet Cytogenet *22*, 1-18.

Kusano, K., Berres, M. E., and Engels, W. R. (1999). Evolution of the RECQ family of helicases: A *Drosophila* homolog, Dmblm, is similar to the human Bloom syndrome gene. Genetics *151*, 1027-39.

Kuzminov, A. (1995). Instability of inhibited replication forks in *E. coli*. Bioessays *17*, 733-41.

Kyoizumi, S., Nakamura, N., Takebe, H., Tatsumi, K., German, J., and Akiyama, M. (1989). Frequency of variant erythrocytes at the *glycophorin-A* locus in two Bloom's syndrome patients. Mutat Res *214*, 215-22.

Langlois, R. G., Bigbee, W. L., Jensen, R. H., and German, J. (1989). Evidence for increased *in vivo* mutation and somatic recombination in Bloom's syndrome. Proc Natl Acad Sci USA *86*, 670-4.

Lebel, M., and Leder, P. (1998). A deletion within the murine Werner syndrome helicase induces sensitivity to inhibitors of topoisomerase and loss of cellular proliferative capacity. Proc Natl Acad Sci USA *95*, 13097-102.

Li, L., Eng, C., Desnick, R. J., German, J., and Ellis, N. A. (1998). Carrier frequency of the Bloom syndrome blm^{Ash} mutation in the Ashkenazi Jewish population. Mol Genet Metab *64*, 286-90.

Lilley, D. M. J. (1997). All change at Holliday junction. Proc Natl Acad Sci USA *94*, 9513-5.

Lindor, N. M., Devries, E. M., Michels, V. V., Schad, C. R., Jalal, S. M., Donovan, K. M., Smithson, W. A., Kvols, L. K., Thibodeau, S. N., and Dewald, G. W. (1996). Rothmund-Thomson syndrome in siblings: evidence for acquired *in vivo* mosaicism. Clin Genet *49*, 124-9.

Lindor, N. M., Furuichi, Y., Kitao, S., Shimamoto, A., Arndt, C., and Jalal, S. (2000). Rothmund-Thomson syndrome due to *RecQ4* helicase mutations: A case report and clinical and molecular comparisons with Bloom syndrome and Werner syndrome. Am. J. Med. Genet, *in press*.

Lloyd, R. G., and Sharples, G. J. (1993a). Dissociation of synthetic Holliday junctions by *E. coli* RecG protein. EMBO J *12*, 17-22.

Lloyd, R. G., and Sharples, G. J. (1993b). Processing of recombination intermediates by the RecG and RuvAB proteins of *Escherichia coli*. Nucleic Acids Res *21*, 1719-25.

Lohman, T. M., and Bjornson, K. P. (1996). Mechanisms of helicase-catalyzed DNA unwinding. Annu Rev Biochem *65*, 169-214.

Lönn, U., Lonn, S., Nylen, U., Winblad, G., and German, J. (1990). An abnormal profile of DNA replication intermediates in Bloom's syndrome. Cancer Res *50*, 3141-5.

Lu, J., Mullen, J. R., Brill, S. J., Kleff, S., Romeo, A. M., and Sternglanz, R. (1996). Human homologues of yeast helicase . Nature *383*, 678-9.

Lüking, A., Stahl, U., and Schmidt, U. (1998). The protein family of RNA helicases. Crit Rev Biochem Mol Biol *33*, 259-96.

Ma, L., Siemssen, E. D., Noteborn, H. M., and van der Eb, A. J. (1994). The xeroderma pigmentosum group B protein ERCC3 produced in the baculovirus system exhibits DNA helicase activity. Nucleic Acids Res *22*, 4095-102.

Maftahi, M., Han, C. S., Langston, L. D., Hope, J. C., Zigouras, N., and Freyer, G. A. (1999). The *top3+* gene is essential in Schizosaccharomyces pombe and the lethality associated with its loss is caused by Rad12 helicase activity. Nucleic Acids Res *27*, 4715-4724.

Mahdi, A. A., Sharples, G. J., Mandal, T. N., and Lloyd, R. G. (1996). Holliday junction resolvases encoded by homologous *rusA* genes in *Escherichia coli* K-12 and phage 82. J Mol Biol *257*, 561-73.

Marciniak, R. A., Lombard, D. B., Johnson, F. B., and Guarente, L. (1998). Nucleolar localization of the Werner syndrome protein in human cells. Proc Natl Acad Sci USA *95*, 6887-92.

Martin, G. M., Sprague, C. A., and Epstein, C. J. (1970). Replicative life-span of cultivated human cells. Effects of donor's age, tissue, and genotype. Lab Invest *23*, 86-92.

Mastrangelo, I. A., Hough, P. V., Wall, J. S., Dodson, M., Dean, F. B., and Hurwitz, J. (1989). ATP-dependent assembly of double hexamers of SV40 T antigen at the viral origin of DNA replication. Nature *338*, 658-62.

Matsumoto, T., Shimamoto, A., Goto, M., Furuichi, Y. (1997). Impaired nuclear localization of defective DNA helicases in Werner's syndrome.Nat Genet *16*, 335-6.

Matsumoto, T., Imamura, O., Goto, M., and Furuichi, Y. (1998). Characterization of the nuclear localization signal in the DNA helicase involved in Werner's syndrome. Int J Mol Med *1*, 71-6.

McDaniel, L. D., and Schultz, R. A. (1992). Elevated sister chromatid exchange phenotype of Bloom syndrome cells is complemented by human chromosome 15. Proc Natl Acad Sci USA *89*, 7968-72.

Mézard, C., George, H., Davies, A. A., van Gool, A. J., Zerbib, D., Stasiak, A., and West, S. C. (1999). *Escherichia coli* $RuvB^{L268S}$: a mutant RuvB protein that exhibits wild- type activities *in vitro* but confers a UV-sensitive *ruv* phenotype *in vivo*. Nucleic Acids Res *27*, 1275-82.

Miozzo, M., Castorina, P., Riva, P., Dalpra, L., Fuhrman Conti, A. M., Volpi, L., Hoe, T. S., Khoo, A., Wiegant, J., Rosenberg, C., and Larizza, L. (1998). Chromosomal instability in fibroblasts and mesenchymal tumors from 2 sibs with Rothmund-Thomson syndrome. Int J Cancer *77*, 504-10.

Monnat, R. J., Jr., Hackmann, A. F., and Chiaverotti, T. A. (1992). Nucleotide sequence analysis of human hypoxanthine phosphoribosyltransferase (HPRT) gene deletions. Genomics *13*, 777-87.

Morozov, V., Mushegian, A. R., Koonin, E. V., and Bork, P. (1997). A putative nucleic acid-binding domain in Bloom's and Werner's syndrome helicases. Trends Biochem Sci *22*, 417-8.

Moser, M. J., Oshima, J., and Monnat, R. J., Jr. (1999). *WRN* mutations in Werner syndrome. Hum Mutat *13*, 271-9.

Murray, J. M., Lindsay, H. D., Munday, C. A., and Carr, A. M. (1997). Role of *Schizosaccharomyces pombe* RecQ homolog, recombination, and checkpoint genes in UV damage tolerance. Mol Cell Biol *17*, 6868-75.

Nakayama, H., Nakayama, K., Nakayama, R., Irino, N., Nakayama, Y., and Hanawalt, P. C. (1984). Isolation and genetic characterization of a thymineless death-resistant mutant of *Escherichia coli* K12: identification of a new mutation (*recQ1*) that blocks the RecF recombination pathway. Mol Gen Genet *195*, 474-80.

Nakayama, K., Irino, N., and Nakayama, H. (1985). The *recQ* gene of *Escherichia coli* K12: molecular cloning and isolation of insertion mutants. Mol Gen Genet *200*, 266-71.

Neff, N. F., Ellis, N. A., Ye, T. Z., Noonan, J., Huang, K., Sanz, M., and Proytcheva, M. (1999). The DNA helicase activity of BLM is necessary for the correction of the genomic instability of Bloom syndrome cells. Mol Biol Cell *10*, 665-76.

Ng, S. W., Liu, Y., Hasselblatt, K. T., Mok, S. C., and Berkowitz, R. S. (1999). A new human topoisomerase III that interacts with SGS1 protein. Nucleic Acids Res *27*, 993-1000.

Ockey, C. H., and Saffhill, R. (1986). Delayed DNA maturation, a possible cause of the elevated sister- chromatid exchange in Bloom's syndrome. Carcinogenesis *7*, 53-7.

Ogburn, C. E., Oshima, J., Poot, M., Chen, R., Hunt, K. E., Gollahon, K. A., Rabinovitch, P. S., and Martin, G. M. (1997). An apoptosis-inducing genotoxin differentiates heterozygotic carriers for Werner helicase mutations from wild-type and homozygous mutants. Hum Genet *101*, 121-5.

Orren, D. K., Brosh, R., Nehlin, J. O., Machwe, A., Gray, M. D., and Bohr, V. A. (1999). Enzymatic and DNA binding properties of purified WRN protein: high affinity binding to single-stranded DNA but not to DNA damage induced by 4NQO. Nucleic Acids Res *27*, 3557-66.

Ortiz-Lombardía, M., Gonzalez, A., Eritja, R., Aymami, J., Azorin, F., and Coll, M. (1999). Crystal structure of a DNA Holliday junction. Nat Struct Biol *6*, 913-7.

Owen-Hughes, T., Utley, R. T., Cote, J., Peterson, C. L., and Workman, J. L. (1996). Persistent site-specific remodeling of a nucleosome array by transient action of the SWI/SNF complex. Science *273*, 513-6.

Parsons, C. A., Stasiak, A., Bennett, R. J., and West, S. C. (1995). Structure of a multisubunit complex that promotes DNA branch migration. Nature *374*, 375-8.

Parsons, C. A., and West, S. C. (1993). Formation of a RuvAB-Holliday junction complex *in vitro*. J Mol Biol *232*, 397-405.

Patel, S. S., and Hingorani, M. M. (1993). Oligomeric structure of bacteriophage T7 DNA primase/helicase proteins. J Biol Chem *268*, 10668-75.

Picketts, D. J., Higgs, D. R., Bachoo, S., Blake, D. J., Quarrell, O. W., and Gibbons, R. J. (1996). ATRX encodes a novel member of the SNF2 family of proteins: mutations point to a common mechanism underlying the ATR-X syndrome. Hum Mol Genet *5*, 1899-907.

Postow, L., Ullsperger, C., and Cozzarelli, N. (1999). A positive supercoil-induced four-way junction in replication intermediates. Abstract from meeting (Molecular mechanisms in DNA replication and recombination), Taos.

Puranam, K. L., and Blackshear, P. J. (1994). Cloning and characterization of RECQL, a potential human homologue of the *Escherichia coli* DNA helicase RecQ. J Biol Chem *269*, 29838-45.

Puranam, K. L., Kennington, E., Sait, S. N., Shows, T. B., Rochelle, J. M., Seldin, M. F., and Blackshear, P. J. (1995). Chromosomal localization of the gene encoding the human DNA helicase *RECQL* and its mouse homologue. Genomics *26*, 595-8.

Rao, B. J., Chiu, S. K., and Radding, C. M. (1993). Homologous recognition and triplex formation promoted by RecA protein between duplex oligonucleotides and single-stranded DNA. J Mol Biol *229*, 328-43.

Rosin, M. P., and German, J. (1985). Evidence for chromosome instability *in vivo* in Bloom syndrome: increased numbers of micronuclei in exfoliated cells. Hum Genet *71*, 187-91.

Rothmund, A. (1868). Über Katarakte in Verbindung mit einer eigenthümlichen Hautdegeneration. Arch. Klin. Exp. Ophthal. *4*, 159-182.

Runyon, G. T., Wong, I., and Lohman, T. M. (1993). Overexpression, purification, DNA binding, and dimerization of the *Escherichia coli uvrD* gene product (helicase II). Biochem *32*, 602-12.

Salk, D. (1982). Werner's syndrome: a review of recent research with an analysis of connective tissue metabolism, growth control of cultured cells, and chromosomal aberrations. Hum Genet *62*, 1-5.

Salk, D., Au, K., Hoehn, H., and Martin, G. M. (1981). Cytogenetics of Werner's syndrome cultured skin fibroblasts: variegated translocation mosaicism. Cytogenet Cell Genet *30*, 92-107.

Salk, D., Au, K., Hoehn, H., and Martin, G. M. (1985). Cytogenetic aspects of Werner syndrome. Adv Exp Med Biol *190*, 541-6.

San Martín, M. C., Stamford, N. P., Dammerova, N., Dixon, N. E., and Carazo, J. M. (1995). A structural model for the *Escherichia coli* DnaB helicase based on electron microscopy data. J Struct Biol *114*, 167-76.

San Martín, M. C., Gruss, C., Carazo, J. M. (1997). Six molecules of SV40 large T antigen assemble in a propeller-shaped particle around a channel. J Mol Biol *268*, 15-20.

Sancar, A. (1996). DNA excision repair. Annu Rev Biochem *65*, 43-81.

Sawaya, M. R., Guo, S., Tabor, S., Richardson, C. C., and Ellenberger, T. (1999). Crystal structure of the helicase domain from the replicative helicase-primase of bacteriophage T7. Cell *99*, 167-77.

Schaeffer, L., Roy, R., Humbert, S., Moncollin, V., Vermeulen, W., Hoeijmakers, J. H., Chambon, P., and Egly, J. M. (1993). DNA repair helicase: a component of BTF2 (TFIIH) basic transcription factor. Science *260*, 58-63.

Schellenberg, G. D., Miki, T., Yu, C.-E., and Nakura, J. (1998). Werner syndrome. In: The genetic basis of human cancer, ed. Vogelstein, B. and Kinzler, K. W., McGraw-Hill, New York.

Scherzinger, E., Ziegelin, G., Barcena, M., Carazo, J. M., Lurz, R., and Lanka, E. (1997). The RepA protein of plasmid RSF1010 is a replicative DNA helicase. J Biol Chem *272*, 30228-36.

Sekelsky, J. J., Brodsky, M. H., Rubin, G. M., and Hawley, R. S. (1999). *Drosophila* and human RecQ5 exist in different isoforms generated by alternative splicing. Nucleic Acids Res *27*, 3762-3769.

Seki, M., Miyazawa, H., Tada, S., Yanagisawa, J., Yamaoka, T., Hoshino, S., Ozawa, K., Eki, T., Nogami, M., Okumura, K., and et al. (1994). Molecular cloning of cDNA encoding human DNA helicase Q1 which has homology to *Escherichia coli* Rec Q helicase and localization of the gene at chromosome 12p12. Nucleic Acids Res *22*, 4566-73.

Seki, T., Wang, W. S., Okumura, N., Seki, M., Katada, T., and Enomoto, T. (1998). cDNA cloning of mouse BLM gene, the homologue to human Bloom's syndrome gene, which is highly expressed in the testis at the mRNA level. Biochim Biophys Acta *1398*, 377-81.

Selby, C. P., and Sancar, A. (1997). Human transcription-repair coupling factor CSB/ERCC6 is a DNA-stimulated ATPase but is not a helicase and does not disrupt the ternary transcription complex of stalled RNA polymerase II. J Biol Chem *272*, 1885-90.

Sen, D., and Gilbert, W. (1988). Formation of parallel four-stranded complexes by guanine-rich motifs in DNA and its implications for meiosis. Nature *334*, 364-6.

Shen, J. C., Gray, M. D., Oshima, J., Kamath-Loeb, A. S., Fry, M., and Loeb, L. A. (1998a). Werner syndrome protein. I. DNA helicase and DNA exonuclease reside on the same polypeptide. J Biol Chem *273*, 34139-44.

Shen, J. C., Gray, M. D., Oshima, J., and Loeb, L. A. (1998b). Characterization of Werner syndrome protein DNA helicase activity: directionality, substrate dependence and stimulation by replication protein A. Nucleic Acids Res *26*, 2879-85.

Shinohara, A., Ogawa, H., Matsuda, Y., Ushio, N., Ikeo, K., and Ogawa, T. (1993). Cloning of human, mouse and fission yeast recombination genes homologous to RAD51 and recA. Nat Genet *4*, 239-43.

Shiratori, M., Sakamoto, S., Suzuki, N., Tokutake, Y., Kawabe, Y., Enomoto, T., Sugimoto, M., Goto, M., Matsumoto, T., and Furuichi, Y. (1999). Detection by epitope-defined monoclonal antibodies of Werner DNA helicases in the nucleoplasm and their upregulation by cell transformation and immortalization. J Cell Biol *144*, 1-9.

Sinclair, D. A., and Guarente, L. (1997). Extrachromosomal rDNA circles-a cause of aging in yeast. Cell *91*, 1033-42.

Sinclair, D. A., Mills, K., and Guarente, L. (1997). Accelerated aging and nucleolar fragmentation in yeast *sgs1* mutants. Science *277*, 1313-6.

Spillare, E. A., Robles, A. I., Wang, X. W., Shen, J. C., Yu, C. E., Schellenberg, G. D., and Harris, C. C. (1999). p53-mediated apoptosis is attenuated in Werner syndrome cells. Genes Dev *13*, 1355-60.

Stasiak, A., Tsaneva, I. R., West, S. C., Benson, C. J., Yu, X., and Egelman, E. H. (1994). The *Escherichia coli* RuvB branch migration protein forms double hexameric rings around DNA. Proc Natl Acad Sci USA *91*, 7618-22.

Stefanini, M., Scappaticci, S., Lagomarsini, P., Borroni, G., Berardesca, E., and Nuzzo, F. (1989). Chromosome instability in lymphocytes from a patient with Werner's syndrome is not associated with DNA repair defects. Mutat Res *219*, 179-85.

Stewart, E., Chapman, C. R., Al-Khodairy, F., Carr, A. M., and Enoch, T. (1997). *rqh1+*, a fission yeast gene related to the Bloom's and Werner's syndrome genes, is required for reversible S phase arrest. EMBO J *16*, 2682-92.

Stillman, B. (1994). Smart machines at the DNA replication fork. Cell *78*, 725-8.

Subramanya, H. S., Bird, L. E., Brannigan, J. A., and Wigley, D. B. (1996). Crystal structure of a DExx box DNA helicase. Nature *384*, 379-83.

Sugino, A. (1995). Yeast DNA polymerases and their role at the replication fork. Trends Biochem Sci *20*, 319-23.

Sun, H., Karow, J. K., Hickson, I. D., and Maizels, N. (1998). The Bloom's syndrome helicase unwinds G4 DNA. J Biol Chem *273*, 27587-92.

Sun, H., Bennett, R. J, Maizels, N. (1999). The *Saccharomyces cerevisiae* Sgs1 helicase efficiently unwinds G-G paired DNAs. Nucleic Acids Res *27*, 1978-84.

Sung, P., Bailly, V., Weber, C., Thompson, L. H., Prakash, L., and Prakash, S. (1993). Human xeroderma pigmentosum group D gene encodes a DNA helicase. Nature *365*, 852-5.

Suzuki, N., Shimamoto, A., Imamura, O., Kuromitsu, J., Kitao, S., Goto, M., and Furuichi, Y. (1997). DNA helicase activity in Werner's syndrome gene product synthesized in a baculovirus system. Nucleic Acids Res *25*, 2973-8.

Suzuki, N., Shiratori, M., Goto, M., and Furuichi, Y. (1999). Werner syndrome helicase contains a 5'-->3' exonuclease activity that digests DNA and RNA strands in DNA/DNA and RNA/DNA duplexes dependent on unwinding. Nucleic Acids Res *27*, 2361-8.

Takayama, K., Salazar, E. P., Broughton, B. C., Lehmann, A. R., Sarasin, A., Thompson, L. H., and Weber, C. A. (1996). Defects in the DNA repair and transcription gene *ERCC2(XPD)* in trichothiodystrophy. Am J Hum Genet *58*, 263-70.

Takeuchi, F., Hanaoka, F., Goto, M., Akaoka, I., Hori, T., Yamada, M., and Miyamoto, T. (1982). Altered frequency of initiation sites of DNA replication in Werner's syndrome cells. Hum Genet *60*, 365-8.

Thacker, J. (1999). A surfeit of *RAD51*-like genes? Trends Genet *15*, 166-8.

Thomson, M. S. (1923). A hitherto undescribed familial disease. Br J Dermatol *35*, 455-462.

Thomson, M. S. (1936). Poikiloderma congenitale. Br J Dermatol *48*, 221-234.

Troelstra, C., van Gool, A., de Wit, J., Vermeulen, W., Bootsma, D., and Hoeijmakers, J. H. (1992). *ERCC6*, a member of a subfamily of putative helicases, is involved in Cockayne's syndrome and preferential repair of active genes. Cell *71*, 939-53.

Tsaneva, I. R., Muller, B., and West, S. C. (1993). RuvA and RuvB proteins of *Escherichia coli* exhibit DNA helicase activity *in vitro*. Proc Natl Acad Sci USA *90*, 1315-9.

Umezu, K., and Nakayama, H. (1993). RecQ DNA helicase of Escherichia coli. Characterization of the helix-unwinding activity with emphasis on the effect of single-stranded DNA-binding protein. J Mol Biol *230*, 1145-50.

Umezu, K., Nakayama, K., and Nakayama, H. (1990). *Escherichia coli* RecQ protein is a DNA helicase. Proc Natl Acad Sci USA *87*, 5363-7.

Usdin, K., and Woodford, K. J. (1995). CGG repeats associated with DNA instability and chromosome fragility form structures that block DNA synthesis *in vitro*. Nucleic Acids Res *23*, 4202-9.

van Heel, M. (1989). Classification of very large electron microscopical image data sets. Optik *82*, 114-126.

van Heel, M., and Frank, J. (1981). Use of multivariate statistics in analysing the images of biological macromolecules. Ultramicroscopy *6*, 187-194.

Vasseur, F., Delaporte, E., Zabot, M. T., Sturque, M. N., Barrut, D., Savary, J. B., Thomas, L., and Thomas, P. (1999). Excision repair defect in Rothmund Thomson syndrome. Acta Derm Venereol *79*, 150-2.

Velankar, S. S., Soultanas, P., Dillingham, M. S., Subramanya, H. S., and Wigley, D. B. (1999). Crystal structures of complexes of PcrA DNA helicase with a DNA substrate indicate an inchworm mechanism. Cell *97*, 75-84.

Vennos, E. M., and James, W. D. (1995). Rothmund-Thomson syndrome. Dermatol Clin *13*, 143-50.

Vijayalaxmi, Evans, H. J., Ray, J. H., and German, J. (1983). Bloom's syndrome: evidence for an increased mutation frequency *in vivo*. Science *221*, 851-3.

Walker, J. E.,.Eberle, A., Gay, N. J., Runswick, M. J., and Saraste, M. (1982). Conservation of structure in protein-translocating ATPases of *Escherichia coli* and mitochondria. Biochem Soc Trans *10*, 203-6.

Walpita, D., Plug, A. W., Neff, N. F., German, J., and Ashley, T. (1999). Bloom's syndrome protein, BLM, colocalizes with replication protein A in meiotic prophase nuclei of mammalian spermatocytes. Proc Natl Acad Sci USA *96*, 5622-7.

Wang, W. S., Seki, M., Yamaoka, T., Seki, T., Tada, S., Katada, T., Fujimoto, H., and Enomoto, T. (1998). Cloning of two isoforms of mouse DNA helicase Q1/RecQL cDNA;

alpha form is expressed ubiquitously and beta form specifically in the testis. Biochim Biophys Acta *1443*, 198-202.

Wasserman, R. A., Austin, C. A., Fisher, L. M., and Wang, J. C. (1993). Use of yeast in the study of anticancer drugs targeting DNA topoisomerases: expression of a functional recombinant human DNA topoisomerase II alpha in yeast. Cancer Res *53*, 3591-6.

Watt, P. M., Hickson, I. D., Borts, R. H., and Louis, E. J. (1996). *SGS1*, a homologue of the Bloom's and Werner's syndrome genes, is required for maintenance of genome stability in *Saccharomyces cerevisiae*. Genetics *144*, 935-45.

Watt, P. M., Louis, E. J., Borts, R. H., and Hickson, I. D. (1995). Sgs1: a eukaryotic homolog of *E. coli* RecQ that interacts with topoisomerase II *in vivo* and is required for faithful chromosome segregation. Cell *81*, 253-60.

Weber, C. A., Salazar, E. P., Stewart, S. A., and Thompson, L. H. (1990). *ERCC2*: cDNA cloning and molecular characterization of a human nucleotide excision repair gene with high homology to yeast RAD3. EMBO J *9*, 1437-47.

Weeda, G., Eveno, E., Donker, I., Vermeulen, W., Chevallier-Lagente, O., Taieb, A., Stary, A., Hoeijmakers, J. H., Mezzina, M., and Sarasin, A. (1997). A mutation in the *XPB/ERCC3* DNA repair transcription gene, associated with trichothiodystrophy. Am J Hum Genet *60*, 320-9.

Weeda, G., van Ham, R. C., Vermeulen, W., Bootsma, D., van der Eb, A. J., and Hoeijmakers, J. H. (1990). A presumed DNA helicase encoded by *ERCC-3* is involved in the human repair disorders xeroderma pigmentosum and Cockayne's syndrome. Cell *62*, 777-91.

Werner, O. (1904). Über Katarakt in Verbindung mit Sklerodermie. Doctoral dissertation,. Kiel University.

West, S. C. (1994). The processing of recombination intermediates: mechanistic insights from studies of bacterial proteins. Cell *76*, 9-15.

West, S. C. (1997). Processing of recombination intermediates by the RuvABC proteins. Annu Rev Genet *31*, 213-44.

Whitby, M. C., Bolt, E. L., Chan, S. N., and Lloyd, R. G. (1996). Interactions between RuvA and RuvC at Holliday junctions: inhibition of junction cleavage and formation of a RuvA-RuvC-DNA complex. J Mol Biol *264*, 878-90.

Williamson, J. R., Raghuraman, M. K., and Cech, T. R. (1989). Monovalent cation-induced structure of telomeric DNA: the G-quartet model. Cell *59*, 871-80.

Wu, L., Davies, S. L., North, P. S., Goulaouic, H., Riou, J.-F., Turley, H., Gatter, K. C., and Hickson, I. D (2000). Functional interaction betwen the Bloom's syndrome gene product and topoisomerase III. J Biol Chem *in press*.

Yamabe, Y., Shimamoto, A., Goto, M., Yokota, J., Sugawara, M., and Furuichi, Y. (1998). Sp1-mediated transcription of the Werner helicase gene is modulated by Rb and p53. Mol Cell Biol *18*, 6191-200.

Yamagata, K., Kato, J., Shimamoto, A., Goto, M., Furuichi, Y., and Ikeda, H. (1998). Bloom's and Werner's syndrome genes suppress hyperrecombination in yeast *sgs1* mutant: implication for genomic instability in human diseases. Proc Natl Acad Sci USA *95*, 8733-8.

Yan, H., Chen, C. Y., Kobayashi, R., and Newport, J. (1998). Replication focus-forming activity 1 and the Werner syndrome gene product. Nat Genet *19*, 375-8.

Yao, N., Hesson, T., Cable, M., Hong, Z., Kwong, A. D., Le, H. V., and Weber, P. C. (1997). Structure of the hepatitis C virus RNA helicase domain. Nat Struct Biol *4*, 463-7.

Ye, L., Nakura, J., Morishima, A., and Miki, T. (1998). Transcriptional activation by the Werner syndrome gene product in yeast. Exp Gerontol *33*, 805-12.

Yu, C. E., Oshima, J., Fu, Y. H., Wijsman, E. M., Hisama, F., Alisch, R., Matthews, S., Nakura, J., Miki, T., Ouais, S., Martin, G. M., Mulligan, J., and Schellenberg, G. D. (1996a). Positional cloning of the Werner's syndrome gene. Science *272*, 258-62.

Yu, X., and Egelman, E. H. (1997). The RecA hexamer is a structural homologue of ring helicases. Nat Struct Biol *4*, 101-4.

Yu, X., Jezewska, M. J., Bujalowski, W., and Egelman, E. H. (1996b). The hexameric *E. coli* DnaB helicase can exist in different quaternary states. J Mol Biol *259*, 7-14.

Zhong, S., Hu, P., Ye, T.-Z., Stan, R., Ellis, N. A., and Pandolfi, P. P (1999). A role for PML and the nuclear body in genomic stability. Oncogene *18*, 7941-47.

Publications arising from this work

Karow, J. K., Chakraverty, R. K., and Hickson, I. D. (1997). The Bloom's syndrome gene product is a 3'-5' DNA helicase. J Biol Chem *272*, 30611-4.

Sun, H., Karow, J. K., Hickson, I. D., and Maizels, N. (1998). The Bloom's syndrome helicase unwinds G4 DNA. J Biol Chem *273*, 27587-92.

Karow, J. K., Newman, R. H., Freemont, P. S., and Hickson, I. D. (1999). Oligomeric ring structure of the Bloom's syndrome helicase. Curr Biol *9*, 597-600.

Wu, L., Karow, J. K., and Hickson, I. D. (1999). Helicases and topoisomerases link up. Curr Biol *9*, R518-R520.

Karow, J. K., Wu, L,. and Hickson, I. D. (2000). RecQ family helicases: roles in cancer and aging. Curr Opin Genet Dev, *in press*.

Karow, J. K., Constantinou, A., West, S. C., .and Hickson, I. D. (*submitted*). The Bloom's syndrome gene product promotes branch migration of Holliday junctions.